

FINAL REPORT

BRAKE PAD PARTNERSHIP:
SAN FRANCISCO BAY
MODELING

Prepared for
Sustainable Conservation
98 Battery Street, Suite 302
San Francisco, CA 94111

December 2007



URS Corporation
1333 Broadway, Suite 800
Oakland, CA 94612

TABLE OF CONTENTS

Section 1	Introduction.....	1-1
Section 2	Methodology	2-1
	2.1 Model Description and Inputs.....	2-1
	2.1.1 Hydrodynamic Module (MIKE 21 HD)	2-1
	2.1.2 ECO Lab Heavy Metal Module	2-7
	2.2 Modeled Scenarios.....	2-14
Section 3	Results	3-1
	3.1 Results of Modeled Scenarios.....	3-1
	3.2 Discussion of Results.....	3-2
	3.2.1 Dissolved Copper in the Bay Water Column.....	3-2
	3.2.2 Benthic Copper in the Bay Sediments	3-3
	3.2.3 Mass Balance	3-4
Section 4	Sensitivity/Uncertainty	4-1
	4.1 Previous Sensitivity Analyses.....	4-1
	4.2 Sensitivity to Copper Loads.....	4-1
	4.3 Sensitivity to Initial Benthic Copper Conditions	4-2
	4.4 Sensitivity to Temperature and Salinity Forcings.....	4-3
	4.5 Model Uncertainty and Limitations	4-3
Section 5	References	5-1

Tables

1	Input Parameters for the MIKE 21 Hydrodynamic Module
2	Modeled Watersheds and Flow Scaling Factors
3	Publicly Owned Treatment Work and Industrial Point Sources
4	Marina Inputs
5	Input Parameters for the ECO Lab Heavy Metal Module
6	Summary of Estimated Contribution of Brake Pad Wear Debris to Ambient Dissolved Copper
7	Summary of Cumulative Probabilities for Mid and Mid-No-BP Modeled Scenarios
8	Benthic Copper Concentrations for Mid and Mid-No-BP Modeled Scenarios by Site

TABLE OF CONTENTS

9	Benthic Copper Concentrations for Mid and Mid-No-BP Modeled Scenarios by Subsection
10	Annual Watershed Copper Loads for Mid Modeled Scenario

Figures

1	Brake Pad Partnership Technical Studies
2	MIKE 21 Model Domain and Bathymetry of San Francisco Bay
3	Watershed Boundaries and Entry Points to Bay
4	Publicly Owned Treatment Work, Industrial Point Source, and Marina Locations
5	Locations of Current and Tide Stations Selected for Hydrodynamic Model Verification
6	Comparison of Measured and Predicted Water Surface Elevations at Tide Stations 4509 and 4317
7	Comparison of Measured and Predicted Water Surface Elevations at Tide Stations 4290 and 5143
8	Modeled Flow Through Carquinez Strait
9	Comparison of Measured and Predicted Current Speeds at Stations C13, C12, and C312
10	Comparison of Measured and Predicted Current Speeds at Stations C9, C306, and C7
11	Comparison of Measured and Predicted Current Speeds at Stations C304, C211, and C16
12	Comparison of Measured and Predicted Current Speeds at Stations C215, C18, and C22
13	Comparison of Measured and Predicted Current Speeds at Stations C23, C316, and C24
14	Summary of Processes Modeled by ECO Lab Heavy Metal Module
15	Sensitivity of Dissolved Copper Concentration to Temperature and Salinity Forcings
16	Locations of Water Quality Stations Selected for Heavy Metal Model Verification
17	Comparison of Measured and Predicted Dissolved Copper Concentrations
18	Comparison of Observed and Predicted 4-Day Running Average Suspended Sediment Concentrations at Point San Pablo Station for 1997 Using 200-meter Model Output
19	Comparison of Observed and Predicted 4-Day Running Average Suspended Sediment Concentrations at Dumbarton Bridge Station for 1997 Using 330-meter Model Output

TABLE OF CONTENTS

20	Comparison of Selected Hourly and Average Copper Concentration Data at Redwood Creek
21	Dissolved Copper Concentrations for Mid and Mid-No-BP Modeled Scenarios
22	Benthic Copper Concentrations for Mid and Mid-No-BP Modeled Scenarios
23	Cumulative Probabilities for Mid and Mid-No-BP Modeled Scenarios
24	Cumulative Probabilities for Scenario Differences at Coyote Creek (In Channel)
25	Annual Copper Loads in Tributary Runoff from Watershed Model
26	Copper Inventory for Lower South San Francisco Bay During 1997 Dry Season (February to September)
27	Copper Inventory for San Francisco Bay During Water Year 1999
28	Copper Inventory for San Francisco Bay During Water Year 2010 Using Hydrology for Water Year 1990
29	Copper Inventory for San Francisco Bay During Water Year 2018 Using Hydrology for Water Year 1998
30	Copper Inventory for San Francisco Bay During Water Year 2020 Using Hydrology for Water Year 2000
31	Sensitivity of Dissolved Copper Concentration to Copper Loads
32	Sensitivity of Benthic Copper Concentration to Copper Loads, Coyote Creek (In Channel)
33	Sensitivity of Dissolved Copper Concentration to Initial Benthic Copper Conditions
34	Sensitivity of Benthic Copper Concentration to Initial Benthic Copper Conditions

TABLE OF CONTENTS

Acronyms

2-D, 3-D	two-, three-dimensional
AD	advection-dispersion
Bay	San Francisco Bay
BPP	Brake Pad Partnership
BPWD	brake pad wear debris
cfs	cubic feet per second
Delta	Sacramento-San Joaquin River Delta
DWR	California Department of Water Resources
g/cell/s	gram(s) per grid cell per second
IEP	Interagency Ecological Program
kg/m ³	kilogram(s) per cubic meter
m/s	meter(s) per second
m ³ /s	cubic meter(s) per second
µg/L	micrograms per liter
µg/m ² /d	microgram per square meter per day
mg/kg	milligrams per kilogram
mg/L	milligrams per liter
MIKE 21 HD	MIKE 21 Hydrodynamic Module
MLLW	Mean Lower Low Water
NAVD	North American Vertical Datum of 1988
NGVD	National Geodetic Vertical Datum of 1929
NOAA	National Oceanic and Atmospheric Administration
NPDES	National Pollutant Discharge Elimination System
POTW	publicly owned treatment work
RMP	Regional Monitoring Program
SSC	suspended sediment concentration
USGS	U.S. Geological Survey
WY	Water Year

This San Francisco Bay (Bay) modeling effort is being conducted as part of a larger study by the Brake Pad Partnership (BPP) that examines the potential impact of copper from brake pad wear debris (BPWD) released to the environment. The BPP's source release inventory, water quality monitoring, air deposition monitoring, and watershed modeling studies were specifically prepared to provide input data for this Bay modeling effort. Other BPP studies, such as air deposition monitoring, procurement of a representative sample of BPWD, and physical and chemical characterization of BPWD indirectly provided information that supported this modeling effort. Partnership studies were completed with the cooperative oversight of the BPP Steering Committee and were peer reviewed by the BPP's Scientific Advisory Team. Figure 1 illustrates the technical approach of the BPP and how preceding studies inform the Bay modeling effort.

As stated in the approved Work Plan for this Bay model study (URS 2006), this report presents results of Bay modeling on the fate of copper from BPWD in the Bay. Results in this report provide a baseline for comparing to any increases or decreases in copper loadings that could occur in the future. By running model scenarios with and without the contributions of copper from BPWD, the effects of BPWD on the dissolved and benthic copper concentrations in the Bay can be determined. In this report, the model scenario that represents the best estimate of all copper contributions, including those from BPWD, is referred to as "Mid." The model scenario that represents the best estimate of all copper contributions excluding those from BPWD is referred to as "Mid-No-BP."

The Bay model for this BPP study is largely built upon a previous Bay model that was developed by URS for the Proposed San Francisco International Airport (SFO) Runway Configuration Project (URS 2003). The calibration and verification of this previous model were subject to extensive peer review (NOAA 2003). The BPP Steering Committee elected to use this model with the understanding that it would be modified as necessary for the BPP study.

2.1 MODEL DESCRIPTION AND INPUTS

MIKE 21 was used in conjunction with the ECO Lab module to simulate the water quality of the San Francisco Bay. MIKE 21 is a two-dimensional (2-D), free-surface flow modeling system developed by the Danish Hydraulic Institute. It simulates hydraulics and hydraulics-related phenomena in estuaries, coastal waters, and seas where vertical stratification can be neglected. It consists of a hydrodynamic module to which other modules can be added to address different phenomena. For the BPP Bay modeling, the ECO Lab module was used with the hydrodynamic module (MIKE 21 HD). A heavy metal template predefined by the Danish Hydraulic Institute served as the basis for the ECO Lab module setup, which was modified from its original version to meet the needs of the BPP project. The ECO Lab module replaces the Heavy Metal (ME) module that was used in an earlier version of MIKE 21. Both the MIKE 21 HD and ECO Lab Heavy Metal modules are described below.

2.1.1 Hydrodynamic Module (MIKE 21 HD)

MIKE 21 HD is the basic hydrodynamic module of the MIKE 21 series. It simulates the changes of water levels and velocities in response to tides, wind, and freshwater inflows. It solves the time-dependent vertically integrated equations of continuity and conservation of momentum in two horizontal dimensions. The equations are solved by a finite difference method. Water levels and flows are resolved on a rectangular grid covering the area of interest. Inputs include bathymetry, bed resistance, wind velocities, and hydrographic boundary conditions (e.g., tides in the Pacific Ocean and inflow from the Sacramento-San Joaquin River Delta [Delta]). Section 2.1.1.1 describes the inputs to MIKE 21 HD.

For the BPP copper modeling, a 200-meter resolution bathymetric grid used in a previously developed Bay model was revised into a coarser, nested grid configuration to balance the spatial resolution of the model with the time required to perform the simulations. The calibration and verification of this previous model have been peer reviewed (NOAA 2003). A 990-meter resolution grid was used to represent the bathymetry of the entire Bay from the mouth of the Delta to a point about 12 kilometers offshore of the Golden Gate Bridge. Two 330-meter resolution grids were nested within the 990-meter grid to provide more detailed bathymetry for the South Bay and Carquinez Strait. The revised model bathymetry is shown on Figure 2. Through verification, this revised bathymetry was determined to be sufficient to adequately model the hydrodynamic processes in the Bay. In addition, although the modeling approach in the Work Plan for this Bay Model study described both short-term and long-term modeling, it was determined upon reviewing the results of the revised grid verification that a separate long-term model was not necessary. Verification of hydrodynamic modeling using the revised bathymetry is described further in Section 2.1.1.2.

The use of a 2-D model rather than a three-dimensional (3-D) model was chosen primarily because the advantages (decreased computation time and good estimate of transport processes when water column is well mixed) outweigh the disadvantages (inability to model density-driven currents for stratified water column and inability to model vertical component of velocity for regions with steeply sloping bathymetry) and because a 3-D copper model of the San Francisco Bay has not been previously developed.

In a previous study of the Bay (URS 2003), salinity simulations of the dry season of a dry year (Water Year [WY]1994) and the wet season of a wet year (WY 1998) were performed using the 2-D MIKE 21 model and the 3-D TRIM model. The MIKE 21 model was able to adequately model the salinity during the dry season. However, the 2-D model did not perform as well to reproduce salinities during the wet season of WY 1998 when conditions were stratified in the main channel throughout most of the Bay. The 3-D model did reproduce the salinities, which indicates that 3-D processes are important during periods of high freshwater flows and stratification (URS 2003). The ability to accurately model salinity is a good indication of the model's ability to simulate the transport of dissolved substances. Based on the previous modeling of salinity, the MIKE 21 model should perform well during the dry season and probably for most of the wet season, as well as for portions of the Bay that are not very stratified, such as the South Bay.

The use of a 2-D versus a 3-D model can also have implications on the hydraulic residence time, which is generally believed to be a key parameter affecting water quality. For example, if the residence time is short, the water quality would be primarily determined by the inflow. If the residence time is long, the water quality would be influenced by bottom inputs and/or biological activity (Fischer et al. 1979). Previous estimates of the hydraulic residence time for the South Bay and for the region south of the Dumbarton Bridge range from 2 weeks to approximately 10 weeks (URS 2003). An unpublished U.S. Geological Survey (USGS) report (Smith and Gross 1997) found that the residence time of a discharge in Coyote Creek ranged from 63 to 67 days using a 2-D model. A later study by Gross (1998) using a 3-D model predicted a residence time south of the Dumbarton Bridge ranging from 19 to 23 days.

A study of hydraulic residence times in the South Bay performed by URS (2003) using the 2-D MIKE 21 model, the TRIM2D model, and the TRIM3D model found that the 3-D model did not produce significantly shorter residence times. Using a discharge in Coyote Creek and hydrologic conditions for 1993, the 2-D models estimated a residence time for the South Bay ranging from 50 to 80 days. The 3-D model estimated a residence time of 50 to 60 days. For the region south of the Dumbarton Bridge, the 2-D models estimated a residence time between 10 to 20 days. The 3-D model estimated a residence time of 10 to 15 days. In general, the estimates using the 3-D model were fairly comparable to the estimates using the 2-D model, which indicates that the transport processes in the South Bay can be adequately modeled using MIKE 21.

2.1.1.1 Inputs to MIKE 21 HD

This section describes the inputs to the MIKE 21 HD module. For a summary of the inputs and for values used in the MIKE 21 HD module, see Table 1.

Bathymetry

The bathymetric grid was developed by combining bathymetric data collected from several sources: a 30-meter resolution Digital Elevation Model of the entire Bay obtained from the National Oceanic and Atmospheric Administration (NOAA) (NOAA/NOS 1999), a 25-meter resolution grid for the South Bay below Dumbarton Bridge developed by the USGS (Smith and Cheng 1994), a 100-meter resolution grid for the Bay (Cheng and Smith 1998), and a grid created by URS from NOAA soundings in the Pacific Ocean. The grids were all projected to Universal Transverse Mercator Zone 10 North American Datum 1927 horizontal projection and rotated 35.40 degrees counterclockwise from north to align flow direction with the model

coordinate system in the South Bay and in San Pablo Bay. The Delta was modeled as a “box” with a surface area of 61,000 acres, an average depth of 5.1 meters (16.7 feet), and a volume of 1,145,000 acre-feet (DWR 1995).

The depths on the NOAA bathymetric grid and the USGS San Francisco Bay grid (Cheng and Smith 1998) were reported relative to local Mean Lower Low Water (MLLW). In contrast, the depths on the USGS Far South San Francisco Bay bathymetric grid (Smith and Cheng 1994) were reported relative to the National Geodetic Vertical Datum of 1929 (NGVD). The depths on the grids that were originally reported relative to MLLW were converted to NGVD based on water-surface elevation data from NOAA tide station benchmark sheets. The correction between MLLW and NGVD varies from approximately 0.9 meter at the Golden Gate to approximately 1.3 meters in the far South Bay (e.g., Coyote Creek) and to about 0.4 meter in Suisun Bay.

The data sources were generally used separately for each specific region where they were applied. The 25-meter USGS grid of the Lower South Bay (Smith and Cheng 1994) was used in preference to other data sources because it incorporated aerial photos to provide more accurate bathymetry in the shallow areas. The 30-meter NOAA/NOS (1999) grid was the primary source from the Dumbarton Bridge through the Central Bay to Carquinez Strait. The 100-meter USGS bathymetric grid (Cheng and Smith 1998) was used to specify the model bathymetry in Suisun Bay and in the Pacific Ocean outside of the Golden Gate. NOAA soundings were used to extend the bathymetry further west in the Pacific Ocean. Once the coverage for the entire Bay was obtained, the grids were all interpolated to a 30-meter resolution before merging them together using the hierarchy specified above. The 30-meter grid was then resampled to create the 330- and 990-meter grids used in the Bay modeling for this study.

Flow Boundary Conditions

At the eastern model boundary, the Delta outflow was specified as the average daily flow rate estimated by the California Department of Water Resources (DWR) Interagency Ecological Program (IEP) using the Dayflow program (DWR IEP 2007). The Dayflow computer program estimates the net Delta outflow by performing a water balance around the boundary of the Delta, taking Chipps Island as the western limit. The net Delta outflow is the sum of the total Delta inflow (including surface water inflows, streamflows, etc.) and runoff from precipitation over the watersheds making up the Delta, minus the Delta-wide consumptive use (e.g., channel depletion) and total Delta exports and diversions. Delta outflow data were obtained from 1980 through 2005.

Delta outflow exhibits a seasonal pattern with high flows in the winter and spring and lower flows in the summer and fall. Winter and spring flows are variable due to the variable amounts of rainfall. In general, Delta outflow exhibits less variation in summers and is usually between 50 and 200 cubic meters per second (m^3/s) (1,800 to 7,000 cubic feet per second [cfs]) or a 4-fold variation from minimum to maximum. In winters the flow range is much larger, and can vary between low values of 400 m^3/s (14,000 cfs) to high values of 18,000 m^3/s (636,000 cfs), a 45-fold variation from minimum to maximum.

Tidal Boundary Conditions

The input data for the Pacific Ocean boundary were taken from the NOAA tide station located at Point Reyes (NOAA Station Number 9415020), which is the closest station to the model

boundary with continuous water-level measurements. Either measured or predicted tidal data were specified along the ocean boundary about 12 kilometers outside of the Golden Gate Bridge.

The measured data at Point Reyes were not available from the NOAA website (<http://tidesandcurrents.noaa.gov/>) prior to 12/31/1995, so the predicted elevations were used from 1/1/1981 through 12/31/1995, and for any data gaps after 12/31/1995. The recorded time series of water-surface elevation, which reflects tidal and nontidal (e.g., wind, barometric pressure) forcing of water surface elevation, was applied from 12/31/1995 to 9/30/2005. The measured water levels were also applied prior to 1/1/1981, since this period had been used for verification of the previously developed 200-meter resolution Bay model.

The water-surface elevation data at Point Reyes were reported relative to MLLW. The data were converted to NGVD by subtracting 0.806 meter. This amount is based on the elevation of the North American Vertical Datum of 1988 (NAVD) published in the NOAA benchmark sheet for Point Reyes (0.008 meter relative to MLLW) and the difference of 0.798 meter between NAVD and NGVD calculated by the VERTCON program (National Geodetic Survey 1994).

Precipitation

Daily rainfall gauge data were applied to each watershed in the BPP study's watershed model (AQUA TERRA 2007). For the Bay model, a high spatial resolution of rainfall data was unnecessary as wet deposition inputs are small relative to tributary and publicly owned treatment work (POTW) discharges to the Bay. The watershed modeling report shows that rainfall onto the Bay is mostly uniform except in the Lower South Bay (AQUA TERRA 2007, Figure 2.2). Therefore, rainfall data from the San Jose gauge station (or Coyote Creek watershed) were applied to the Lower South Bay, and rainfall data from the Berkeley gauge station (or Contra Costa West watershed) were applied to the rest of the Bay. This distribution of available rainfall data was considered sufficient to represent rainfall throughout the Bay.

Eddy Viscosity

The eddy viscosity parameterizes horizontal mixing of momentum. The eddy viscosity is determined using the Smagorinsky formula based on velocity, with a Smagorinsky coefficient ranging from 0.05 to 0.5. The Smagorinsky coefficients were determined during calibration of the previous model (URS 2003).

Resistance

Resistance is represented by a bottom roughness coefficient, or Manning's n . The roughness coefficients were determined during calibration of the previous model (URS 2003).

Tributary Sources

Mean daily tributary flows were obtained from the BPP-supplied watershed modeling results (AQUA TERRA 2007). The watershed boundaries used in the watershed model differed from those used in the identification of catchment entry points in the Bay model. The watershed model identified 22 "subwatersheds," whereas the previous Bay model identified 70 catchments, most of which aggregate into the subwatersheds. The Bay model defines an entry point for each catchment. Figure 3 shows the locations of the catchment entry points and the various watershed delineations. Since the revised bathymetric grid does not include the small channels in the South and Lower South bays that connect inflow to the Bay, some of the entry points were moved from their geographically true locations to prevent placement in a grid cell that was periodically dry.

To maintain the same number and location of catchment entry points as in the previous Bay model, the flows from the watershed model were adapted to the catchment areas used in the Bay model by applying area-based scaling factors. The flow produced by a subwatershed was scaled to the area of a corresponding catchment by multiplying the flow by a ratio of the catchment area to the subwatershed area. Areas that contribute to major reservoirs (e.g., Upper San Leandro Reservoir, Crystal Springs Reservoir, Lake Chabot, etc.) were excluded in the calculation of the flow scaling factors, as reservoirs are not directly connected to the Bay. Also, exclusion of the areas above major reservoirs is consistent with the watershed model. Table 2 shows the corresponding subwatershed and its flow-scaling factor for each catchment.

For catchments not included in any of the subwatersheds used in the watershed model, flows from the subwatershed closest to the catchment of interest were used. To derive the flows for each of these catchments not included in the subwatersheds, the flows from the nearby subwatersheds were scaled by multiplying them with the ratio of the corresponding catchment area to the subwatershed area. These catchment/subwatershed pairings are identified in Table 2.

The watershed model identified stream reaches downstream of four upper subwatersheds—Upper San Francisquito Creek, Upper Alameda, Upper Colma, and Upper Corte Madera—to provide direct connections to the Bay. The flows of these subwatersheds were added to those at existing catchment entry points that were considered closest to the approximated connection points. In all cases, the approximated connection points were either the same as or very close to existing catchment entry points. These catchment/subwatershed pairings are identified in Table 2.

A misplacement of Upper Alameda's downstream reach was noted during an initial review after the model had been run for 20 years. In the Bay model, the Upper Alameda subwatershed connects to the Bay via the A11 catchment entry point. The correct connection point should have been at A12, which is the Alameda Creek Federal Flood Channel mouth. However, the effects of this error would only cover a small area because A11 and A12 are adjacent to each other (separated by 12 330-meter resolution grid cells), and discharges from the entry points are quickly mixed in the Bay. Thus, to be consistent with the previous 20 years of the simulation, the error was not corrected for the subsequent modeling. Point source inputs to ECO Lab consist of flow, concentration, and velocity data. The flow and concentration are used to determine the copper load, while the velocity is used to provide the flow with initial momentum. A flow velocity of 0.1 meter per second (m/s) was estimated as a reasonably small value compared to the current speeds of the Bay. Because the model grid size is 330 meters or larger, and because the model is not a near-field model, discharge from the source would be quickly mixed.

Publicly Owned Treatment Work and Industrial Point Sources

A total of 36 industrial and wastewater treatment plant sources were included in the Bay model. These sources are listed in Table 3 and locations are shown on Figure 4. Daily average flows were input when electronic data were available; otherwise monthly averages based on 1996 and 1997 National Pollutant Discharge Elimination System (NPDES) self-monitoring reports were applied to the entire simulation period. As for the tributary sources, a velocity of 0.1 m/s was applied to all flows.

Marina Inputs

The locations and copper release rates of 90 marinas included in the Bay model were provided by a BPP-supplied copper release study (Rosselot 2006). The copper released from marinas includes copper from pressure-treated wood used in marine construction and copper released from antifouling coatings used on boats (Rosselot 2006). Copper loads from algaecides released to shoreline surface waters were also included in the model for the five counties with reported usage (Rosselot 2006). These loads were treated as point sources located near the center of each county's shoreline. Even though the loads should be more distributed, this assumption should not unduly influence the results because the copper loads from algaecides are relatively small compared to other copper releases to the Bay, including the total copper releases from marinas.

The marinas and counties are listed in Table 4 and locations are shown on Figure 4. The locations were provided as latitude and longitude coordinates. For the Bay model, these coordinates were converted into MIKE 21 grid cell coordinates. Some of the marina sites were moved from their geographically true locations to prevent placement in a grid cell that was periodically dry.

The heavy metal template of the ECO Lab module requires that the point source loads are input as a flow and a concentration with an initial velocity. The marina and algaecide loads from Rosselot (2006) were converted to a concentration using a specified flow rate. The flow rates at the marinas and for the algaecide releases were assumed to be small, as they do not represent large tributary or POTW discharges. A small daily flow rate of $0.001 \text{ m}^3/\text{s}$ was selected to represent the volume of water that contained the daily copper released at each point source. A default velocity of 0.1 m/s was applied to all flows.

Wind

Hourly wind direction and speed data collected at San Francisco International Airport were applied to the entire Bay. These data were downloaded from the National Climatic Data Center website (NCDC 2007).

2.1.1.2 Verification of Hydrodynamics with Coarser Grid

The MIKE 21 model has the option for increasing the resolution of the bathymetry by nesting grids that increase in resolution by a factor of three compared to the encompassing grid. The MIKE 21 model dynamically couples the nested grids within the larger grids such that the numerical calculations are performed using the most detailed bathymetry available for each region. A dynamic exchange of both momentum and mass occurs between the coarse grid and the finer nested grids.

A MIKE 21 hydrodynamic and heavy metal model of the Bay was previously developed and calibrated using bathymetry with a 200-meter resolution (URS 2003). To speed up the simulation time for the BPP Bay modeling, 330- and 990-meter grids were created with the same data used to create the previous 200-meter grid. The South Bay and Carquinez Strait were defined using 330-meter resolution grids nested within the larger 990-meter grid. The revised model bathymetry is shown on Figure 2.

To verify that the hydrodynamic model based on the revised bathymetry was performing adequately, the predicted water levels and current speeds were compared to measured data from several stations located throughout the Bay. Figure 5 shows the locations of the tide and current

stations used in the model verification. The revised output was also compared to the previous model output using the 200-meter grid.

The comparisons of predicted and measured water levels are shown on Figures 6 and 7. Figure 6 shows the water levels at the Dumbarton Bridge (Station 4509) and the Bay Bridge (Station 4317). The predicted results using the coarser grids are essentially the same as the results using the 200-meter grid, and they represent the measured data quite well. Figure 7 shows the water levels at the Golden Gate (Station 4290) and Carquinez Strait (Station 5143). The results at the Golden Gate are similar to those shown on Figure 6, where the predicted results using the coarser grids are basically the same as the results using the 200-meter grid, and they both agree with the measured data. At Carquinez Strait, the water levels are probably more influenced by the local bathymetry, so the results using the coarser grids show a slightly reduced tidal range compared to both the results using the 200-meter grid and the measured data. However, the modeled flows through Carquinez Strait are not significantly different using the coarse grids compared to the 200-meter grid, as shown on Figure 8.

The comparisons of current speeds are shown on Figures 9 through 13. At some stations, current speeds were measured at multiple depths in the water column. For this situation, only the measurements from the current meter located closest to mid-depth were shown for comparison to the depth-averaged model output. The current speed is generally much more affected by the local bathymetry than the water level, so it is not expected that the modeled output would completely match the measured data at locations where the current speeds vary at a finer resolution than the model grid. Since the model output represents the depth-averaged current speeds, it may also be less likely to match the measured data if the measured current speed varies significantly with depth. Given the above considerations, overall, the model output from the coarse grid provides a good estimate of the current speeds throughout the Bay. The only location where the agreement is not as good is through Raccoon Strait at C16 shown on Figure 11, likely due to the narrow channel. Given that this channel is not the only flowpath in or out of the Bay, it did not seem necessary to resolve the bathymetry with finer detail than the 990-meter grid.

2.1.2 ECO Lab Heavy Metal Module

The ECO Lab Heavy Metal module was used to simulate the fate and transport of copper. This module incorporates the four primary processes governing the concentrations of heavy metals, listed below. The first three processes are shown on Figure 14.

1. Adsorption and desorption of metals
2. Sedimentation and resuspension of particulate metal
3. Diffusive transport of dissolved metals at the sediment/water interface
4. Transport of dissolved and particulate metal in the water column by advection and dispersion

The first process, adsorption/desorption, is the essential link between metals in the aqueous and solid phases. Adsorption is the process by which dissolved metal ions or complexes attach themselves to the surface of particulate matter. Desorption is the detachment of the metal from the particulate surface and its return to the dissolved state. In the ECO Lab Heavy Metal module, adsorption also includes the processes of absorption (incorporation of the metal into the solid phase) and surface precipitation.

The second important process is resuspension and sedimentation of particulate matter within the Bay. When metals are sorbed onto the solid phase, their concentration in the water column is partly controlled by the turbulent shear stresses induced by wind, tidal, or fluvial advection. These stresses cause sediments to become resuspended, thereby increasing water-column metals concentrations. Conversely, as turbulence is reduced, the particles and associated metals are again able to settle to the Bay floor as depicted on Figure 14.

The third process illustrated on Figure 14 is diffusion of metal-enriched water between the ambient Bay and porewater, depending on the concentration gradient. Diffusion rates are dependent on the chemical environment in the pore spaces of the sediment, which may be significantly different than the overlying water. Adsorption and desorption rate constants are used to represent chemical transformation in the porewater.

The final process incorporated into the ECO Lab Heavy Metal module is advection and dispersion of dissolved and adsorbed metals. Both dissolved and adsorbed metals are modeled simultaneously in ECO Lab, and parameters calculated in the simultaneous runs of MIKE 21 HD and ECO Lab govern this process.

In addition to the ecological, chemical, and settling processes shown on Figure 14, heavy metals are also influenced by hydrodynamic processes. ECO Lab includes an advection-dispersion (AD) component, which uses the information from MIKE 21 HD. The temporal and spatial changes to heavy metal concentrations are determined by solving combined AD and biogeochemical process equations.

The inputs to ECO Lab include the initial benthic sediment concentrations, point sources (POTWs, industrial wastewater sources, and BPP-supplied marina releases), tributary loads from the BPP-supplied watershed model, air deposition rates from the BPP-supplied air deposition model, initial concentrations in the Bay water column, and boundary conditions at the Pacific Ocean and Delta. Descriptions of the inputs to ECO Lab are provided in Section 2.1.2.1.

As described in Section 2.1.1, a 200-meter resolution bathymetric grid that was used in the development and calibration of a previous Bay model was revised to meet the needs of the BPP copper modeling. Verification of water quality modeling using the revised bathymetry is described further in Section 2.1.2.2.

2.1.2.1 Inputs

This section describes the inputs to the ECO Lab Heavy Metal module. For a summary of the inputs and for values used in the ECO Lab Heavy Metal module, see Table 5.

Initial Concentrations in the Bay Water Column

The initial concentrations of dissolved copper, adsorbed copper, and suspended sediment in the water column were arbitrarily set to the initial concentrations used in the calibration of the previous Bay model (URS 2003). The initial concentrations were not considered to be critical to the performance of the model after the first several days of the simulation because the physical processes dictate the concentrations.

Initial Concentrations in the Benthic Sediment

The initial dissolved copper concentration, adsorbed copper concentration, and sediment thickness were set to the initial conditions used in the calibration of the previous Bay model

(URS 2003). Toxic hotspots identified by the Bay Protection and Toxic Cleanup Program were overlain on existing sediment fields (SFBRWQCB 1999). Each hotspot was assigned to a single grid cell representing the location of the sample. Sensitivity of the model results to these initial conditions was investigated in this study and is described in Section 4.3.

Boundary Conditions

The concentrations of dissolved copper, adsorbed copper, and suspended sediment at the Pacific Ocean boundary were set to the concentrations used in the calibration of the previous Bay model (URS 2003). Distribution coefficients for the Pacific Ocean boundary were derived from the average of all measurements from the Regional Monitoring Program (RMP) monitoring station outside of the Bay (Golden Gate station, SFEI 1994–1999). Dissolved and adsorbed copper concentrations were then calculated from the relationship between the distribution coefficient and the dissolved, adsorbed, and total copper concentrations in the water column measured in the northern Pacific Ocean (Burton and Statham 1990). The input concentrations for the Pacific Ocean boundary were constant in time.

The same methods used in the previous Bay model (URS 2003) for calculating the concentrations of dissolved copper, adsorbed copper, and suspended sediment at the Delta boundary were used for this study. Suspended sediment concentrations (SSCs) measured at the USGS Mallard Island station were used to estimate the SSCs at the Delta boundary. Measured suspended sediment data were available from 2/9/1994 through 9/30/2004. The arithmetic mean of concentrations measured by sensors installed at the top and bottom of the water column at the Mallard Island station was taken as the depth-averaged value. For this study, 3-hour averages of the 15-minute data were applied at the Delta boundary. The previously determined relationship between daily Delta outflow and sediment inflow was used to calculate SSCs outside the period of measured data (DWR IEP 2007). The SSCs ranged from 9 to 400 milligrams per liter (mg/L).

Distribution coefficients and metal concentrations on suspended sediment for the Delta boundary were derived from the average of all measurements from the San Joaquin and Sacramento RMP monitoring stations for 1993–1998 (SFEI 1994–1999).

Based on the average concentration of copper adsorbed on the sediment of 60 milligrams per kilogram (mg/kg) and the average distribution coefficient of 35,738 liters/kilogram, the concentration of dissolved copper in the water column was calculated to be 1.7 micrograms per liter (µg/L). The adsorbed metal concentration in the water column was then calculated from the time-series of suspended sediment using the following equation:

$$AMW = \frac{(AMS \times SSC)}{10^3}$$

where:

AMW = the adsorbed metal concentration in the water (µg_{Cu}/L_{water})

AMS = the adsorbed metal concentration on the sediment (mg_{Cu}/kg_{sediment})

SSC = the suspended sediment concentration (mg_{sediment}/L_{water})

The adsorbed copper concentrations in the water at the Delta boundary ranged from 0.6 to 24 µg/L.

Tributary Sources

The BPP-supplied watershed model provided mean daily flow, total copper, dissolved copper, and SSCs for each watershed and for each of the modeled scenarios (AQUA TERRA 2007). The tributary inputs for the Mid scenario differed from those for the Mid-No-BP scenario. For input into ECO Lab, the adsorbed copper concentration in the water was calculated as the difference between the total and dissolved copper concentrations.

As described in Section 2.1.1.1, the watersheds defined in the watershed model differed from those in the Bay model. However, because most of the catchments lay within one of the 22 subwatersheds, the concentration data for each subwatershed were directly used for each of their corresponding catchments. Table 2 shows the corresponding subwatershed for each catchment. For catchments not included in any of the subwatersheds used in the watershed model, concentrations from the subwatershed closest to the catchment of interest were used. These catchment/subwatershed pairings are identified in Table 2. For subwatersheds without a corresponding catchment entry point, concentrations for each of these subwatersheds were added to the catchment entry point closest to the approximated Bay connection point, as identified in Table 2.

Publicly Owned Treatment Work and Industrial Point Sources

A total of 36 industrial and wastewater treatment plant sources were included in the Bay model. These sources are listed in Table 3 and locations are shown on Figure 4. Daily average concentrations were input when electronic data were available; otherwise, monthly averages based on 1996 and 1997 NPDES self-monitoring were applied to the entire simulation period. Metals were conservatively assumed to be in the dissolved state since SSCs were generally low.

Marina Inputs

The locations and annual copper release rates of 90 marinas and five county point sources were provided by a BPP-supplied copper release study (Rosselot 2006). The marinas and counties are listed in Table 4 and locations are shown on Figure 4. As described in Section 2.1.1.1, the copper released from marinas includes copper from pressure-treated wood used in marine construction and copper released from antifouling coatings used on boats. Using the representative marina volume determined for the daily flow rate (see Section 2.1.1.1), the annual mass of copper released at each marina was converted into a constant mean daily concentration for input into ECO Lab. The resulting concentration input for each marina is shown in Table 4.

Air Deposition

Wet and dry deposition inputs were derived from the deposition rates determined by the BPP study's air deposition model (Atmospheric and Environmental Research 2007). This model described the atmospheric deposition of copper resulting from BPWD released into the air. Daily rainfall, which is described in Section 2.1.1.1, dictates whether the air deposition for a given day is in the form of wet deposition via rainfall or dry deposition. On days without rain, only dry deposition occurs; on days with rain, only wet deposition occurs.

Wet deposition is the contribution of copper from rainfall. The wet deposition rate was determined to be 0.85 microgram per square meter per day ($\mu\text{g}/\text{m}^2/\text{d}$). By dividing this rate by the rainfall depth for each day, the wet deposition rate was converted into a time series of daily dissolved copper concentration in rainfall for input into ECO Lab.

Dry deposition refers to particulate copper pollution from the atmosphere. The dry deposition rate was determined to be $0.81 \mu\text{g}/\text{m}^2/\text{d}$. Because ECO Lab required the dry deposition input to be in units of grams per grid cell per second ($\text{g}/\text{cell}/\text{s}$), this value was converted to the appropriate units depending on the location and area of the grid cell. Grid cells in the main 990-meter grid are $980,100 \text{ m}^2$, while grid cells in either of the two nested 330-meter grids are $108,900 \text{ m}^2$. As a result, the dry deposition input for grid cells in the main grid was $9.19 \times 10^{-6} \text{ g}/\text{cell}/\text{s}$, and the input for grid cells in the nested grids was $1.02 \times 10^{-6} \text{ g}/\text{cell}/\text{s}$.

The Mid-No-BP scenario does not include the contribution of copper from BPWD; therefore, the Bay model run for the Mid-No-BP scenario did not include air deposition of copper.

Adsorption and Desorption Coefficients for the Bay Water Column and Sediment Porewater

Adsorption and desorption are reverse reactions for the transition of a heavy metal between solute and solid phases. The forward reaction, from solute to solid, proceeds at a rate given by the adsorption rate constant. The reverse reaction, from solid to solute, proceeds at a rate given by the desorption rate constant. These reactions occur in both the water column and the water contained in the sediment layer, i.e., sediment porewater. Because the characteristics of particulate matter in the water column and sediment differ, the adsorption and desorption rate constants for each medium also differs.

The adsorption and desorption rate constants previously used were approximated based on site-specific data and laboratory studies conducted on samples collected in the Bay (URS 2003). In the previous model, one set of adsorption and desorption rate constants for the water column were used to calibrate the model for the wet season (December 1995 to April 1996), while another set was used to calibrate for the dry season (March 1997 to August 1997). The rate constants for the sediment porewater were the same for both seasons. For the BPP Bay model, the dry season parameters were applied throughout the simulation period to allow the model to run through both seasons. The effect of using a single value was checked in the verification process.

Sediment Characteristics and Parameters

The density of sediment porewater is the mass of water per volume of porewater. The previous model used a constant value of 1,030 kilograms per cubic meter (kg/m^3), which is equivalent to the density of seawater, for the whole Bay (URS 2003). This density was used in the Bay model for this study.

The density of dry sediment is the mass of dry sediment particles per volume of dry sediment particles. The previous model used a constant value of $2,500 \text{ kg}/\text{m}^3$ for the whole Bay (URS 2003). This density was used in the Bay model for this study.

The benthic sediment porosity is the fraction of bulk sediment mass comprised of water on a gravimetric basis. The previous model used a constant value of 0.8 for the whole Bay (URS 2003). This porosity was used in the Bay model for this study.

The diffusive boundary layer is a thin, stagnant layer of water at the water/sediment interface. It is through this layer that the direct exchange of dissolved copper between the water column and sediment porewater occurs. The previous model used a constant boundary layer thickness of 0.1 millimeter for the whole Bay (URS 2003). This thickness was used in the Bay model for this study.

The diffusion coefficient helps describe the flux rate of dissolved metal between the water column and sediment porewater through the diffusive boundary layer. The previous model used a constant diffusion coefficient of $6 \times 10^{-10} \text{ m}^2/\text{s}$ for the whole Bay (URS 2003). This coefficient was used in the Bay model for this study.

Suspended sediment is affected by a sedimentation process, which is described by a settling velocity. The settling velocity varies spatially throughout the Bay with the smallest values in the mudflats near the Dumbarton Bridge and the highest values in the deep water at the Golden Gate. Wet season and dry season velocities are the same. The settling velocities were determined during calibration of the previous model (URS 2003).

The rate at which settled sediment becomes resuspended in the water column varies spatially throughout the Bay with the lowest values near the Golden Gate and highest values in the mudflats of San Pablo, Suisun, and Honker bays. Because the Bay is dominated by high winds and fetch during the dry season, dry season resuspension rates are generally greater than wet season resuspension rates. The resuspension rates were determined during calibration of the previous model (URS 2003). For this study, dry season values were applied throughout the entire simulation period because they provided a better fit to the measured dissolved copper concentrations than the wet season values. Also, because the dry season values produced satisfactory results, it was unnecessary to specify resuspension rates weighted by the duration of wet and dry periods.

Suspended matter can be produced in the water column by biological primary production. The rate of particle production is described by a coefficient that is constant in time. The previous model used a constant particle production rate of $0.1 \text{ g/m}^2/\text{day}$ for the whole Bay (URS 2003). This coefficient was used in the Bay model for this study.

Sediments can be resuspended when the current speed exceeds a critical value. The critical velocity for resuspension of sediment varies spatially throughout the Bay with the lowest values in the mudflats south of the Dumbarton Bridge and highest values near the Golden Gate. In the previous model, wet season and dry season velocities were the same except near the Golden Gate, where wet season values were approximately 10 to 15 percent lower than during the dry season. The critical velocities were determined during calibration of the previous model (URS 2003). For the BPP Bay model, dry season values were applied throughout the entire simulation period.

Forcings

Forcing functions express the dependence of adsorption and desorption on various water and sediment characteristics: pH, reduction-oxidation (redox) potential, salinity, and temperature. ECO Lab uses these inputs, which may be constant in time and space or variable in both time and space, and calculates a factor that adjusts the adsorption and desorption rates.

The previous model incorporated temperature and salinity dependencies (URS 2003). Both the temperature and salinity input data were temporally and spatially variable and were available for only the calibration time periods. Due to the limited amount of time available to locate and process additional temperature and salinity data for the entire simulation period, this study investigated the sensitivity of dissolved copper to forcing functions to determine the necessity of these forcing functions. This sensitivity analysis is described further in Section 4.4. From this analysis, it was determined that the dependence of dissolved copper on temperature and salinity

was not significant enough to warrant using forcing functions in the Bay model. Also, as shown on Figure 15, a comparison of the two model runs—where one included both temperature and salinity forcing functions and the other included neither—against measured data at selected sites showed that the run without forcing functions generally agreed with the measured data better than the run with forcing functions. Furthermore, verification of the model demonstrated that the model without forcing functions was able to provide a good estimate of dissolved copper concentrations. Verification is described in the following section.

2.1.2.2 Verification of Heavy Metal with Coarser Grid

As described in Section 2.1.1, a 200-meter resolution bathymetric grid used in the development and calibration of a previous Bay model was revised to meet the needs of the BPP copper modeling. The revised model bathymetry is shown on Figure 2. Input data for the revised grid were created using the same data as the previous model. To verify that the heavy metal model based on the revised grid was performing adequately, the predicted dissolved copper concentrations were compared to measured data from selected RMP stations located throughout the Bay and City of San Jose monitoring stations in the South Bay (Shafer, pers. comm., 2007; SFEI 2007). Figure 16 shows the locations of the water quality stations used in the heavy metal model verification. The previous model was calibrated to dissolved copper concentrations measured during the 1996 wet season (December 1995 to April 1996) and the 1997 dry season (March 1997 to August 1997) (URS 2003). To capture both these time periods, the model based on the revised bathymetry ran from December 1995 to August 1997 using the 1997 dry season calibration parameters from the previous model. The output from this run was used to verify that the model was reproducing dissolved copper concentrations. Because copper toxicity in the aquatic environment is due to the dissolved fraction rather than total copper, and because regulatory water quality objectives are based on dissolved copper, this study focuses only on the dissolved fraction of copper.

The comparisons of measured and predicted dissolved copper concentrations are shown on Figure 17, starting at the Delta (San Joaquin River RMP station shown on Figure 17a) and moving southward to the Lower South Bay (San Jose station SB05 shown on Figure 17w). The predicted results using the coarser grids are generally within the range of the measured data. However, several noticeable and consistent discrepancies exist between the predicted and measured data. Predicted data for several North Bay stations did not capture the relatively low concentrations measured in April 1996 (Figures 17c through 17f). Also, predicted data for Lower South Bay stations tend to disagree with the measured data from the City of San Jose in February and March 1997, which were lower than predicted (Figures 17s through 17v). Since the model output represents depth-averaged concentrations, it is less likely to match the measured data if the measured concentration varies significantly with depth. Water samples were collected just below the water surface by the RMP at varying tide levels and at depths varying between approximately 1 to 2 feet, adding to the difficulty of predicting actual conditions (AMS 2001). Also, the model output represents concentrations within grid cells that are hundreds of meters on each side, whereas the measured data represent one point in space. Other reasons for the differences between measured and predicted values include the inaccuracy of the model and the lab variability. Given the above considerations, overall, the model output from the coarse grid provides a good estimate of the dissolved copper concentrations throughout the Bay. For a discussion of uncertainty and sensitivity, see Section 4.

2.1.2.3 Verification of Suspended Sediment

The previous heavy metal model of the Bay that used a 200-meter resolution bathymetric grid was calibrated for SSC during a dry season period and a wet season period. An example of the previous Bay model calibration results are shown on Figure 18 for the wet season period from January 1, 1997, through May 1, 1997 (URS 2003). The SSCs are shown as 4-day running averages to be comparable to 4-day average dissolved copper concentrations, as stipulated in the Cal Toxics regulatory guidance (URS 2003). The example plot is shown for a site in the North Bay at Point San Pablo. The observed SSCs were based on a sensor located near the surface of the water column. In general, the previous model showed less variability than the measured data and tended to underestimate the peak SSCs.

An example of the SSC output from the BPP copper model that uses a 990-meter grid for the whole Bay and nested 330-meter grids in the South Bay and at Carquinez Strait is shown for the same wet season period at the Dumbarton Bridge station on Figure 19. Once again, the observed SSCs were from a sensor near the surface. This plot shows that the model both under- and overpredicts the SSC, with more of a tendency to underpredict the concentration. Less variability occurs in the modeled output than in the measured SSCs. The highest modeled values near Dumbarton Bridge are almost as high as some of the measured peak values, although they are not occurring at the same time.

As discussed in the previous Bay model study, the lack of a wind-based forcing function in the sediment module for MIKE 21 ME (and, equivalently, ECO Lab) is a limitation of the model and is especially important during low spring tides where wind-induced resuspension in shallow water can cause substantial increases in suspended sediment that are not captured by the model. By not including wind as a forcing function, underprediction of short-term variations in suspended sediment can result and may also result in an overprediction of sediment deposition. The results of the BPP copper model showed that rather than having the Bay as a whole in quasi-equilibrium as might be expected, the model consistently predicted greater deposition than erosion, with a net increase of approximately 3 centimeters per year. However, the intended results of both the previous model and the BPP Bay model are predicted 4-day average dissolved copper concentrations. The results of the suspended sediment and sediment deposition rates are never used directly in the assessment of changes in dissolved copper due to BPWD.

2.2 MODELED SCENARIOS

Two scenarios were modeled for a 40-year simulation period from WYs 1981 to 2020 (October 1, 1980, to September 30, 2020). Initially, it was requested that the Bay model run for a 20-year simulation period, from WYs 1981 to 2000. After a preliminary review of the results from the first 20 years, the BPP Steering Committee requested to run the simulation for an additional 20 years through WY 2020. Time-varying input data, such as precipitation, wind, point sources, and the BPP-supplied tributary sources, for the first 20 years were repeated for the last 20 years. That is, the input data for the simulation from WYs 2001 to 2020 mirror the input data for the simulation from WYs 1981 to 2000. However, the initial copper conditions for WY 2001 were set to the conditions at the end of WY 2000.

The mid-level (Mid) scenario represents baseline copper conditions using estimated BPWD contributions to the Bay. The other scenario represents copper conditions without BPWD

contributions (Mid-No-BP). To reiterate the model input descriptions in Section 2.1, the Bay model inputs for the Mid and Mid-No-BP scenarios differ in two major ways. First, each scenario had a unique set of tributary inputs as provided by the watershed model (AQUA TERRA 2007). Second, the Mid scenario included air deposition inputs from the BPP-supplied air deposition model, whereas the Mid-No-BP scenario did not include any air deposition. By modeling scenarios with and without the contributions of copper from the BPWD, the effects of BPWD on the dissolved and benthic copper concentrations in the Bay can be determined.

The BPP and the watershed model study also investigated low-level (with and without BPWD) and high-level (with and without BPWD) scenarios. The low-level scenario represented the midpoint fluxes minus one standard deviation of the estimate for all BPWD sources, and plus one standard deviation for all non-BPWD sources. The high-level scenario represented the midpoint fluxes plus one standard deviation of the estimate for all BPWD sources, and minus one standard deviation for all non-BPWD sources. The results of the watershed model showed that even though some spatial variability in copper loads occurs between scenarios, the total copper loads to the Bay did not vary significantly between each level of contributions (AQUA TERRA 2007). Modeling the Mid and Mid-No-BP scenarios shows how sensitive the Bay model is to changes in copper loads. Due to computer processing time constraints, Bay model runs of the low- and high-level scenarios were not included in this study. As differences were apparent between the Mid and Mid-No-BP scenarios, the BPP may choose to run the low- and high-level scenarios in future studies.

3.1 RESULTS OF MODELED SCENARIOS

For presentation in this report, dissolved copper concentrations are shown as 4-day averages and benthic copper concentrations are shown as 30-day averages. Results are based on hourly output from the model. The dissolved copper concentrations were averaged every 4 days to be consistent with the chronic site-specific objective for dissolved copper in the Lower South San Francisco Bay of 6.9 µg/L, which is based on a 4-day average (SFBRWQCB 2007). Because benthic copper concentrations change very gradually, the 30-day averages were shown. A comparison of the hourly concentrations and their averaged counterparts at Redwood Creek from February through May 2006 is shown on Figure 20. The frequent fluctuations in the dissolved copper concentrations are smoothed by averaging the data (Figure 20a). For benthic copper (Figure 20b), the averaged concentrations are not significantly different from the hourly concentrations, which already form a smooth curve.

To limit the amount of model output to be analyzed, the ECO Lab output was saved every hour for the months of February and September for each year of the simulation. These months were selected to represent wet season and dry seasons, respectively. ECO Lab and MIKE 21 HD output was saved for a selection of 10 transects throughout the Bay every hour for the entire simulation period. Most of the transects extend linearly from the western shoreline to the eastern shoreline, but the Golden Gate and San Pablo Bay transects extend from the northern shoreline to the southern shoreline. A grid cell along each transect represents a site that is approximately the same as one of the deep channel RMP water quality stations shown on Figure 16. The sites that are outside the channel in mudflats are also depicted on Figure 16. These sites were selected to provide a basis for comparison against RMP measured data, as well as to show differences between in-channel and mudflat results. The sites, starting in the North Bay and moving towards the Lower South Bay, are:

- San Pablo Bay
- Golden Gate
- Bay Bridge/Yerba Buena Island
- Alameda
- Oyster Point
- San Bruno Shoal (in the deep channel and in the mudflats along the eastern shoreline)
- Redwood Creek
- Dumbarton Bridge
- South Bay
- Coyote Creek (in the deep channel and in the mudflats along the western shoreline)

The model results are discussed in Section 3.2.

3.2 DISCUSSION OF RESULTS

The model results for dissolved and benthic copper concentrations are shown on Figures 21 and 22, respectively. The results for the Mid and Mid-No-BP scenarios are shown in the upper half of each page, and the differences between the scenarios (Mid minus Mid-No-BP) are shown in the lower half. The resulting concentrations shown in the upper half of each page are plotted on a different scale than the scenario differences shown in the lower half of each page. Different scales were used so that the variation in differences would be more apparent. Dissolved copper results are discussed in Section 3.2.1 and benthic copper results are discussed in Section 3.2.2.

3.2.1 Dissolved Copper in the Bay Water Column

The results of the 40-year simulation provided on Figure 21 show a seasonally fluctuating, yet otherwise fairly constant, level of dissolved copper in the Bay. Overall, the concentrations and differences appear to be trending upwards, suggesting an increasing influence of BPWD to dissolved copper in the Bay. However, this upward trend is very slight and could be an effect of variations in annual runoff amounts rather than the behavior of BPWD-related copper in the Bay. The differences in concentration between the Mid and Mid-No-BP scenarios are primarily attributed to the different tributary loads.

The results show that when BPWD sources of copper are removed, dissolved copper in the Bay decreases. The differences between the Mid and Mid-No-BP dissolved copper results (i.e., Mid results minus Mid-No-BP results) shown on Figure 21 are nearly always positive. The range of differences tends to increase moving from the North Bay towards the Lower South Bay. It appears that the greater the concentration, the greater the difference between the Mid and Mid-No-BP scenarios. Likewise, during times when concentrations are lowest, the difference between the scenarios is zero or close to zero. As shown in each pair of concentration and difference plots on Figure 21, the fluctuating pattern in the difference plots mirrors the seasonal pattern of the concentrations. These results indicate that, from a spatial perspective, copper contribution of BPWD is highest in the Lower South Bay. From a temporal perspective, copper contribution from BPWD is highest during the wet season. The dissolved copper concentrations peak during storm events. These periods also show the largest differences between the Mid and Mid-No-BP scenarios, which implies that the contribution from BPWD is highest during storm events. Essentially the only contribution from BPWD during the dry season is from air deposition.

Table 6 provides a summary of the contribution of BPWD to copper concentrations in the Bay during the wet season and across the entire water year. Over the course of a year, BPWD contributes less than 1 percent to the dissolved copper concentrations at the North Bay sites, while BPWD contributions are approximately 6 percent in the South Bay and 9 percent in the Lower South Bay. During the wet season, BPWD contributes less than 1 percent to the dissolved copper concentrations at the North Bay sites, while BPWD contributions have an upper range of 10 percent in the South Bay and 14 percent in the Lower South Bay. The results in Table 6 reflect the spatial and temporal patterns described above, that is, the contribution of BPWD to copper concentration in the Bay tends to be highest in the Lower South Bay and lowest in the North Bay. Also, the contribution of BPWD is highest during the wet season. The large ranges (25th to 75th percentile) in BPWD contributions in the Lower South Bay sites are indicative of the high variability in dissolved copper concentrations that are modeled in the Lower South Bay.

The cumulative probability plots on Figure 23 present the model results over the entire 40-year simulation period without time dependence. An accompanying table, Table 7, summarizes minimum and maximum 4-day average dissolved copper concentrations as well as the concentrations representing the 50 and 90 percent probabilities for both modeled scenarios at each site. For a discrete random variable X , a cumulative probability function (or cumulative distribution function) F is given by:

$$F(x_i) = p(X \leq x_i)$$

Where, for this study:

- F = the cumulative probability function
- x_i = the 4-day average dissolved copper concentration for which the probability function is being calculated (e.g., $F(1.5)$ calculates the probability that X is less than or equal to 1.5 $\mu\text{g/L}$)
- X = the actual 4-day average dissolved copper concentration given by the model results

The cumulative probability plots indicate the same conclusions as above. The differences in dissolved copper concentrations between the Mid and Mid-No-BP scenarios are almost unnoticeable in the North Bay and much more pronounced in the South and Lower South bays. Also, the differences are greater when concentrations are higher, and almost nonexistent when the concentrations are lowest.

Figure 24 shows the cumulative probabilities of the differences between the Mid and Mid-No-BP dissolved copper results at Coyote Creek (in the channel), which is representative of the cumulative probability distribution in the Lower South Bay. Small differences under 0.1 $\mu\text{g/L}$ occur approximately half of the simulation period, whereas differences that exceed 0.1 $\mu\text{g/L}$ are more variable and can reach up to 1.4 $\mu\text{g/L}$.

3.2.2 Benthic Copper in the Bay Sediments

The results of the 40-year simulation show that for the selected points, in general, the benthic copper concentrations increased from the initial concentration. Benthic copper concentrations at San Bruno Shoal (in the eastern mudflats) (Figure 22g) and Redwood Creek (Figure 22h) remained relatively constant. Significant decreases occurred at the San Pablo Bay site (Figure 22a), the Bay Bridge site (Figure 22c), and the Coyote Creek site (in the western mudflats) (Figure 22i). The time it takes to start reaching equilibrium generally ranges from about 3 to 10 years. Most of the sites established equilibrium within the 40-year simulation period, but some, such as Dumbarton Bridge (Figure 22i), still showed trends by the end of the simulation.

As with dissolved copper, the results for benthic copper confirm that when BPWD sources of copper are removed, benthic copper in the Bay decreases. The difference between the Mid and Mid-No-BP dissolved copper results (i.e., Mid results minus Mid-No-BP results) shown on Figure 22 are nearly always positive. The differences between the Mid and Mid-No BP scenarios are trending upwards over time, which suggests that the Bay sediment requires long timescales (e.g., decades) to reach equilibrium with copper inputs. Also, the differences tend to increase from the North Bay to the Lower South Bay. Like the differences between scenarios for dissolved copper, the differences for benthic copper increase with concentration. The differences

in concentration between the Mid and Mid-No-BP scenarios are primarily attributed to the different tributary loads.

Tables 8 and 9 show how the average benthic copper concentrations at a given location change over the 40-year simulation period. The concentrations shown in Table 8 are the results at a single grid cell representing a given site, whereas the concentrations in Table 9 are averages of all the grid cells within the specified subsection. It is useful to present the benthic copper results in both ways because the concentrations at a specific site (one grid cell) are not representative of the subsection of the Bay in which it is located. For example, Table 8 and Figure 22j show that the benthic copper concentration at the South Bay site increased from 52 to 90 mg/kg after 40 years. Conversely, as shown in Table 9, the subsection of the Bay in which the South Bay site is located (between Dumbarton Bridge and the southern tip of the Bay) is decreasing in benthic copper, from 52 to 29 mg/kg.

These differences in benthic copper from site to site within a subsection of the Bay are also evident when comparing the channel and mudflat results for San Bruno Shoal and Coyote Creek. At San Bruno Shoal (Table 8, Figures 22f and 22g), the channel site experiences a significant increase in benthic copper, while benthic copper concentrations at the mudflat site appear to be stable. Overall, Table 9 shows that benthic copper concentrations in this subsection of the Bay, from the Bay Bridge to the Dumbarton Bridge, are increasing, though not as dramatically as at the San Bruno Shoal channel site. At Coyote Creek (Table 8, Figures 22k and 22l), benthic copper at the channel site increases, then equilibrates near 80 mg/kg, but at the mudflat site, it decreases, then equilibrates near 20 mg/kg. Table 9 shows that benthic copper concentrations in the Lower South Bay, below Dumbarton Bridge, initially decrease, then equilibrate near 30 mg/kg. Benthic copper concentrations are clearly different depending not only on the subsection of the Bay, but also along each transect of the Bay.

During the last 30 years of the simulations, the grid-averaged benthic copper concentrations for subsections of the Bay increase except for the Lower South Bay, below the Dumbarton Bridge. The northernmost subsections exhibit significant increases and are generally 50 mg/kg or greater, while the two subsections below San Bruno Shoal show benthic copper concentrations at or near equilibrium and are less than 50 mg/kg. The Lower South Bay dropped to the lowest benthic copper concentrations and equilibrated relatively quickly, reaching 30 mg/kg after the first 10 years of the simulation. In terms of the differences in results between the Mid and Mid-No-BP scenarios, the differences (i.e., the contribution of BPWD to benthic copper concentrations) increase in all subsections of the Bay. Furthermore, the differences are greatest in the South and Lower South bays. In these southernmost subsections, the differences reach up to 3.5 percent after 40 years of simulation.

3.2.3 Mass Balance

The results from the Mid scenario were used to gain perspective on how seasonal and annual copper loadings contribute to the overall balance of copper in the Bay. The variability in annual copper loads from the tributary runoff (excluding flows entering the Bay from the Delta) is shown on Figure 25. These are the same loads used as input to the model between 1981 and 2000 and repeated for the next 20 years between 2001 and 2020. The loads were based on output provided from the BPP-supplied watershed model for the Mid scenario and are also shown in

Table 10 from 1981 to 2005. The total copper loads varied between approximately 18,000 kg and 100,000 kg with an average of 47,000 kg.

As described in more detail below, the various components contributing to the overall mass of copper in the Bay were inventoried on an annual basis for several years covering a range of copper loads from runoff. The tributary loads for the selected years ranged from approximately 20,000 kg (for modeled WY 2010, based on loads from WY 1990) to 93,000 kg (for modeled WY 2018, based on loads from WY 1998). The mass of copper in the Lower South Bay was also inventoried for a period consisting mainly of the dry season of 1997.

Figure 26 shows the copper inventory based on model output for the Lower South Bay from February through September 1997. This period generally had low Delta outflow, rainfall, and runoff loads, as is typical for the dry season. The largest component of the copper inventory is the 2,600,000 kg in the sediment, which is 99.96 percent of the total copper in the system. The contributions of copper from watershed runoff, wastewater discharge, marinas, and air deposition totaled approximately 1,800 kg. The net mass of copper leaving the Lower South Bay past the Dumbarton Bridge totaled 7,700 kg, leading to removal of approximately 6,000 kg of copper from the Lower South Bay during the dry season. The model results actually showed an increase in the mass of copper in the bed during this period. However, since the mass of copper in the bed sediment is so much larger than any of the other components in the inventory, an error in the initial or final values of less than 1 percent would be enough to account for this difference. A large percentage of the Lower South Bay includes mudflats that regularly go dry. The wetting and drying typically leads to small errors in sedimentation calculations, which could explain the discrepancy in the copper mass balance. A likely source of the net export of copper is the suspension and transport of bed particulate copper out of the Lower South Bay during the dry season. This explanation is supported by an observed decrease of 0.11 mg copper /kg in the benthic sediment during this period. This decrease accounts for the net export.

Figure 27 shows the copper inventory of the entire Bay out to the Golden Gate Bridge during WY 1999 (from September 1998 through September 1999). This period had a total copper load from tributaries of 36,000 kg, which is slightly below the calculated average annual tributary load of 47,000 kg. The contributions of copper from Delta outflow totaled 110,000 kg. The contributions of copper from other watershed runoff, wastewater discharge, marinas, and air deposition totaled approximately 76,000 kg. Of the 76,000 kg, 8,750 kg are due to brake pad sources. The net mass of copper leaving the Bay past the Golden Gate Bridge totaled 170,000 kg leading to a net gain in the mass of copper in the Bay of 13,000 kg. Since the mass of copper in the bed is over 4 orders of magnitude larger, a difference of 13,000 kg is relatively small. It would appear that the entire Bay was essentially neither gaining nor losing copper during WY 1999.

Similar inventories are provided on Figures 28 through 30. Figure 28 is for WY 2010, which had the minimum annual load from tributary runoff of the years selected for the inventories. For this year, the model showed a net export of copper in the Bay of approximately 43,000 kg. This is consistent with the expectation that during periods with minimal amounts of runoff and minimal associated copper loads, copper would tend to be exported from the Bay.

This compares to Figure 29, which had the maximum annual load from tributary runoff of the years selected for the inventories. For WY 2018, the model showed a net accumulation of copper in the Bay of approximately 170,000 kg. This is consistent with the expectation that during

periods with large amounts of runoff and large associated copper loads, copper would tend to build up in the Bay.

Figure 30 shows the inventory for WY 2020, which had an annual tributary load of 43,000 kg, which is close to the calculated annual average. This year resulted in a net accumulation of approximately 48,000 kg.

In general, the model tends to calculate an accumulation of copper. As mentioned in Section 2.1.2.3, the model calculated an overall annual increase in deposition of 3 centimeters per year. This value is fairly large in part due to the fact that the model treats the sediment bed as a single layer and does not include any consolidation or changes to bathymetry based on the amount of deposition. This may lead to an underprediction in the effect that removing copper from brake pads may have on lowering the dissolved copper concentrations in the Bay because as cleaner sediment is deposited on the bed, the model mixes it with the entire reservoir of deposited sediment instead of burying the underlying sediment. Since the bed sediment makes up such a large percentage of the total mass of copper in the Bay, this has the effect of significantly increasing the residence time of copper in the Bay and increasing the amount of time it would take to see a beneficial change in the concentrations of dissolved copper when input sources of copper are removed.

The quality of the model results depends on the quality of the inputs. In a previous modeling study of copper in the Bay, the sensitivity of the dissolved copper concentration to a variety of input parameters was analyzed (Bessinger et al. 2006; URS 2003). In this study, additional model runs were performed to analyze the sensitivity of dissolved and benthic copper concentrations to copper loads, initial benthic copper conditions, and temperature and salinity forcings. A discussion of the uncertainty in determining the effect of BPWD on copper levels in the Bay is also provided.

4.1 PREVIOUS SENSITIVITY ANALYSES

Sensitivity analyses on the previous Bay model were conducted for seven input parameters: tributary copper concentration, Delta copper concentration, Pacific Ocean copper concentration, benthic sediment copper concentration, adsorption rate constant, benthic diffusion coefficient, and sediment settling velocity (Bessinger et al. 2006, URS 2003). Sensitivity runs were performed to model simulations with upper and lower bounded estimates of the variability that could occur in the Bay over a 4-day averaging period. The results of the sensitivity analyses indicate that the magnitude of tributary source loads affects predicted dissolved copper concentrations. The effects are greater during the wet season, when tributary sources are a larger fraction of the total mass of copper introduced to the water column.

Another source of uncertainty in the model is the adsorption and desorption rate constants selected during calibration. Initial estimates were based on a single experiment and are only valid for the set of chemical conditions present during the experiment. The greatest difference in predictions due to changes in rate constants would be near tributary sources and Bay segment boundaries.

Although the initial sediment porewater concentration does not greatly affect the predicted dissolved concentration, porewater concentrations can affect the predicted importance of sorption processes. Assuming that porewater copper concentrations are approximately equal to water column concentrations over long time periods, and assuming copper partitioning is predominantly governed by an equilibrium distribution coefficient, the importance of desorption would be greater than predicted by the model. This greater importance is because a smaller (or negative) diffusive flux would require more copper desorption from suspended sediment to maintain equilibrium.

4.2 SENSITIVITY TO COPPER LOADS

To analyze the sensitivity of copper concentrations in the Bay to copper loads, the dissolved and adsorbed copper in all the Delta, POTW, industrial, tributary, marina, and air deposition inputs were removed. The SSCs for these sources remained the same. The sensitivity run was performed only for the baseline (Mid) scenario. Final conditions at the end of WY 1990 from the Mid scenario results were used to initialize this sensitivity run because benthic copper conditions appeared to be closer to equilibrium by this time. (See Section 3.2.2 for benthic copper results.) The simulation period for this sensitivity run was from WY 1991 through WY 1992, as this length of time was considered sufficient for the analysis.

Figure 31 shows the comparison of the sensitivity run against the Mid scenario results for dissolved copper at selected locations throughout the Bay. Figure 31 also shows the difference

between the two runs (i.e., Mid results minus sensitivity results). In general, the sensitivity run concentrations are usually lower than the Mid scenario concentrations because of the lack of external copper sources. The sensitivity results in San Pablo Bay (Figure 31a) are more uniform and less variable with the external sources removed compared to the baseline results. In the South Bay (Figures 31b through 31f), the results clearly show that the change in copper loads has an effect on the dissolved copper concentrations in the South Bay, especially during the wet season when runoff carries more BPWD to the Bay. These differences increase moving from the North Bay towards the Lower South Bay. This increase may be due to the larger ratio of watershed area to Bay area as one proceeds south along the Bay.

Figure 32 compares the results and the differences between the two runs for benthic copper at Coyote Creek, where the differences were greatest. Benthic copper concentrations at sites selected for the analysis decreased by less than 1 mg/kg over the modeled years due to removing the copper loads. The differences are very small compared to the benthic copper concentrations of approximately 20 mg/kg to over 100 mg/kg for selected sites in the Bay. These results show that benthic copper concentrations are not sensitive to copper loads over the relatively short time scale used in this sensitivity analysis.

The low- and high-level scenarios briefly described in Section 2.2 were modeled as part of the BPP watershed modeling study. The results of these modeled scenarios provided reasonable lower and upper limits of the uncertainty in the tributary loads (AQUA TERRA 2007). This uncertainty, as well as any other uncertainty inherent in the watershed model, is carried over to the Bay model results. Because these low- and high-level scenarios were not modeled for this Bay modeling study, the uncertainty in dissolved copper concentrations due to the uncertainty in the tributary loads cannot be quantified. Similarly, uncertainty in atmospheric copper loads estimated by the air deposition model (Atmospheric and Environmental Research 2007) will affect the Bay model results, as well.

4.3 SENSITIVITY TO INITIAL BENTHIC COPPER CONDITIONS

To analyze the sensitivity of the predicted copper contribution of BPWD (i.e., Mid scenario results minus Mid-No-BP scenario results) to initial benthic copper conditions, final conditions at the end of WY 2000 from the Mid scenario results were used to initialize the sensitivity run for the Mid scenario. For the Mid-No-BP scenario, final conditions at the end of WY 2000 for the Mid-No-BP scenario were used. The output from WY 2000 showed that the benthic copper concentrations were at or were approaching equilibrium (see Section 3.2.2 for benthic copper results). Except for sites at San Pablo Bay, Bay Bridge, San Bruno Shoal (in the eastern mudflats), Redwood Creek, and Coyote Creek (in the western mudflats), the benthic copper concentration in the majority of the Bay sites increased. The simulation period for these sensitivity runs was from WYs 1980 to 1982, which was considered a sufficient length of time to observe the effect of the different initial benthic copper conditions on copper concentrations.

Figure 33 compares the scenario differences (Mid minus Mid-No-BP) resulting from the sensitivity run against those of the BPP modeled, or “production,” runs for dissolved copper at selected locations throughout the Bay. Furthermore, Figure 33 also shows how much the scenario differences between the sensitivity and production runs differ (i.e., the scenario differences from the sensitivity run minus the scenario differences from the production run). These comparisons illustrate how sensitive the apparent contribution of BPWD to dissolved

copper in the Bay is to initial benthic copper conditions. It appears that by setting the initial benthic copper conditions to at or near equilibrium values, the model generally predicts a greater contribution of BPWD to dissolved copper in the Bay except for instances in the wet season at Coyote Creek (Figure 33f). The heightened sensitivity of dissolved copper to BPWD might be a result of the benthic sediment losing its buffering capacity, or ability to sequester copper loads from the water column, when benthic copper is at equilibrium. Figure 34 compares the scenario differences resulting from the sensitivity run against those of the production run for benthic copper. Overall, the scenario differences from the sensitivity run are greater than the scenario differences from the production run, indicating that the predicted BPWD contribution to benthic copper in the Bay sediment is higher when initial benthic copper conditions are at or approaching equilibrium values. However, the scenario differences resulting from the production run appear to be approaching the scenario differences from the sensitivity run over time. These similar results are likely due to the benthic concentrations remaining stable or increasing slightly over time when the model was initialized to equilibrated benthic concentrations. Although this analysis demonstrates that the model is sensitive to initial benthic conditions, the differences in the predicted contribution of BPWD are probably more attributable to the model approaching equilibrium rather than a direct affect of initial benthic copper. In the long term as benthic copper concentrations reach equilibrium, the differences are likely to be insignificant.

4.4 SENSITIVITY TO TEMPERATURE AND SALINITY FORCINGS

As described in Section 2.1.2.1, the temperature and salinity forcing functions are calculated by ECO Lab from spatially and temporally varying temperature and salinity forcing fields. These forcing functions adjust the adsorption and desorption rates depending on the temperature and salinity conditions at a given location and time step. To determine whether or not to include these forcings in the BPP Bay model, results from a run that included the forcings used in the earlier model were compared to results from a run that did not include temperature and salinity forcings. The simulation period for this analysis was limited to the 1996 wet season (December 1995 to April 1996), since the results from the earlier run that included the temperature and salinity field input files for this period were already available from the previous model. As shown on Figure 15, while the resulting dissolved copper concentrations differed, the differences between the two runs were relatively small. This analysis indicates that dissolved copper is not highly sensitive to temperature and salinity forcings over the range studied.

4.5 MODEL UNCERTAINTY AND LIMITATIONS

While it is possible to quantify the sensitivity of the modeled copper to specific model inputs, some aspects of the uncertainty in the model results are not easily quantified. These include uncertainty related to:

- 1) Contribution from BPWD in Delta loads;
- 2) Resolution of the bathymetry;
- 3) Quality and quantity of data available for calibration;
- 4) Use of a 2-D, depth-averaged model;
- 5) Lack of a robust sediment model.

For this study, the contribution from BPWD in the Delta copper loads was not determined. The results in Section 4.2 showed that the model is sensitive to the external sources of copper loads. The Delta loads are a significant source of copper to the Bay, and would presumably lead to decreased copper concentrations in the Bay if the copper contributions from BPWD were removed.

The resolution of the bathymetric grid affects the transport of copper through advection and dispersion. By having grids with 330-meter and 990-meter resolution, the ability to accurately model transport through smaller channels is reduced. Some of this uncertainty can be quantified during the process of calibration. However, this also depends on the quality and quantity of data available for calibration.

When more data are available for calibration, the accuracy of the modeled copper concentrations can be improved. Data available for calibration and verification of the Bay model are generally from a specific instant in time and at one particular depth. Without measurements that capture the variability in concentrations of suspended sediment and copper at different parts of the tide cycle and at different depths in the water column, it is difficult to know how to adjust the model input parameters to more accurately represent the conditions in the Bay. Having measurements collected at only one location in the channel instead of across an entire transect, as is typical of the measured data in the Bay, makes it difficult to know whether the copper loads are being accurately transported through various segments of the Bay. This leads to a certain level of uncertainty in the modeled copper concentrations.

Some of the limitations of using a 2-D rather than a 3-D model were discussed in Section 2.1.1. The 2-D model will not perform as well during periods of high Delta outflow and tributary runoff in portions of the Bay that become stratified. The transport of copper due to density-driven currents would be excluded. It is difficult to determine how this would affect the resulting copper concentrations and the apparent contribution from BPWD.

The ECO Lab Heavy Metal module has a fairly simplified sediment component. The bed sediment is modeled as one layer. Copper associated with sediment that is deposited on the bed is fully mixed with the underlying sediment. For the BPP Bay model, this probably results in a slower response to changes such as removing copper from BPWD in the external loading sources. Time constraints precluded creating and calibrating a more complex sediment model that would include additional processes, such as sediment compaction and wind-wave resuspension.

- Applied Marine Sciences (AMS). 2001. *Field Sampling Manual for the Regional Monitoring Program for Trace Substances*. February.
- AQUA TERRA Consultants. 2007. *Watershed Modeling of Copper Loads to San Francisco Bay Draft Report*. Mountain View, CA. June 21.
- Atmospheric and Environmental Research, Inc. 2007. *Air Deposition of Copper from Brake Pad Wear Debris Technical Memorandum*. San Ramon, CA. January 24.
- Bessinger, Brad, T. Cooke, B. Forman, V. Lee, P. Mineart, and L. Armstrong. 2006. A kinetic model of copper cycling in San Francisco Bay. *San Francisco Estuary and Watershed Science* 4 (1). February.
- Burton, J.D., and P.J. Statham. 1990. Trace metals in seawater. In *Heavy Metals in the Marine Environment*, R.W. Furness and P.S. Rainbow, eds., pp. 5-25. Boca Raton, FL: CRC Press.
- California Department of Water Resources (DWR). 1995. *Delta Atlas*.
- California Department of Water Resources, Interagency Ecological Program (DWR IEP). 2007. Daily Net Delta Outflow from Dayflow program. Data downloaded on August 27, 2007, from <http://iep.water.ca.gov/dayflow/output/index.html>.
- Cheng, R.T. and R.E. Smith. 1998. A nowcast model for tides and tidal currents in San Francisco Bay, California. *Ocean Community Conference '98, Proceedings*, Baltimore, MD, Marine Technology Society, Nov. 15-19, 1998, pp. 537-543.
- Fischer, H.B., E.J. List, R.C.Y. Koh, J. Imberger, and N.H. Brooks. 1979. *Mixing in Inland and Coastal Waters*. New York: Academic Press.
- Gross, E.S. 1998. Numerical modeling of hydrodynamics and scalar transport in an estuary. PhD dissertation, Stanford University, Stanford, CA.
- National Climatic Data Center (NCDC). 2007. Hourly wind direction and speed data at the San Francisco International Airport (SFO). Downloaded on August 24, 2007, from NCDC Climate Data Online, <http://cdo.ncdc.noaa.gov>.
- National Geodetic Survey. 1994. Program VERTCON (Vertical Conversion) Version 2.0. September.
- National Oceanic and Atmospheric Administration (NOAA). 2003. *Predicted Changes in Hydrodynamics, Sediment Transport, Water Quality, and Aquatic Biotic Communities Associated with SFO Runway Reconfiguration Alternatives BX-6, A3, and BX-R*. Independent peer review panel final report. November.
- National Oceanic and Atmospheric Administration/National Ocean Service (NOAA/NOS). 1999. Bathymetric data for San Francisco Bay, 7.5-inch (30-meter) quads. ARCINFO data file downloaded from <http://sposerver.nos.noaa.gov>.
- Rosselot, Kirstin S. Process Profiles. 2006. *Copper Released from Non-Brake Sources in the San Francisco Bay Area Final Report*. Calabasas, CA. January. Revised March 2007.
- San Francisco Bay Regional Water Quality Control Board (SFBRWQCB). 1999. Bay Protection and Toxic Cleanup Program. Final Regional Toxic Hot Spot Cleanup Plan. March.

- SFBRWQCB. 2007. *San Francisco Bay Basin (Region 2) Water Quality Control Plan*. Oakland, CA. January 18.
- San Francisco Estuary Institute (SFEI). 1994. *1993 Annual Report: San Francisco Estuary Regional Monitoring Program for Trace Substances*. Richmond, CA.
- SFEI. 1995. *1994 Annual Report: San Francisco Estuary Regional Monitoring Program for Trace Substances*. Richmond, CA.
- SFEI. 1996. *1995 Annual Report: San Francisco Estuary Regional Monitoring Program for Trace Substances*. Richmond, CA.
- SFEI. 1997. *1996 Annual Report: Regional Monitoring Program for Trace Substances*. Richmond, CA. December.
- SFEI. 1998. *1997 Annual Report: San Francisco Estuary Regional Monitoring Program for Trace Substances*. Richmond, CA.
- SFEI. 1999. *1998 Annual Report: San Francisco Estuary Regional Monitoring Program for Trace Substances*. Richmond, CA.
- SFEI. 2007. Regional Monitoring Program station locations. Downloaded on May 4, 2007, from SFEI website, <http://www.sfei.org/rmp/maps/2002-2005-WaterLatLongs.xls>.
- Shafer, Peter . 2007. City of San Jose South Bay Water Quality Data. Electronic communication with Terrence Cooke, URS Corp., February 1, 2007.
- Smith, R.E., and R.T. Cheng. 1994. *Defining intertidal bathymetry of the southern extreme of South San Francisco Bay*. U.S. Geological Survey Report. Menlo Park, CA.
- Smith, L.E. and E.S. Gross. 1997. Effects of tides and wind on water residence time during summer in South San Francisco Bay. *U.S. Geological Survey Preliminary Draft Open-File Report*. Sacramento, CA.
- URS. 2003. *Proposed SFO Runway Reconfiguration Project, Predicted Changes in Hydrodynamics, Sediment Transport, Water Quality, and Aquatic Biotic Communities Associated with SFO Runway Reconfiguration Alternatives BX-6, A3, and BX-R, Final Technical Report*. Oakland, CA. June.
- URS. 2006. *San Francisco Bay Modeling for the Environmental Fate and Transport of Copper from Vehicle Brake Bad Wear Debris Work Plan*. Oakland, CA. August 15.

Table 1 Input Parameters for the MIKE 21 Hydrodynamic Module

Parameter	Approximate Value or Range of Values	Unit	Data Source(s)
Bathymetry	-70 to 3	m	NOAA/NOS 1999, Smith and Cheng 1994, Cheng and Smith 1998, DWR 1995
Flow Boundary Conditions	-17,825 to 824	m ³ /s	DWR IEP 2007
Tidal Boundary Conditions	-1.5 to 1.8 m NGVD	m NGVD	NOAA web site, National Geodetic Survey 1994
Precipitation	0 to 89 in Lower South Bay, 0 to 104 in rest of the Bay	mm	AQUA TERRA 2007
Smagorinsky Coefficient (for eddy viscosity calculated from Smagorinsky formula based on velocity)	0.05 to 0.5	dimensionless	URS 2003
Resistance (given by Manning's n)	0.015 to 0.034	dimensionless	URS 2003
Tributary Sources	Varies by watershed	m ³ /s	AQUA TERRA 2007
Publicly Owned Treatment Work and Industrial Point Sources	Varies by source	m ³ /s	NPDES self-monitoring reports, URS 2003
Marina Inputs	0.001	m ³ /s	Assumed default value
Wind	Speed: 0.5 to 25.7 Direction: 0 to 360	Speed: m/s, Direction: degrees from North	NCDC 2007

Table 2 Modeled Watersheds and Flow Scaling Factors

Subwatershed	Catchment (Entry Point) Within Subwatershed	Scaling Factor	Sum of Scaling Factors
Contra Costa Central	CC9	0.01	1.00
	CC10	0.02	
	CC11	0.07	
	CC12	0.02	
	CC13	0.68	
	CC14	0.06	
	CC15	0.15	
Contra Costa West	CC1	0.62	1.00
	CC2	0.04	
	CC3	0.15	
	CC4	0.04	
	CC5	0.11	
	CC6	0.02	
	CC7	0.02	
	CC8	0.01	
Coyote	SC1	1.00	1.00
East Bay Central	A4	0.04	1.00
	A5	0.13	
	A6	0.02	
	A7	0.19	
	A8	0.03	
	A9	0.07	
	A11 ¹	0.29	
	A12	0.22	
Upper San Lorenzo	A10	1.00	1.00
East Bay North	A1	0.15	1.00
	A2	0.28	
	A3	0.19	
	A13	0.39	
East Bay South	SC4	1.00	1.00
Marin North	MN9	0.13	1.00
	MN10	0.20	
	MN11	0.67	
Marin South	MN1	0.09	1.00
	MN2	0.09	
	MN3	0.11	
	MN4	0.18	
	MN5	0.06	
	MN6 ²	0.21	
	MN7	0.20	
	MN8	0.05	
Napa	NR1 ³	1.00	1.00

Table 2 Modeled Watersheds and Flow Scaling Factors

Subwatershed	Catchment (Entry Point) Within Subwatershed	Scaling Factor	Sum of Scaling Factors
Peninsula	SM2	0.05	1.00
	SM3	0.02	
	SM4 ⁴	0.05	
	SM5	0.04	
	SM6	0.08	
	SM7	0.01	
	SM8	0.02	
	SM9	0.01	
	SM10	0.06	
	SM11	0.04	
	SM12	0.10	
	SM13	0.05	
	SM14	0.28	
	SM15	0.19	
Petaluma River	PR1	1.00	1.00
Santa Clara Central	SC2	1.00	1.00
Santa Clara Valley West	SC3 ⁵	1.00	1.00
Solano West (Green Valley Creek)	FF1	0.09	1.01
	FF2	0.20	
	FF3	0.72	
Solano West (Montezuma Slough)	FF5	0.57	1.03
	FF6	0.46	
Solano West (Suisun Creek)	FF4	1.00	1.00
Sonoma	SN1 ⁶	1.00	1.00
<p align="center">Catchments not included in the subwatersheds</p> <p align="center">Flow and concentration data from the subwatershed closest to the specified catchment were used to derive flow and concentration data for this catchment. The subwatershed from which data were derived is listed in the left-hand column.</p>			
Contra Costa Central	AX1	0.05	Not applicable
Solano West (Montezuma Slough)	AX2	0.08	Not applicable
Peninsula	SF1	0.10	Not applicable
Peninsula	SM1	0.22	Not applicable

Notes:

¹ This catchment entry point includes flow and concentration from the Upper Alameda subwatershed. As noted in the text, the placement of the Upper Alameda outflow at A11 was an error and should have been placed at A12.

² This catchment entry point includes flow and concentration from the Upper Corte Madera subwatershed.

³ This catchment includes Upper Napa.

⁴ This catchment entry point includes flow and concentration from the Upper Colma subwatershed.

⁵ This catchment entry point includes flow and concentration from the Upper San Francisquito subwatershed.

⁶ This catchment includes Upper Sonoma.

**Table 3 Publicly Owned Treatment Work and
Industrial Point Sources**

Source	ID Shown on Figure 4
San Jose/Santa Clara Water Pollution Control Plant	PS1
Sunnyvale, City of	PS2
Palo Alto, City of	PS3
San Francisco, City and County of, Southeast	PS4
East Bay Dischargers Authority (EBDA) + Dublin San Ramon Services District (DSRSD) + Livermore	PS5
San Francisco International Airport + South San Francisco/San Bruno Water Quality Control Plant + Burlingame + Millbrae	PS6
San Mateo, City of	PS7
South Bayside System Authority (SBSA)	PS8
Central Contra Costa Sanitary District	PS9
Benicia, City of	PS10
Contra Costa County Sanitary District No. 5	PS11
Vallejo Sanitation & Flood Control District	PS12
Pinole-Hercules, Cities of	PS13
Rodeo Sanitary District	PS14
Novato Sanitary District	PS15
Central Marin Sanitation Agency	PS16
West County Agency	PS17
Marin County Sanitary District	PS18
Sewerage Agency of Southern Marin	PS19
Sausalito-Marín City Sanitary District	PS20
East Bay Municipal Utilities District (EBMUD)	PS21
General Chemical Corporation	PS22
Tosco Corporation Avon Refinery	PS23
Tosco Corporation Rodeo Refinery	PS24
Rhodia Basic Chemicals	PS25
Martinez Refining Company	PS26
Valero Benicia Refinery	PS27
C & H Sugar Company	PS28
Chevron Richmond Refinery	PS29
Zeneca Ag Products	PS30
Dow Chemical Company	PS31
GWF Power Systems (Site V - Nichols Street)	PS32
GWF Power Systems (Site I -Third Street)	PS33
USS Posco	PS34
Pacific Gas & Electric (Hunters Point)	PS35
Southern Energy Delta LLC Potrero Power Plant	PS36

Source: URS 2003.

Table 4 Marina Inputs

Marina Name/County Shoreline	Total Copper Released to Bay Waters¹ (kg/y)	Calculated Mean Daily Dissolved Copper Concentration for Model Input (mg/L)
Aeolian Yacht Club	125	3.4
Alameda Marina	597	16.4
Ballena Isle Marina	484	13.3
Barnhill Marina	38	1.0
Berkeley Marina	1527	41.8
Berkeley Marine Center	75	2.1
Embarcadero Cove Marina	163	4.5
Emery Cove Yacht Harbor	599	16.4
Emeryville Marina	404	11.1
Encinal Yacht Club	0	0.0
Fifth Avenue Marina	120	3.3
Fortman Marina	548	15.0
Grand Marina	553	15.2
Marina Village Yacht Harbor	743	20.4
Marinemax	31	0.8
Mariner Square	59	1.6
Oakland Yacht Club/Pacific Marina	220	6.0
Park Street Landing Marina	35	1.0
Port of Oakland	589	16.1
Portobello Marina/D Anna Yacht Center	64	1.8
San Leandro Marina	571	15.6
Brickyard Cove Marina	326	8.9
Channel Marina	80	2.2
Keefe Kaplan Maritime Inc. (KKMI)	28	0.8
Marina Bay Yacht Harbor	1000	27.4
Martinez Marina	319	8.7
McAvoy Harbor	540	14.8
Pittsburg Marina	682	18.7
Point San Pablo Yacht Harbor	140	3.8
Richmond Yacht Club	302	8.3
Richmond Yacht Harbor Ltd.	14	0.4
Rodeo Marina	9	0.2
Sugar Dock Marina	14	0.4
145 Marina	11	0.3
American Oceanics	9	0.2
Angel Island State Park	1	0.0
Arques Shipyard and Marina	55	1.5
Bel Marin Keys Yacht Club	72	2.0
Cass Marina	37	1.0
Clipper Yacht Harbor	875	24.0

Table 4 Marina Inputs

Marina Name/County Shoreline	Total Copper Released to Bay Waters¹ (kg/y)	Calculated Mean Daily Dissolved Copper Concentration for Model Input (mg/L)
Corinthian Yacht Club	109	3.0
Dolphin Marin and Lofts	7	0.2
Galilee Harbor	45	1.2
Hi Tide Boat Sales & Services	5	0.1
Liberty Ship Marina	67	1.8
Loch Lomond Marina	689	18.9
Lowrie Yacht Harbor	115	3.2
Marin Boat House	13	0.4
Marin Yacht Club	165	4.5
Marina Plaza Harbor	142	3.9
Paradise Cay Yacht Harbor	141	3.9
Pelican Harbor	126	3.5
Richardson Bay Marina	279	7.6
San Francisco Yacht Club	153	4.2
San Rafael Yacht Club	11	0.3
San Rafael Yacht Harbor	159	4.4
Sausalito Marine	57	1.6
Sausalito Yacht Harbor	568	15.6
Schoonmaker Point Marina	208	5.7
Shelter Cove Marina	18	0.5
The Cove Apartments & Marina	39	1.1
Trade Winds Marina	36	1.0
Travis Marina	76	2.1
Napa Valley Marina	243	6.7
Napa Yacht Club ²	0	0.0
Fisherman's Wharf & Hyde St. Harbor	129	3.5
Mission Creek Harbor	43	1.2
Pier 39 Marina	433	11.9
San Francisco Marina East Harbor	351	9.6
San Francisco Marina West Harbor	477	13.1
South Beach Harbor	819	22.4
Treasure Island Marina	118	3.2
Bair Island Marina	133	3.6
Brisbane Marina	809	22.2
Coyote Point Marina	677	18.5
Docktown Marina	156	4.3
Marine Collection LLC	15	0.4
Oyster Cove Marina	216	5.9
Oyster Point Marina	352	9.6
Pete's Harbor	240	6.6
Port of Redwood City Yacht Harbor	254	7.0

Table 4 Marina Inputs

Marina Name/County Shoreline	Total Copper Released to Bay Waters¹ (kg/y)	Calculated Mean Daily Dissolved Copper Concentration for Model Input (mg/L)
South Bay Yacht Club	9	0.2
Benicia Marina	402	11.0
Glen Cove Marina	259	7.1
Suisun City Marina	208	5.7
Vallejo Marina	834	22.8
Vallejo Yacht Club	188	5.2
Gilardi's Lakeville Marina	12	0.3
Petaluma Marina	155	4.2
Port of Sonoma Marina	183	5.0
Santa Clara County	5	0.1
San Mateo County	32	0.9
Contra Costa County	1	0.0
Marin County	847	23.2
Napa County	427	11.7

Notes:

¹ Total copper released to Bay waters includes copper from pressure-treated wood used in marine construction, copper released from antifouling coatings used on boats (specified at each marina), and copper in algaecides released to shoreline surface waters (specified by county).

² Coordinates for Napa Yacht Club were not available. For the Bay model, the grid cell coordinates for Napa Valley Marina were applied to Napa Yacht Club. However, the accuracy of these coordinates is irrelevant since zero copper releases were estimated for Napa Yacht Club.

Source: Rosselot 2006.

Table 5 Input Parameters for the ECO Lab Heavy Metal Module

Parameter	Approximate Value or Range of Values	Unit	Data Source(s)
Initial Concentrations in the Bay Water Column	Dissolved copper: 0.26 to 3.2	µg/L	URS 2003
	Adsorbed copper: 0.01 to 24	µg/L	
	Suspended sediment: 1 to 88	mg/L	
Initial Concentrations in the Benthic Sediment	Dissolved copper in porewater: 8.9	µg/L	URS 2003
	Adsorbed copper: 52.4 throughout Bay with hotspots ranging from 30 to 62	mg/kg	SFBRWBCB 1999; URS 2003
	Sediment thickness: 0.1	m	URS 2003
Pacific Ocean Boundary Conditions	Dissolved copper: 0.044	µg/L	Burton and Statham 1990; SFEI 1994–1999
	Adsorbed copper: 0.032	µg/L	
	Suspended sediment: 20	mg/L	
Delta Boundary Conditions	Dissolved copper: 1.7	µg/L	DWR IEP 2007; SFEI 1994–1999
	Adsorbed copper: 0.6 to 24	µg/L	
	Suspended sediment: 9 to 400	mg/L	
Tributary Sources	Varies by watershed	Dissolved and adsorbed copper: µg/L Suspended sediment: mg/L	AQUA TERRA 2007
Publicly Owned Treatment Work and Industrial Point Sources	Varies by source. Adsorbed copper concentrations are zero.	Dissolved and adsorbed copper: µg/L Suspended sediment: mg/L	NPDES self-monitoring reports; URS 2003
Marina Inputs	Dissolved copper concentrations vary by marina. See Table 4. Adsorbed copper and suspended sediment concentrations are zero.	Dissolved and adsorbed copper: µg/L, Suspended sediment: mg/L	Rosselot 2006
Wet Deposition	0 to 0.05	mg/L	Atmospheric and Environmental Research 2007
Dry Deposition	1.02×10^{-6} to 9.19×10^{-6}	g/cell/s	Atmospheric and Environmental Research 2007
Adsorption Coefficients in the Bay Water Column	0.012 in the North Bay, 0.015 in the Central Bay, 0.011 in the South Bay, 0.005 in the Lower South Bay	1/day/(mg/L)	URS 2003

Table 5 Input Parameters for the ECO Lab Heavy Metal Module

Parameter	Approximate Value or Range of Values	Unit	Data Source(s)
Desorption Coefficients in the Bay Water Column	0.47	1/day	URS 2003
Adsorption Coefficients in the Benthic Sediment Porewater	10	1/day/(mg/L)	URS 2003
Desorption Coefficient in the Benthic Sediment Porewater	0.01	1/day	URS 2003
Density of Sediment Porewater	1,030	kg/m ³	URS 2003
Density of Dry Sediment	2,500	kg/m ³	URS 2003
Sediment Porosity	0.8	dimensionless	URS 2003
Diffusive Boundary Layer Thickness	0.1 mm	mm	URS 2003
Diffusion Coefficient	6×10^{-10}	m ² /s	URS 2003
Settling Velocity	0 to 5	m/day	URS 2003
Resuspension Rate	0.6 to 500	g/m ² /day	URS 2003
Particle Production Rate	0.1	g/m ² /day	URS 2003
Critical Velocity for Resuspension	0.003 to 1.2	m/s	URS 2003

Table 6 Summary of Estimated Contribution of Brake Pad Wear Debris to Ambient Dissolved Copper

Site	Wet Season ¹						Water Year ²					
	Dissolved Copper Concentration from BPWD (µg/L) ³			Percentage of Dissolved Copper Concentration from BPWD (%) ⁴			Dissolved Copper Concentration from BPWD (µg/L) ³			Percentage of Dissolved Copper Concentration from BPWD (%) ⁴		
	25th Percentile	50th Percentile (Median)	75th Percentile	25th Percentile	50th Percentile (Median)	75th Percentile	25th Percentile	50th Percentile (Median)	75th Percentile	25th Percentile	50th Percentile (Median)	75th Percentile
San Pablo Bay ⁵	0.00	0.00	0.00	-0.1 ⁶	0.0	0.0	0.00	0.00	0.00	-0.1 ⁶	0.0	0.0
Golden Gate ⁵	0.00	0.00	0.00	0.1	0.2	0.4	0.00	0.00	0.00	0.1	0.2	0.3
Bay Bridge ⁵	0.00	0.00	0.00	0.0	0.0	0.0	0.00	0.00	0.00	0.0	0.0	0.0
Alameda ⁵	0.00	0.00	0.00	0.1	0.1	0.3	0.00	0.00	0.00	0.1	0.2	0.3
Oyster Point	0.02	0.03	0.05	1.3	1.7	2.7	0.02	0.03	0.04	1.4	1.7	2.5
San Bruno Shoal (In Channel)	0.03	0.05	0.08	1.8	2.5	4.2	0.03	0.04	0.07	1.8	2.3	3.5
San Bruno Shoal (In Eastern Mudflats)	0.07	0.11	0.20	4.0	5.6	9.5	0.03	0.08	0.12	1.9	4.0	6.2
Redwood Creek	0.04	0.09	0.15	2.4	4.6	7.6	0.03	0.05	0.11	1.9	2.9	5.7
Dumbarton Bridge	0.07	0.22	0.45	2.8	7.9	14.0	0.04	0.08	0.26	1.8	3.4	9.0
South Bay	0.08	0.29	0.60	2.3	7.5	13.6	0.05	0.10	0.34	1.3	2.7	8.6
Coyote Creek (In Channel)	0.07	0.26	0.59	1.7	6.1	12.3	0.05	0.10	0.34	1.2	2.5	7.9
Coyote Creek (In Western Mudflats)	0.05	0.20	0.44	1.6	5.1	10.1	0.04	0.09	0.29	1.5	2.6	7.4

Notes:
Data shown in this table represent 4-day average dissolved copper concentrations from the last 10 years of the simulation (Water Years 2010 through 2020). The last 10 years of the simulation were selected to capture the 10-year trend that minimizes effects due to model equilibration.
¹ Wet season is from October 1 to March 31.
² Water year is from October 1 to September 30.
³ Dissolved copper concentration from brake pad wear debris is the difference between the Mid and Mid-No-BP concentrations. The 25th percentile represents the concentration below which 25 percent of the modeled 4-day average concentrations are found. Similarly, the 50th and 75th percentiles represent the concentrations below which 50 and 75 percent of the concentrations are found, respectively.
⁴ Percentage of dissolved copper from brake pad wear debris is calculated by dividing the difference between the Mid and Mid-No-BP concentration by the 4-day average Mid concentration of the corresponding date and time. The 25th percentile represents the relative contribution of brake pad wear debris below which 25 percent of the modeled contributions are found. Similarly, the 50th and 75th percentiles represent the relative contributions below which 50 and 75 percent of the contributions are found, respectively.
⁵ Dissolved copper concentrations from BPWD at sites in the North and Central bays are very small and, thus, displayed above as 0.00 µg/L. The concentrations are beyond the resolution of the model.
⁶ Negative percentages are due to model variability. Mid-No-BP results can sometimes exceed Mid results in the North Bay, resulting in a negative contribution of copper from BPWD. However, these negative scenario differences are minor and occur in the low end of the probable range (25th percentile).

**Table 7 Summary of Cumulative Probabilities for Mid and Mid-No-BP
Modeled Scenarios**

Site	Modeled Scenario	4-Day Average Dissolved Copper Concentration (µg/l)			
		0 Percent (Minimum)	50 Percent (Median)	90 Percent	100 Percent (Maximum)
San Pablo Bay	Mid	0.80	1.29	1.56	2.16
	Mid-No-BP	0.80	1.29	1.56	2.16
Golden Gate	Mid	0.53	0.93	0.93	1.13
	Mid-No-BP	0.53	0.93	1.00	1.12
Bay Bridge	Mid	0.96	1.02	1.04	1.24
	Mid-No-BP	0.95	1.02	1.04	1.24
Alameda	Mid	1.04	1.10	1.17	1.61
	Mid-No-BP	1.04	1.10	1.17	1.59
Oyster Point	Mid	1.31	1.72	1.87	2.20
	Mid-No-BP	1.31	1.69	1.83	2.12
San Bruno Shoal (In Channel)	Mid	1.31	1.87	1.99	2.35
	Mid-No-BP	1.31	1.83	1.93	2.23
San Bruno Shoal (In Eastern Mudflats)	Mid	1.18	1.81	2.12	2.86
	Mid-No-BP	1.18	1.74	1.97	2.40
Redwood Creek	Mid	1.47	1.85	2.04	2.45
	Mid-No-BP	1.47	1.80	1.91	2.35
Dumbarton Bridge	Mid	2.06	2.56	3.20	4.72
	Mid-No-BP	2.02	2.49	2.84	3.63
South Bay	Mid	2.73	3.62	4.41	6.28
	Mid-No-BP	2.71	3.52	3.92	4.91
Coyote Creek (In Channel)	Mid	3.29	3.99	4.79	6.46
	Mid-No-BP	3.26	3.88	4.33	5.51
Coyote Creek (In Western Mudflats)	Mid	2.32	3.26	4.62	6.29
	Mid-No-BP	2.29	3.13	4.25	5.87

BP = Brake Pad

Table 8 Benthic Copper Concentrations for Mid and Mid-No-BP Modeled Scenarios by Site

Site	Time from Beginning of Simulation	Initial Condition	At Year 10	At Year 20	At Year 30	At Year 40
	Scenario	Benthic Copper Concentration (mg/kg)				
San Pablo Bay	Mid	52.4	5.3	4.7	4.9	4.6
	Mid-No-BP	52.4	5.3	4.7	4.9	4.6
	Concentration Difference	0.0	0.0	0.0	0.0	0.0
	Percent Difference	0.0%	0.0%	-0.2%	-0.1%	-0.1%
Golden Gate	Mid	52.4	90.8	101.5	108.2	112.6
	Mid-No-BP	52.4	90.7	101.5	108.1	112.5
	Concentration Difference	0.0	0.0	0.1	0.1	0.1
	Percent Difference	0.0%	0.1%	0.1%	0.1%	0.1%
Bay Bridge	Mid	52.4	11.8	8.9	8.7	8.3
	Mid-No-BP	52.4	11.8	8.9	8.7	8.3
	Concentration Difference	0.0	0.0	0.0	0.0	0.0
	Percent Difference	0.0%	0.0%	0.0%	0.0%	0.0%
Alameda	Mid	52.4	96.7	108.2	115.3	120.1
	Mid-No-BP	52.4	96.7	108.1	115.2	120.0
	Concentration Difference	0.0	0.0	0.1	0.1	0.1
	Percent Difference	0.0%	0.0%	0.0%	0.1%	0.1%
Oyster Point	Mid	52.4	74.2	79.2	82.6	84.3
	Mid-No-BP	52.4	74.2	78.6	81.9	83.5
	Concentration Difference	0.0	0.0	0.6	0.7	0.8
	Percent Difference	0.0%	0.0%	0.7%	0.9%	1.0%
San Bruno Shoal (In Channel)	Mid	52.4	83.3	91.4	96.4	99.2
	Mid-No-BP	52.4	83.3	90.2	95.0	97.6
	Concentration Difference	0.0	0.0	1.2	1.4	1.6
	Percent Difference	0.0%	0.0%	1.3%	1.4%	1.6%
San Bruno Shoal (In Eastern Mudflats)	Mid	52.4	53.3	56.2	55.8	56.7
	Mid-No-BP	52.4	53.3	54.1	53.6	54.1
	Concentration Difference	0.0	0.0	2.1	2.2	2.6
	Percent Difference	0.0%	0.0%	3.7%	3.9%	4.6%
Redwood Creek	Mid	52.4	53.4	52.3	51.8	51.3
	Mid-No-BP	52.4	53.4	50.9	50.3	49.7
	Concentration Difference	0.0	0.0	1.4	1.5	1.6
	Percent Difference	0.0%	0.0%	2.7%	2.8%	3.2%
Dumbarton Bridge	Mid	52.4	121.4	141.7	150.4	157.0
	Mid-No-BP	52.4	121.4	136.3	144.4	150.3
	Concentration Difference	0.0	0.0	5.4	6.0	6.7
	Percent Difference	0.0%	0.0%	3.8%	4.0%	4.3%
South Bay	Mid	52.4	80.3	86.9	88.7	89.9
	Mid-No-BP	52.4	80.3	83.7	85.3	86.2
	Concentration Difference	0.0	0.0	3.2	3.4	3.7
	Percent Difference	0.0%	0.0%	3.7%	3.8%	4.1%

Table 8 Benthic Copper Concentrations for Mid and Mid-No-BP Modeled Scenarios by Site

Site	Time from Beginning of Simulation	Initial Condition	At Year 10	At Year 20	At Year 30	At Year 40
	Scenario	Benthic Copper Concentration (mg/kg)				
Coyote Creek (In Channel)	Mid	52.4	74.0	77.5	78.0	78.4
	Mid-No-BP	52.4	74.0	74.9	75.5	75.6
	Concentration Difference	0.0	0.0	2.5	2.5	2.7
	Percent Difference	0.0%	0.0%	3.3%	3.2%	3.5%
Coyote Creek (In Western Mudflats)	Mid	52.4	26.6	24.9	23.4	23.4
	Mid-No-BP	52.4	25.9	23.9	22.5	22.4
	Concentration Difference	0.0	0.7	1.0	0.9	1.1
	Percent Difference	0.0%	2.5%	4.1%	4.0%	4.5%

BP = Brake Pad

Table 9 Benthic Copper Concentrations for Mid and Mid-No-BP Modeled Scenarios by Subsection

	Time from Beginning of Simulation	Initial Condition	At Year 10	At Year 20	At Year 30	At Year 40
Subsection of Bay	Scenario	Benthic Copper Concentration (mg/kg) Grid-Averaged by Subsection				
From Carquinez Strait to Bay Bridge	Mid	52.4	47.2	51.0	53.9	56.0
	Mid-No-BP	52.4	47.2	51.0	53.9	56.0
	Concentration Difference	0.0	0.0	0.0	0.0	0.0
	Percent Difference	0.0%	0.0%	0.0%	0.0%	0.0%
From Carquinez Strait to San Bruno Shoal	Mid	52.4	55.0	59.5	62.7	65.0
	Mid-No-BP	52.4	54.9	59.3	62.5	64.7
	Concentration Difference	0.0	0.1	0.2	0.2	0.3
	Percent Difference	0.0%	0.2%	0.4%	0.4%	0.4%
From Bay Bridge to Dumbarton Bridge	Mid	52.4	60.2	63.9	66.3	68.1
	Mid-No-BP	52.4	59.4	63.0	65.3	67.0
	Concentration Difference	0.0	0.7	0.9	0.9	1.1
	Percent Difference	0.0%	1.2%	1.4%	1.4%	1.7%
From San Bruno Shoal to Dumbarton Bridge	Mid	52.4	44.9	45.8	46.0	46.7
	Mid-No-BP	52.4	44.0	44.5	44.6	45.1
	Concentration Difference	0.0	0.9	1.4	1.4	1.6
	Percent Difference	0.0%	2.1%	3.0%	3.1%	3.5%
From Dumbarton Bridge to southern tip of Bay	Mid	52.4	30.0	30.1	29.9	30.1
	Mid-No-BP	52.4	29.5	29.4	29.2	29.3
	Concentration Difference	0.0	0.5	0.7	0.7	0.8
	Percent Difference	0.0%	1.7%	2.5%	2.5%	2.7%

BP = Brake Pad

Table 10 Annual Watershed Copper Loads for Mid Modeled Scenario

Water Year	Copper Load (kg/year)		
	Dissolved	Adsorbed	Total
1981	7,209	11,105	18,314
1982	20,254	71,302	91,557
1983	25,158	76,124	101,281
1984	10,726	17,926	28,652
1985	9,169	19,742	28,911
1986	19,515	58,850	78,365
1987	7,915	13,054	20,969
1988	9,188	12,110	21,297
1989	9,267	11,239	20,506
1990	8,715	11,097	19,812
1991	10,963	14,539	25,502
1992	14,801	21,189	35,990
1993	24,260	46,829	71,088
1994	11,055	9,685	20,739
1995	29,271	64,333	93,604
1996	21,162	48,927	70,089
1997	17,663	43,705	61,368
1998	28,510	64,775	93,285
1999	13,768	22,609	36,377
2000	15,071	28,121	43,192
2001	10,554	11,870	22,424
2002	13,323	25,011	38,334
2003	15,236	36,924	52,160
2004	13,222	28,423	41,645
2005	18,342	27,455	45,798
Minimum	7,209	9,685	18,314
Mean	15,373	31,878	47,250
Maximum	29,271	76,124	101,281

Source: AQUA TERRA 2007.

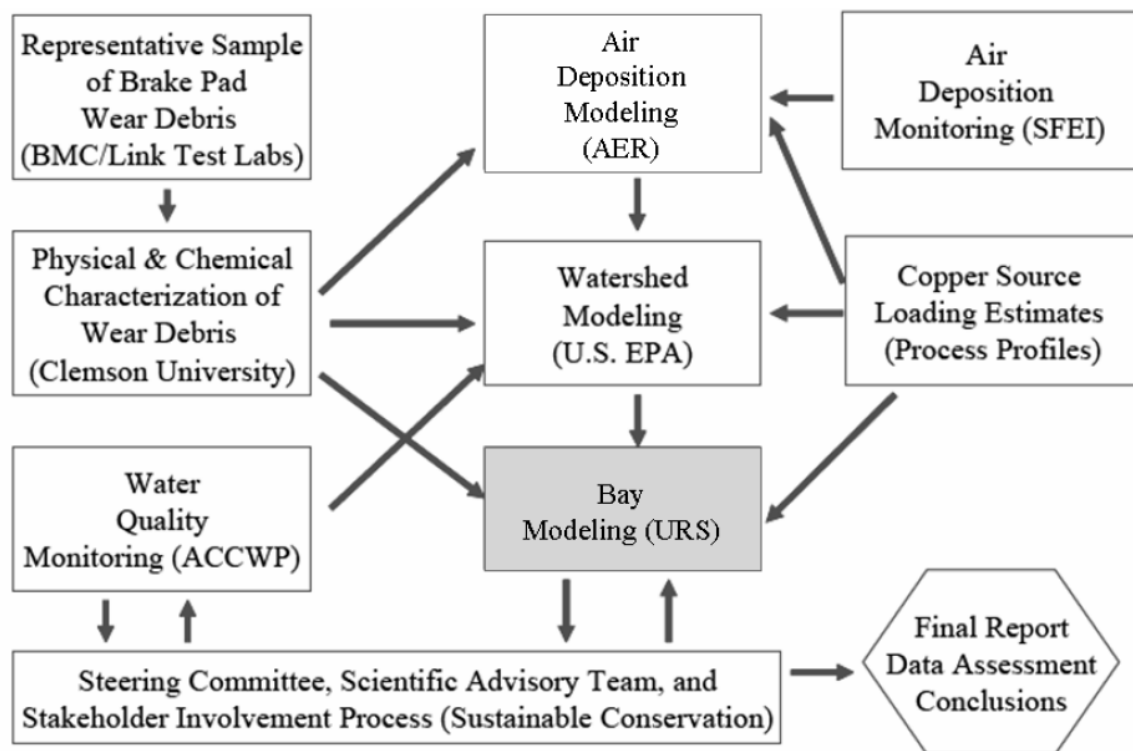
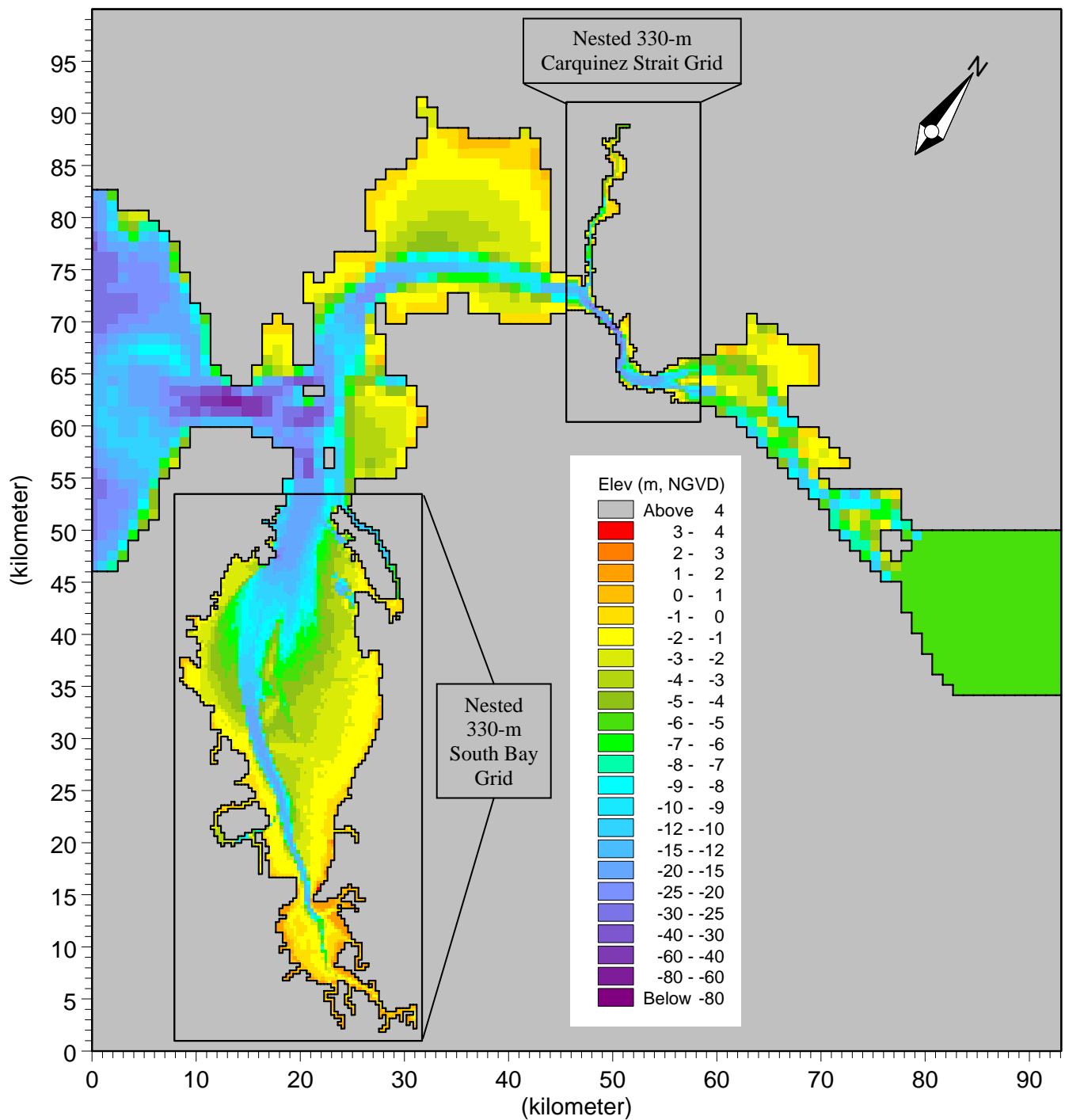
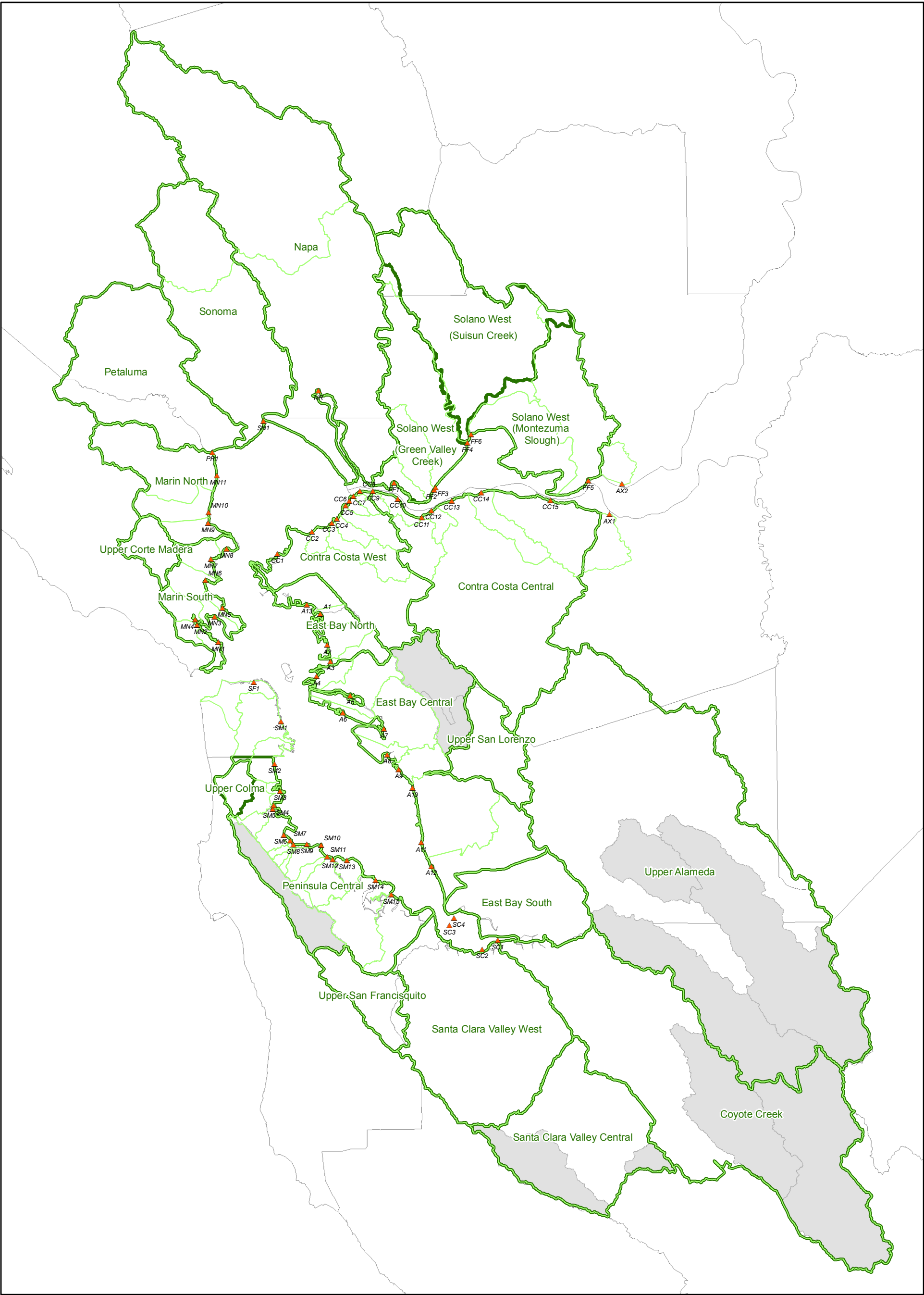


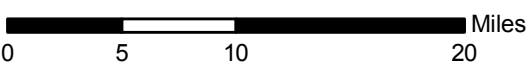
Figure 1 Brake Pad Partnership Technical Studies

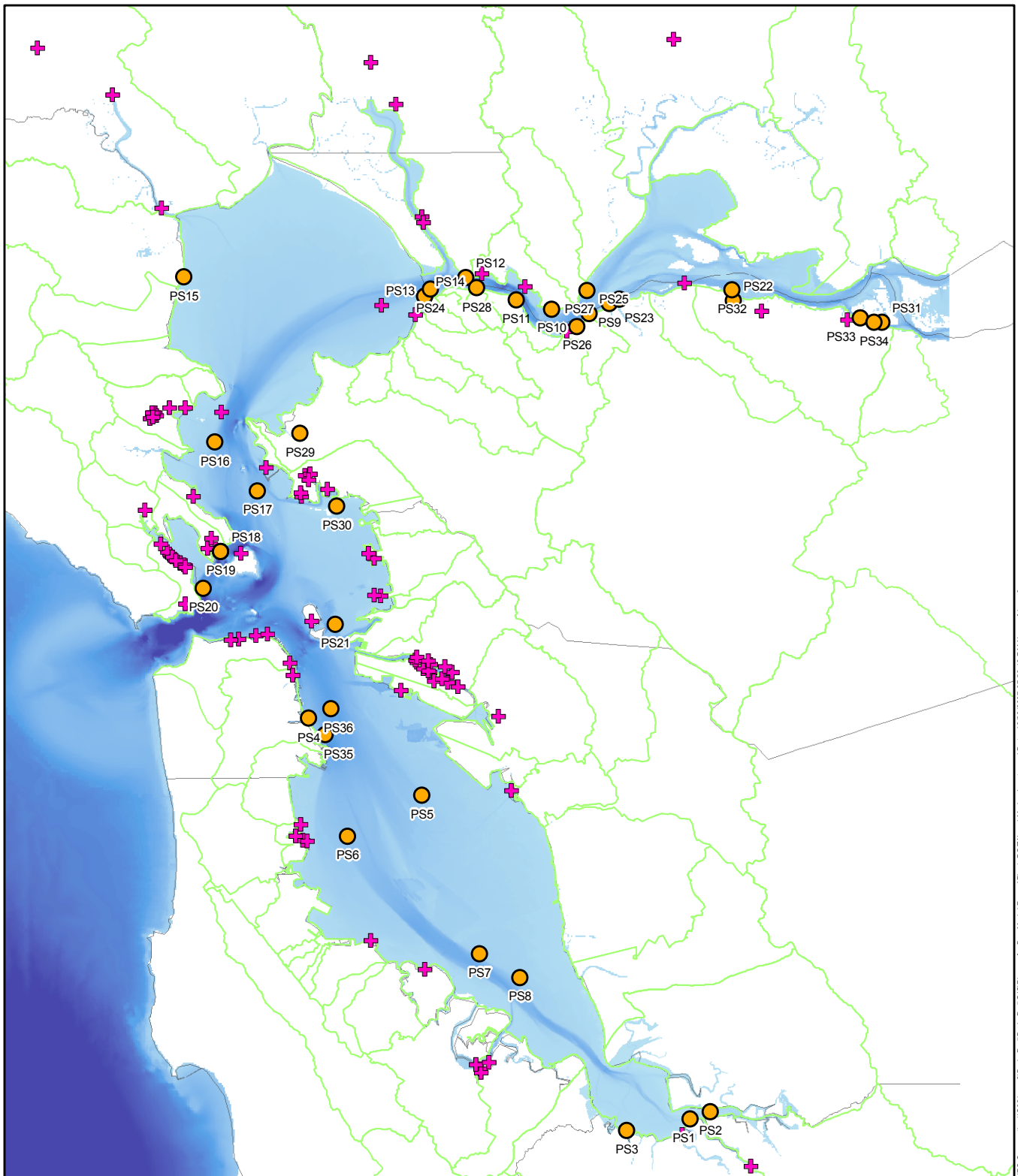




Source: AQUA TERRA 2007, URS 2003.

- ▲ Modeled catchment entry point (labeled with ID shown in Table 2)
- ▭ Catchment used in Bay Model
- ▭ Subwatershed used in Watershed Model
- ▭ Areas excluded from Watershed and Bay Models
- ▭ County line

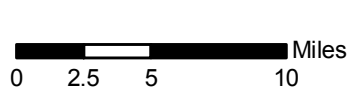





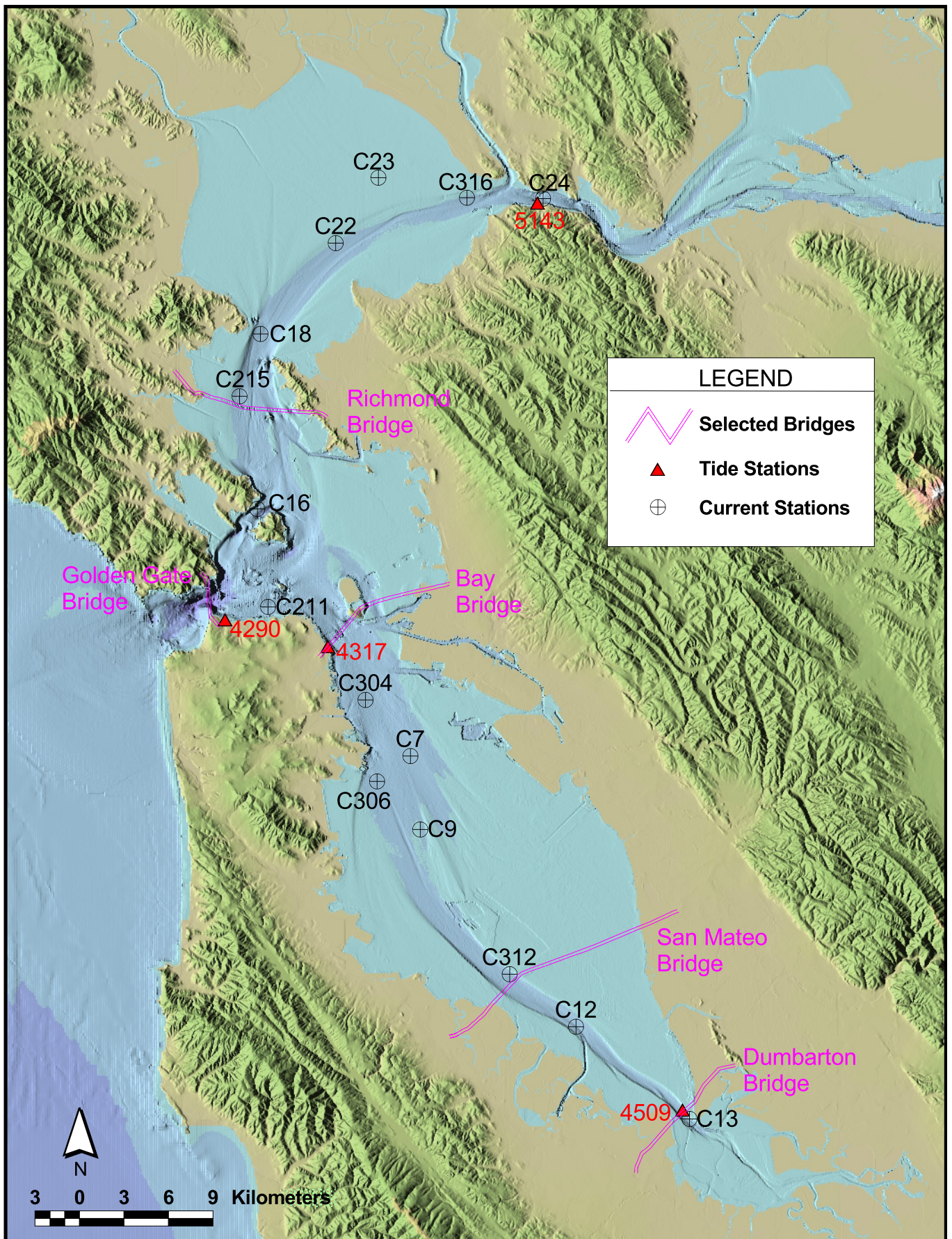
URS Corporation \\S02\emc2\BrakePad\GIS\Figures for Bay Model Report\Fig 4_POTW and Marina Inputs.mxd Date: 10/09/2007 07:56:16 PM Name: maulx0

- Publicly Owned Treatment Work or Industrial Point Source (labeled with ID shown in Table 3)
- ✚ Marina

Sources: Rosselot 2006, URS 2003.



	Brake Pad Partnership	Publicly Owned Treatment Work, Industrial Point Source, and Marina Locations	Figure 4
	26814617		

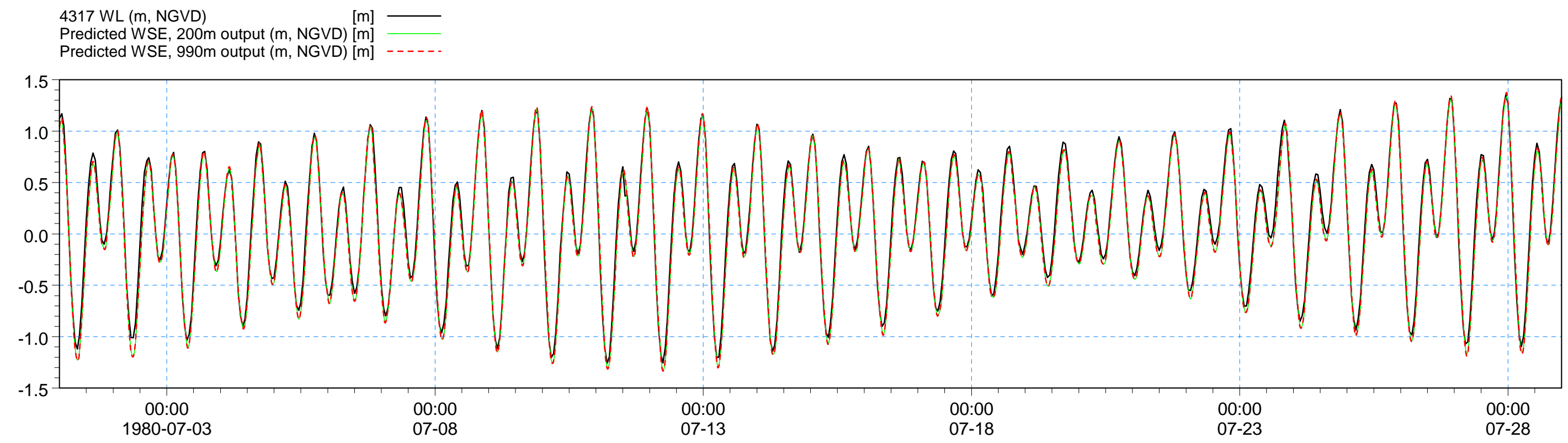
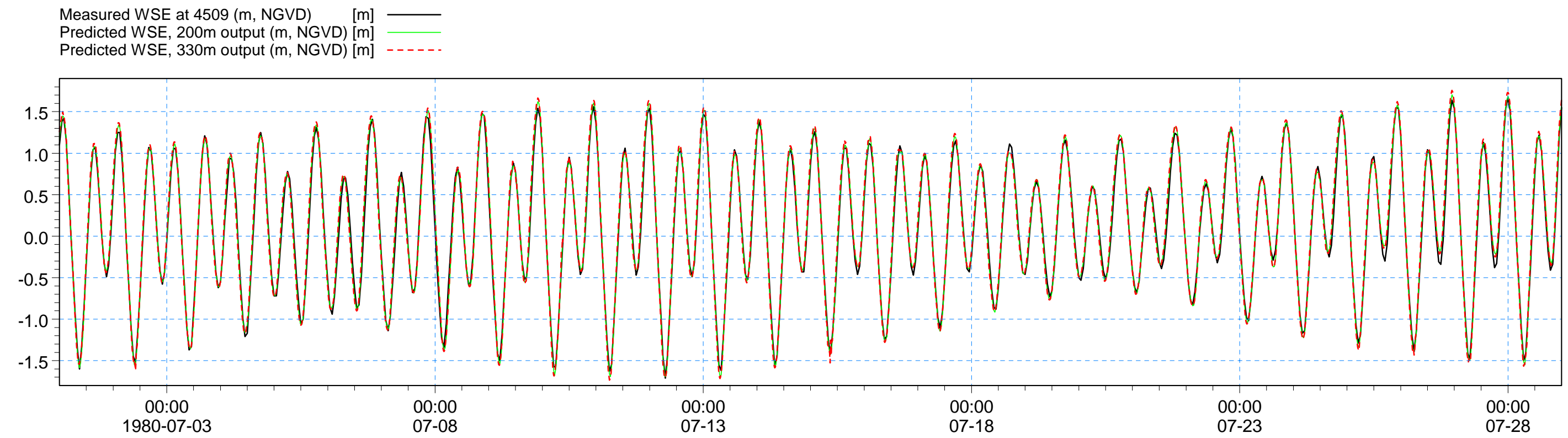


San Francisco
Bay Modeling

26814617

Locations of Current and Tide
Stations Selected for
Hydrodynamic Model Verification

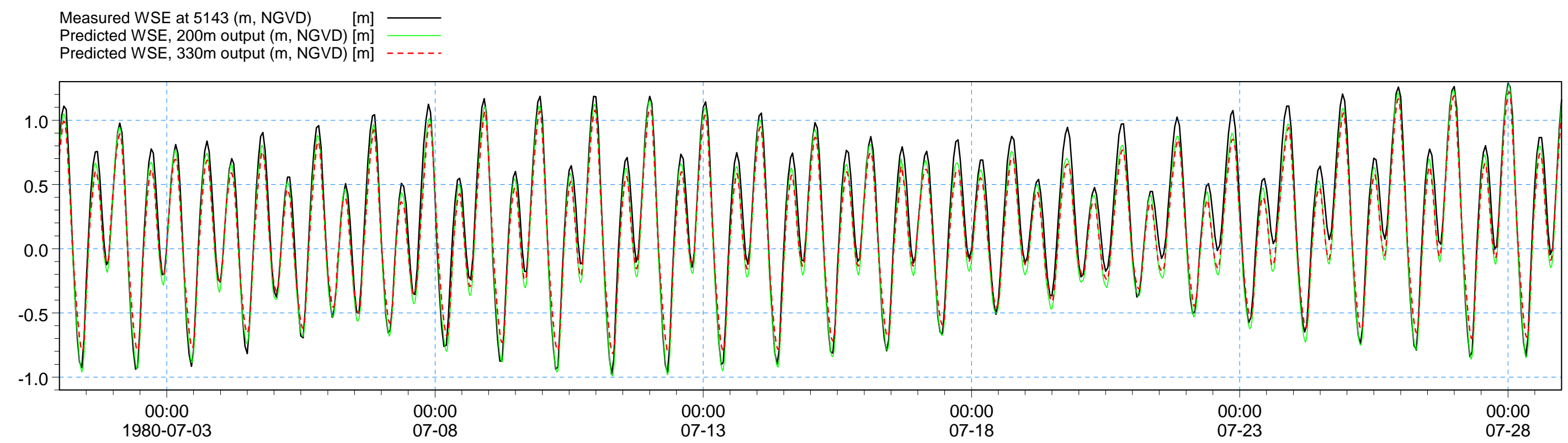
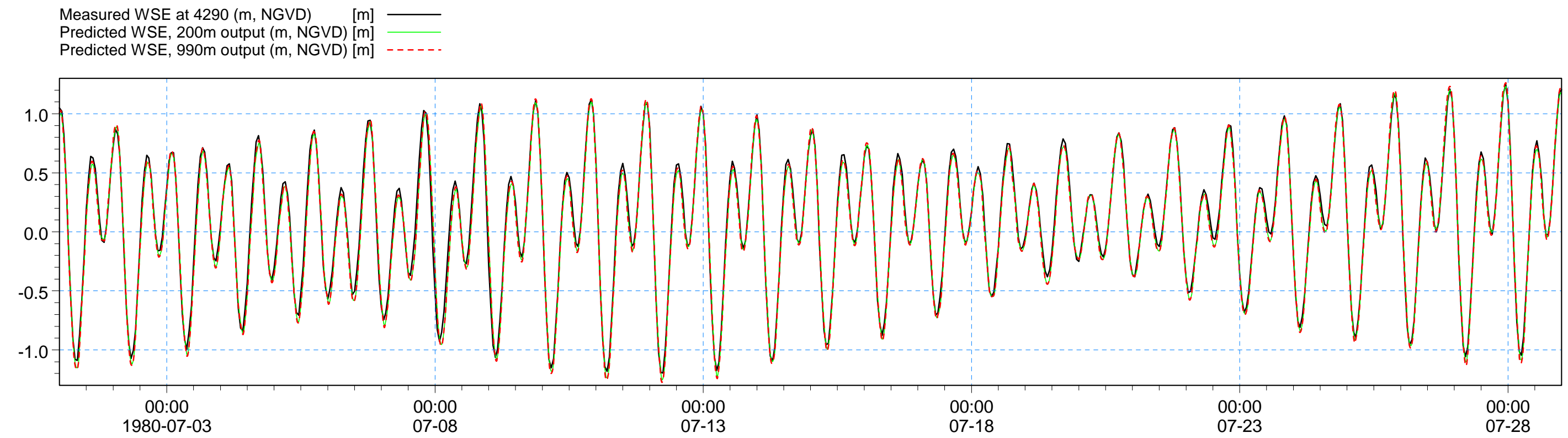
FIGURE
5



San Francisco
Bay Modeling

Comparison of Measured and Predicted Water Surface
Elevations at Tide Stations 4509 and 4317

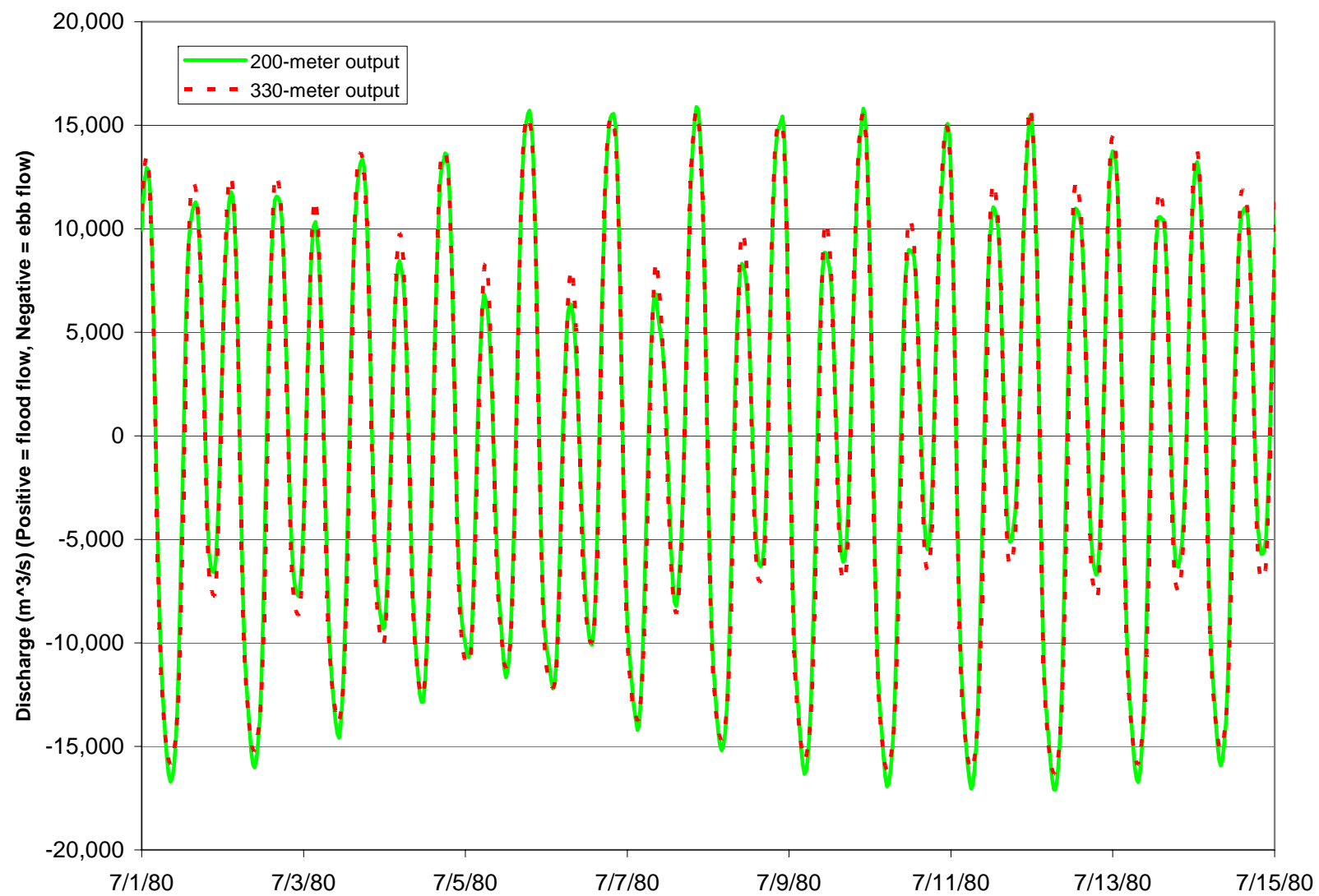
FIGURE
6



San Francisco
Bay Modeling

Comparison of Measured and Predicted Water Surface
Elevations at Tide Stations 4290 and 5143

FIGURE
7

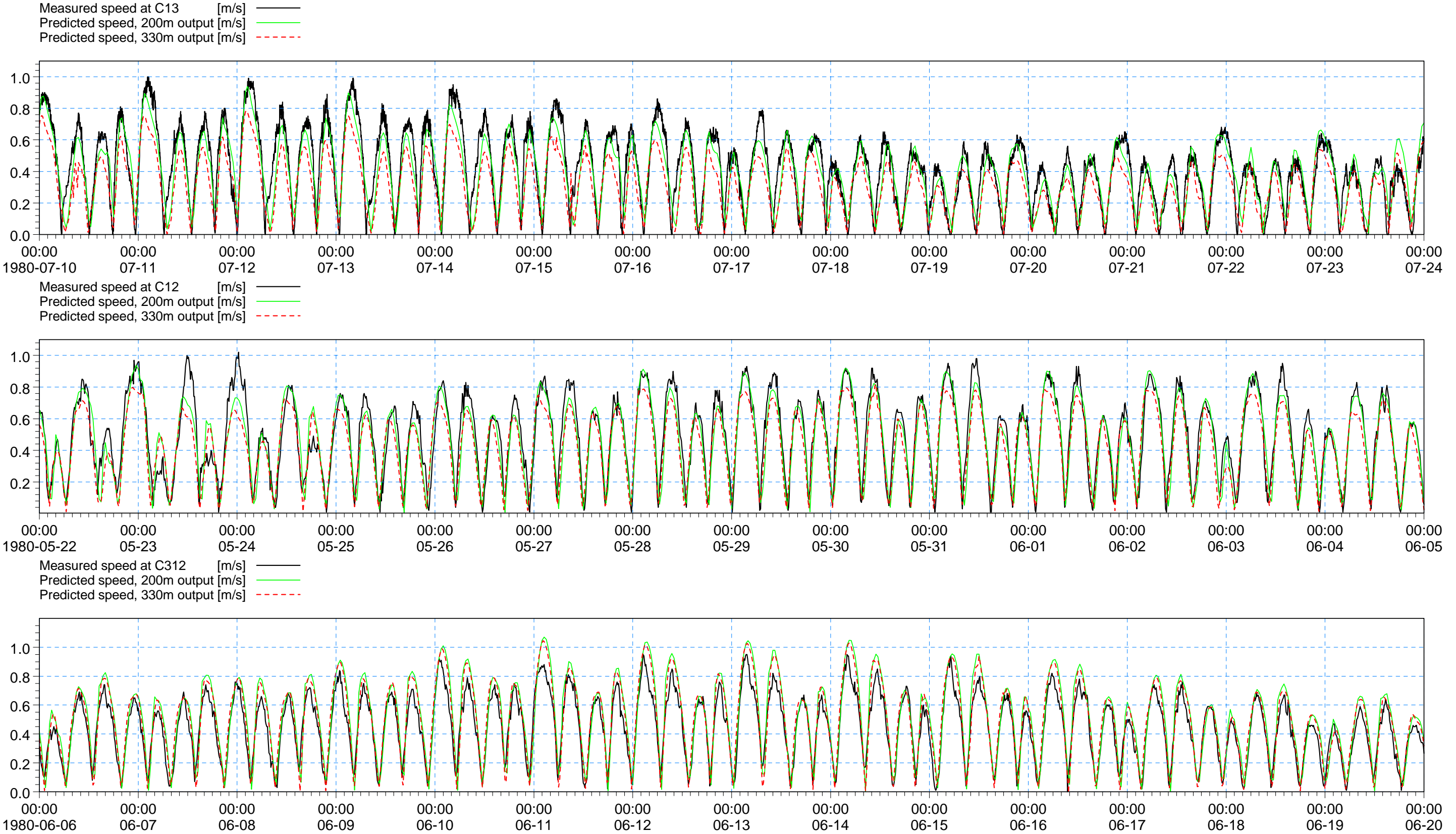


URS

San Francisco
Bay Modeling

Modeled Flow Through Carquinez Strait

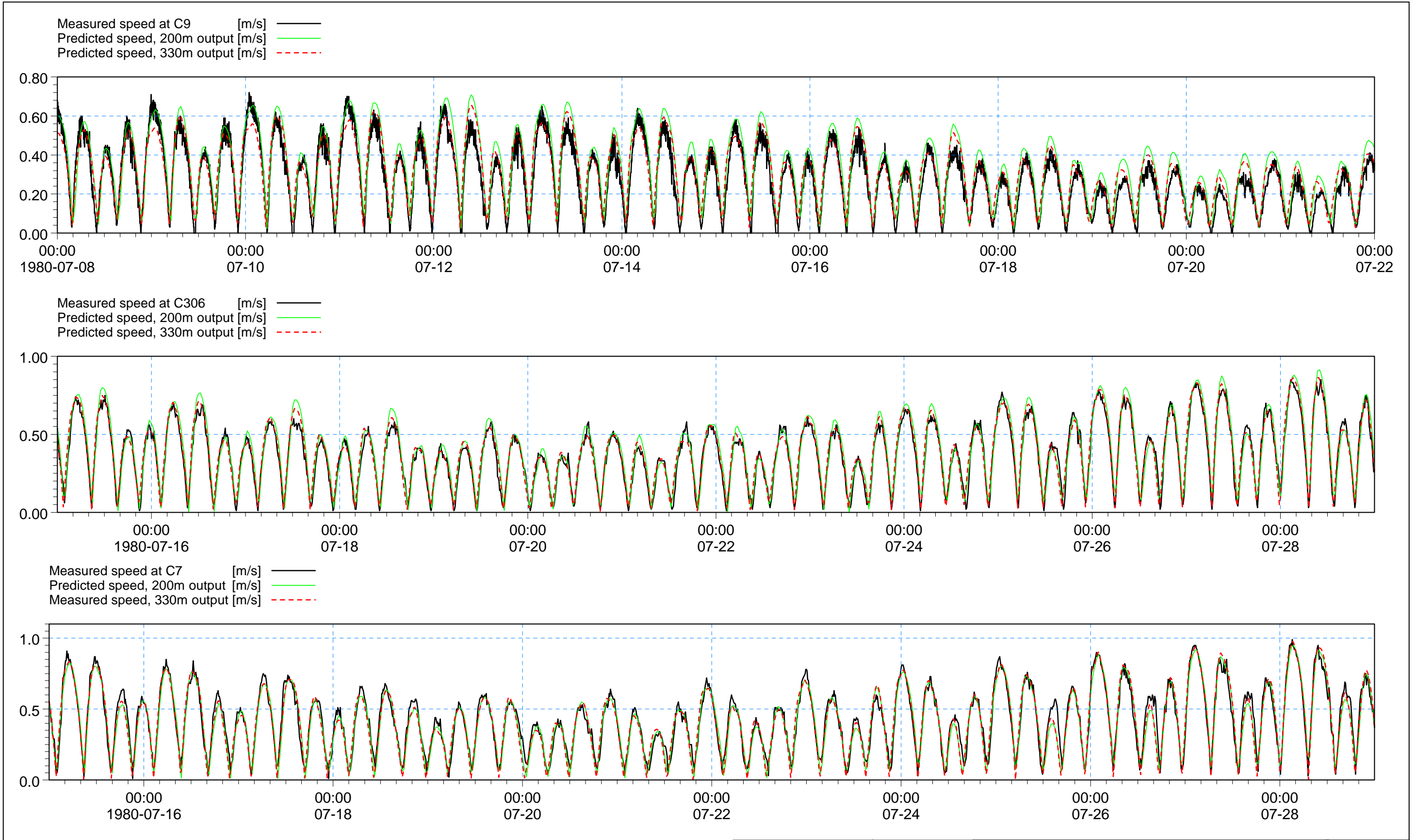
FIGURE
8

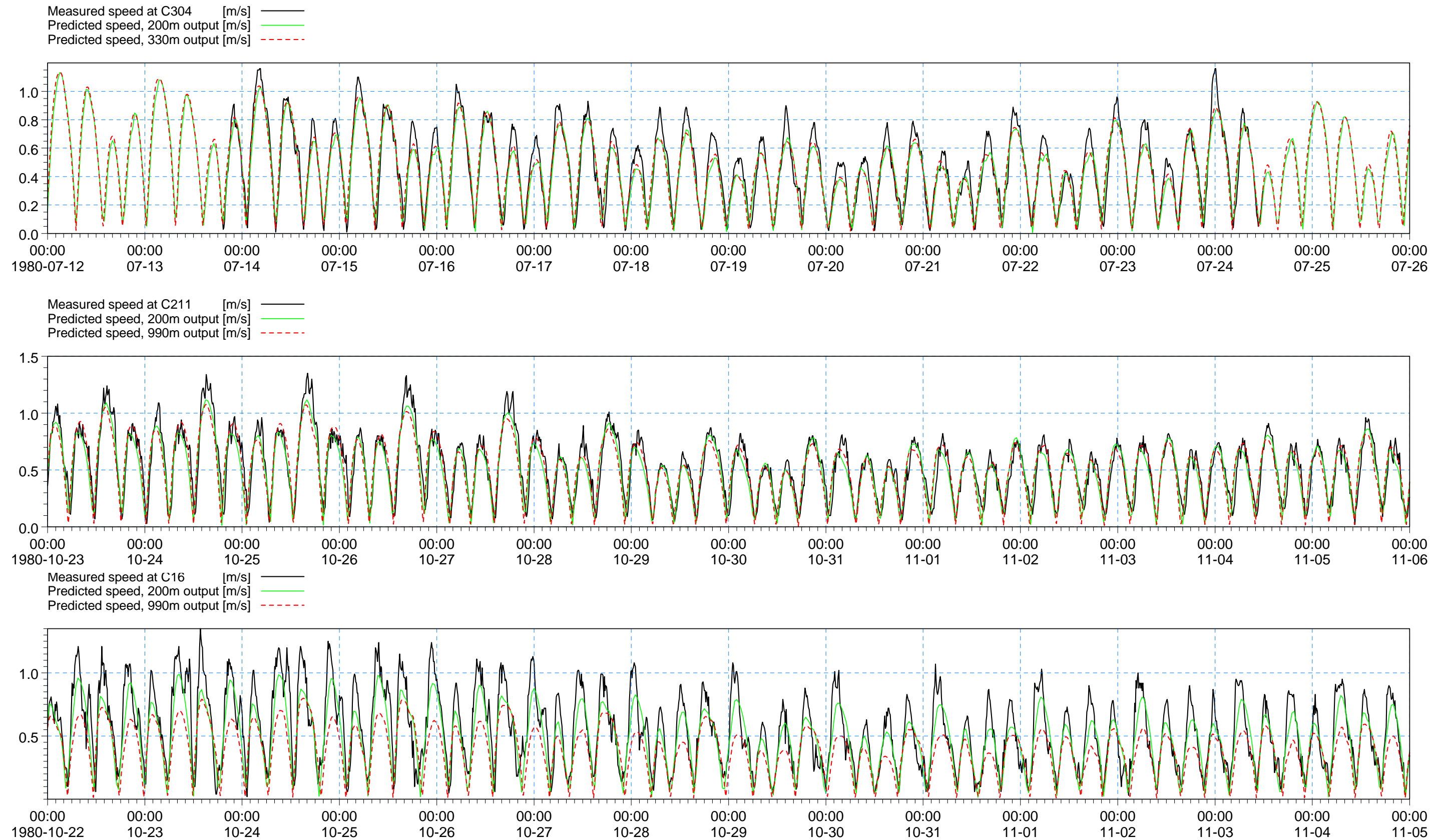


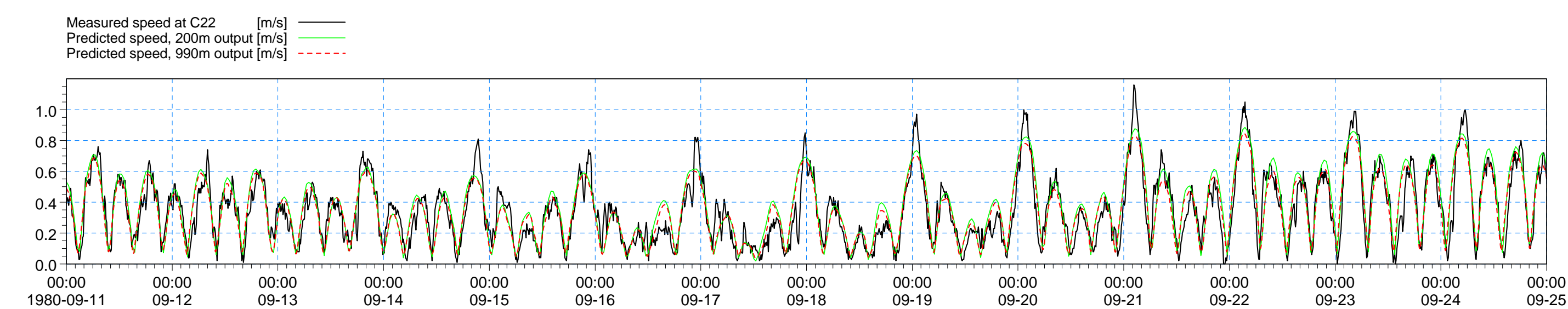
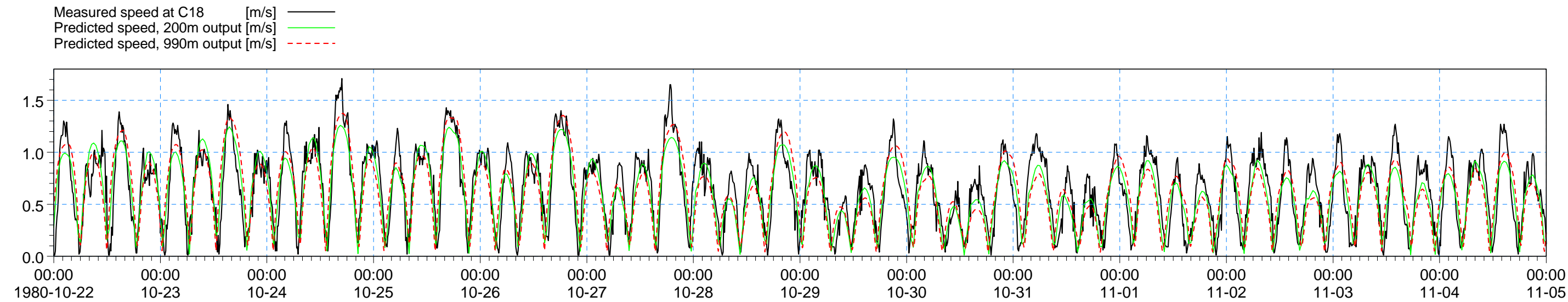
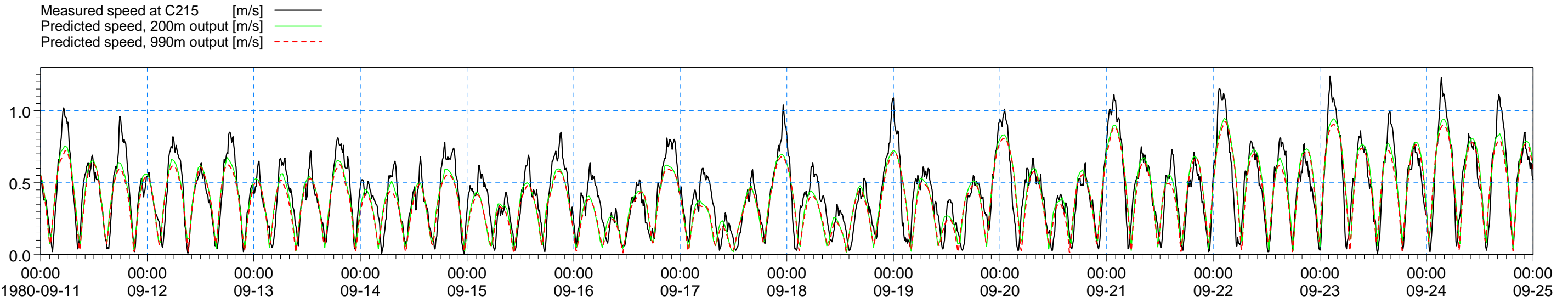
San Francisco
Bay Modeling

Comparison of Measured and Predicted Current
Speeds at Stations C13, C12, and C312

FIGURE
9



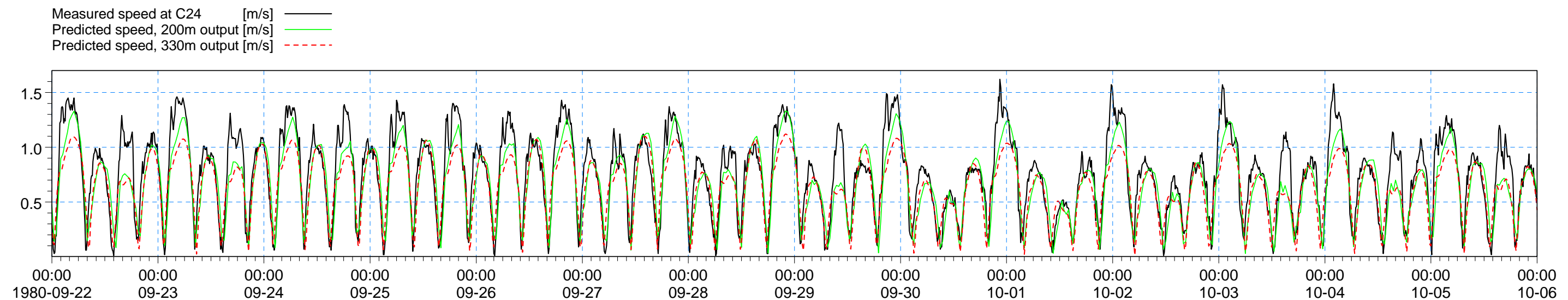
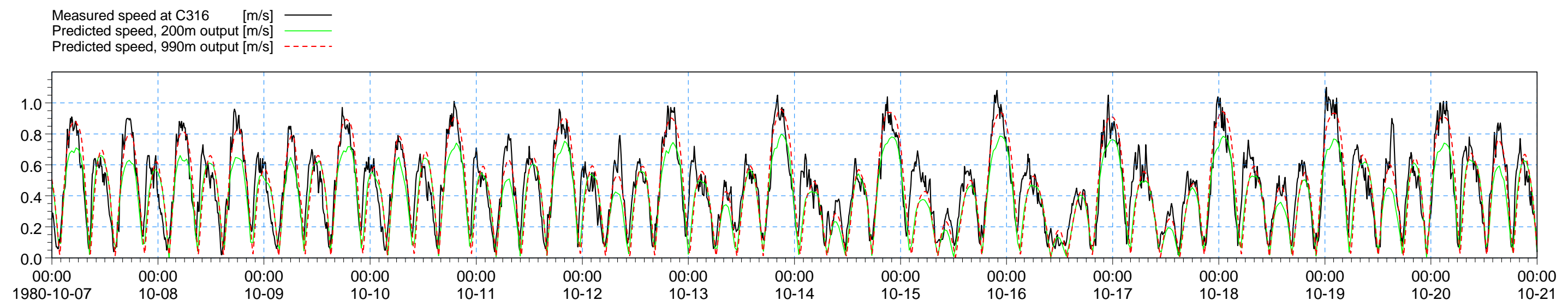
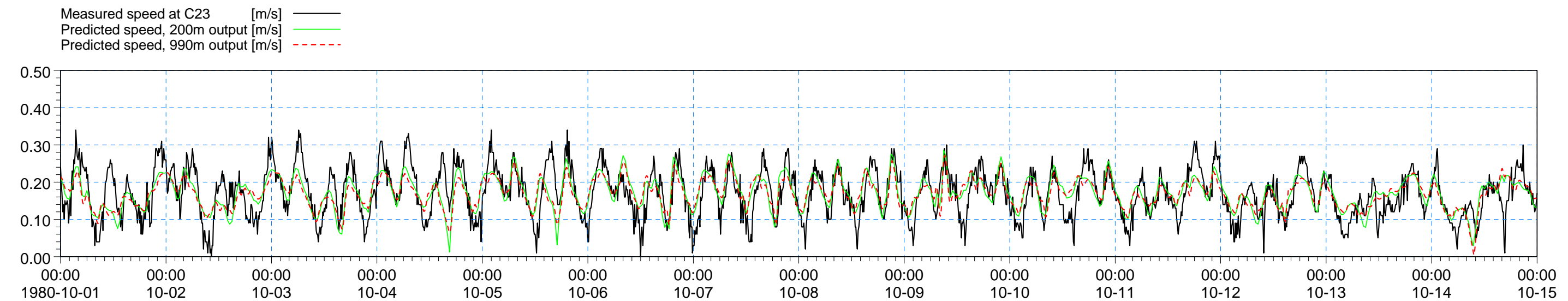




San Francisco
Bay Modeling

Comparison of Measured and Predicted Current
Speeds at Stations C215, C18, and C22

FIGURE
12



San Francisco
Bay Modeling

Comparison of Measured and Predicted Current
Speeds at Stations C23, C316, and C24

FIGURE
13

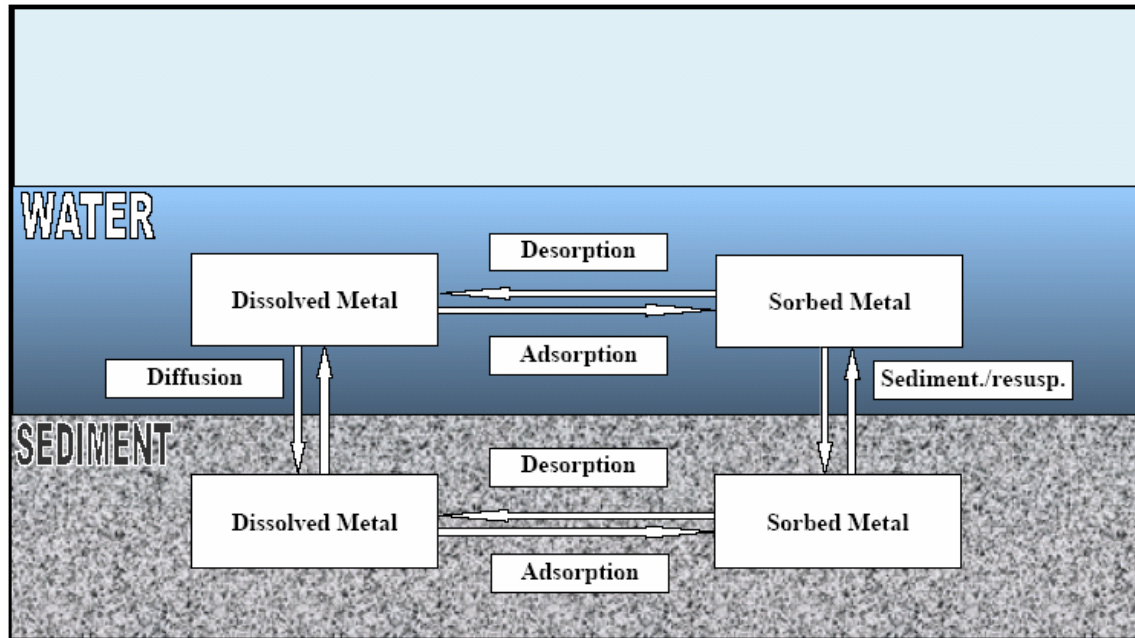
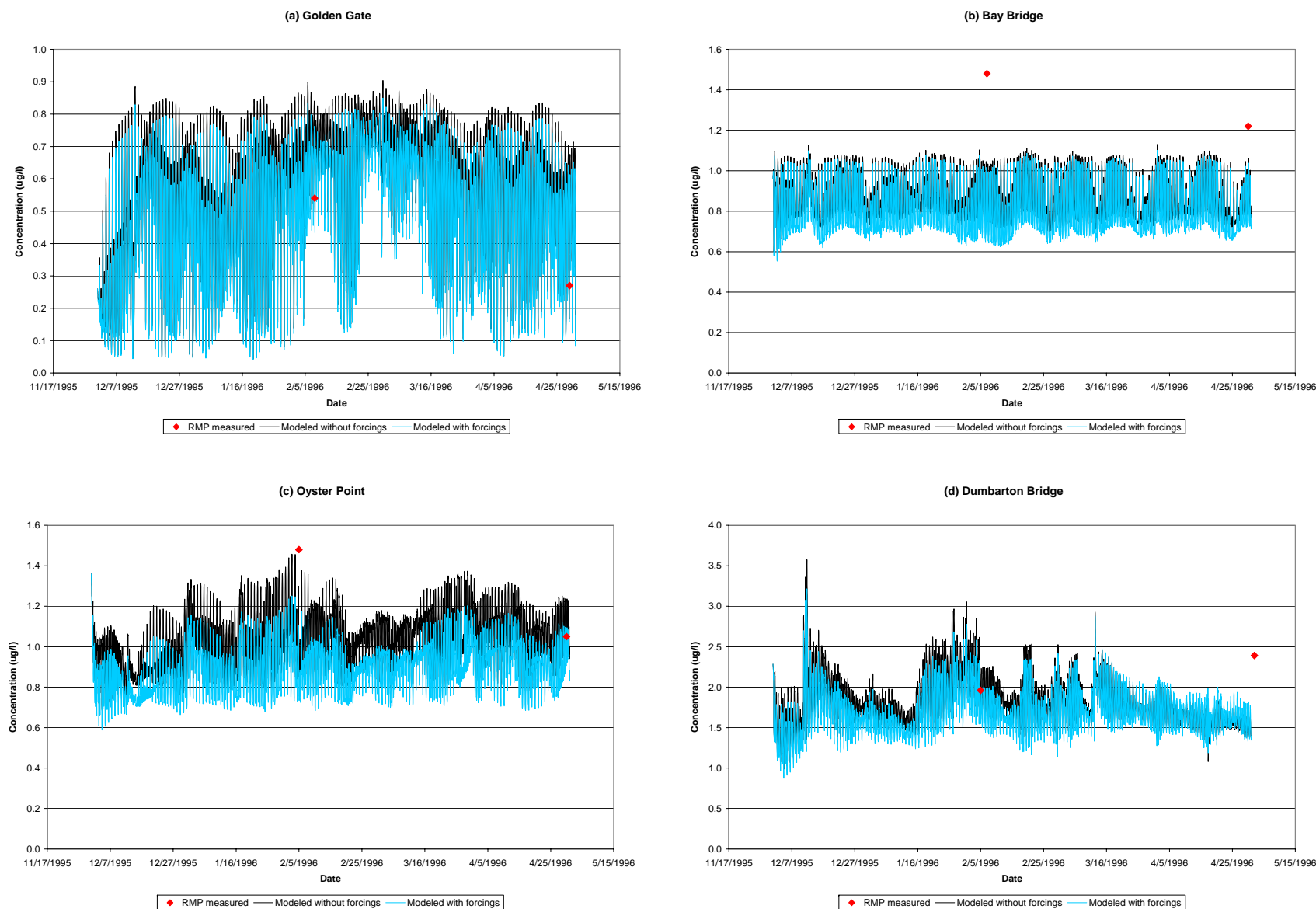
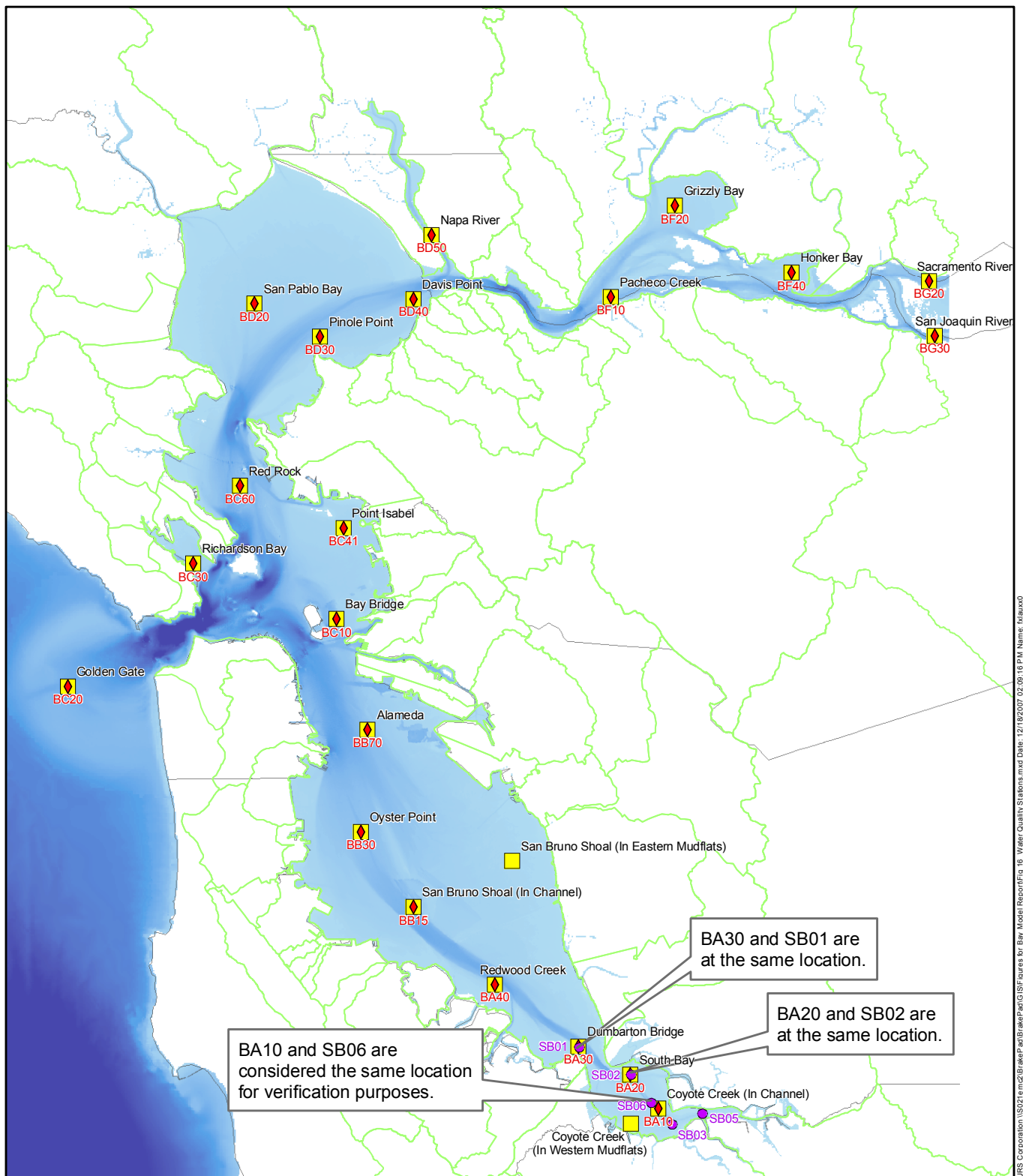


Figure 14 **Summary of Processes Modeled by ECO Lab Heavy Metal Module**

Figure 15. Sensitivity of Dissolved Copper Concentration to Temperature and Salinity Forcings





- ◆ Regional Monitoring Program Monitoring Station (labeled with ID)
- City of San Jose South Bay Monitoring Station (labeled with ID)
- Site of Interest (labeled with name)

Sources: San Jose 2007, SFEI 2007.

0 2.5 5 10 Miles




	Brake Pad Partnership	Locations of Water Quality Stations Selected for Heavy Metal Model Verification	Figure 16
	26814617		

Figure 17. Comparison of Measured and Predicted Dissolved Copper Concentrations

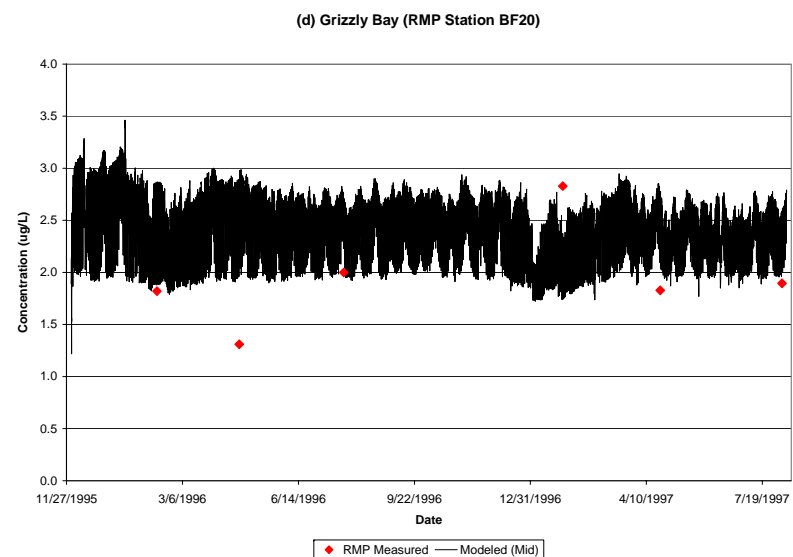
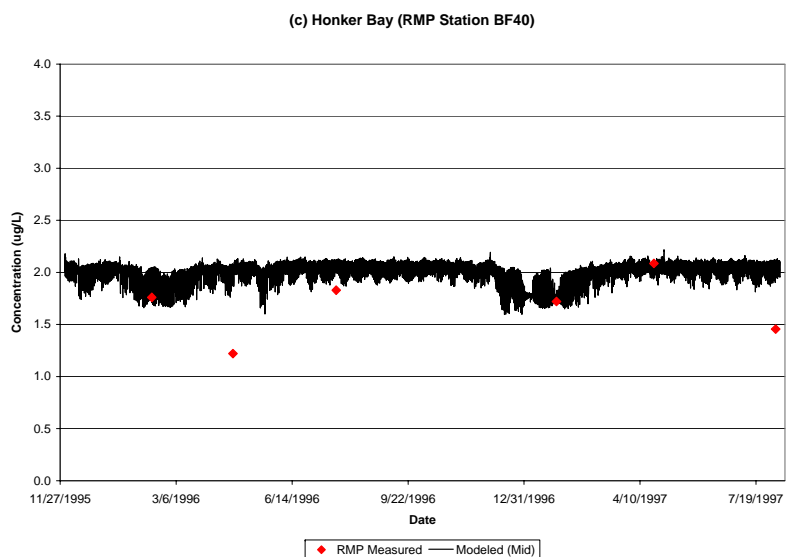
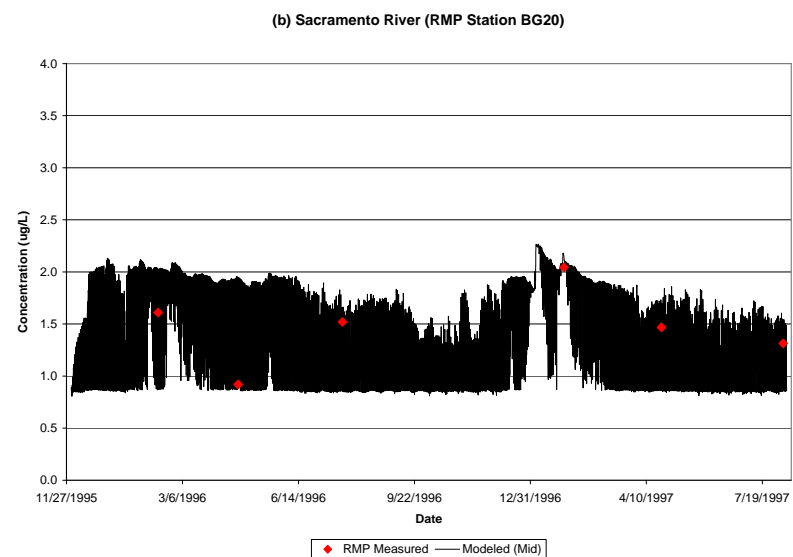
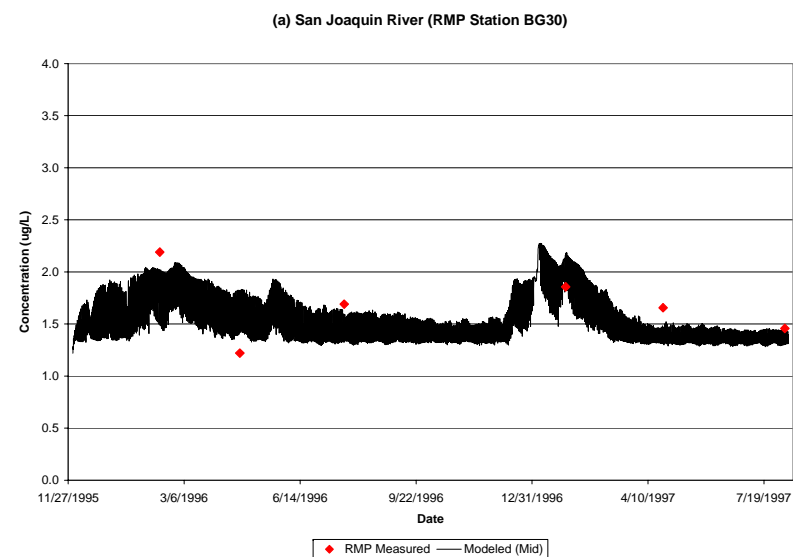


Figure 17. Comparison of Measured and Predicted Dissolved Copper Concentrations (continued)

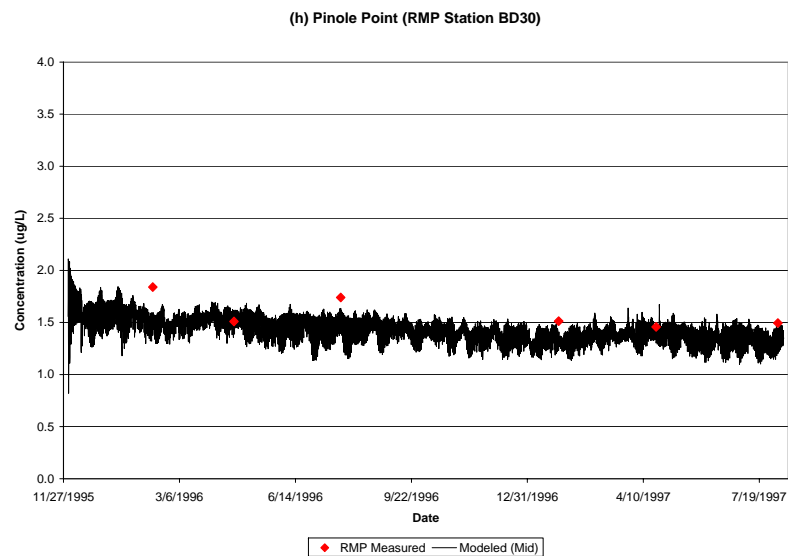
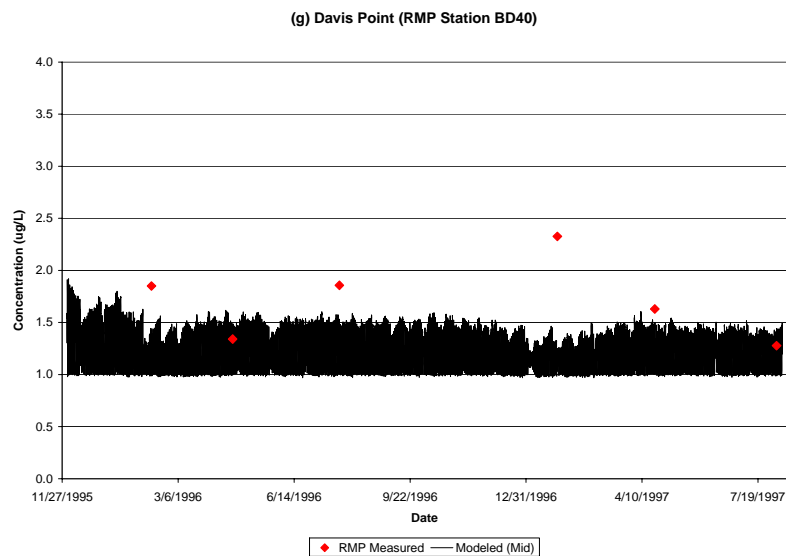
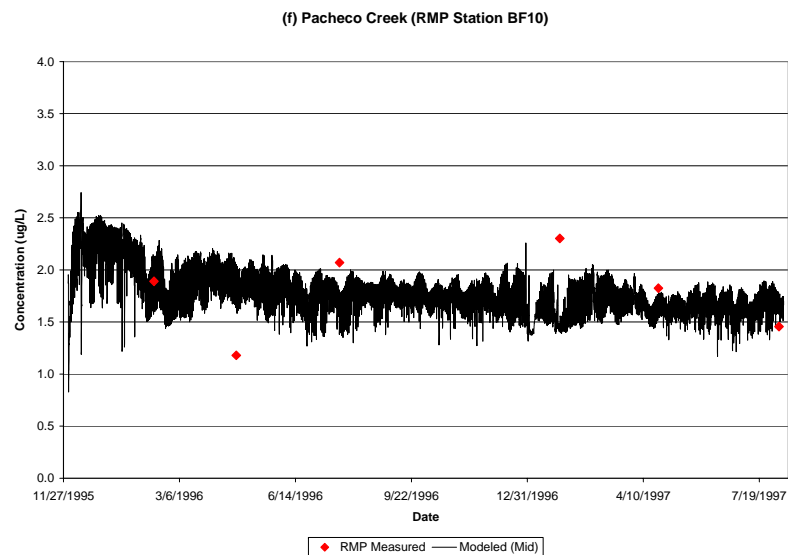
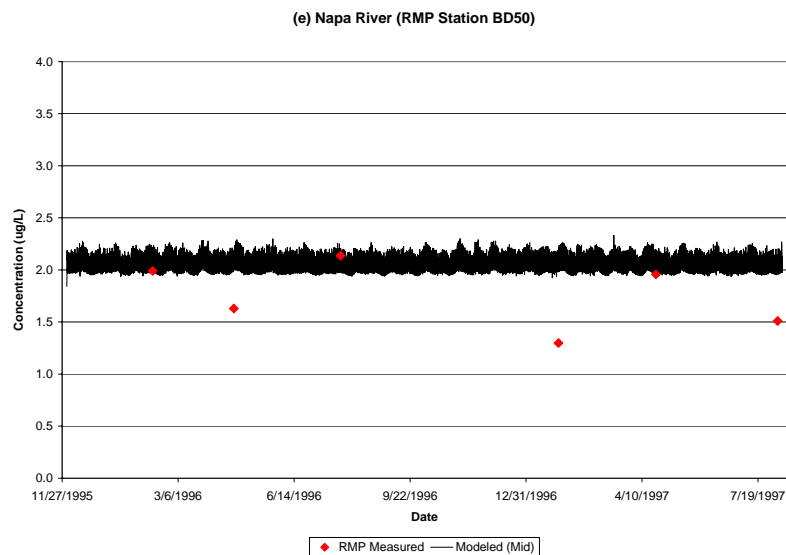


Figure 17. Comparison of Measured and Predicted Dissolved Copper Concentrations (continued)

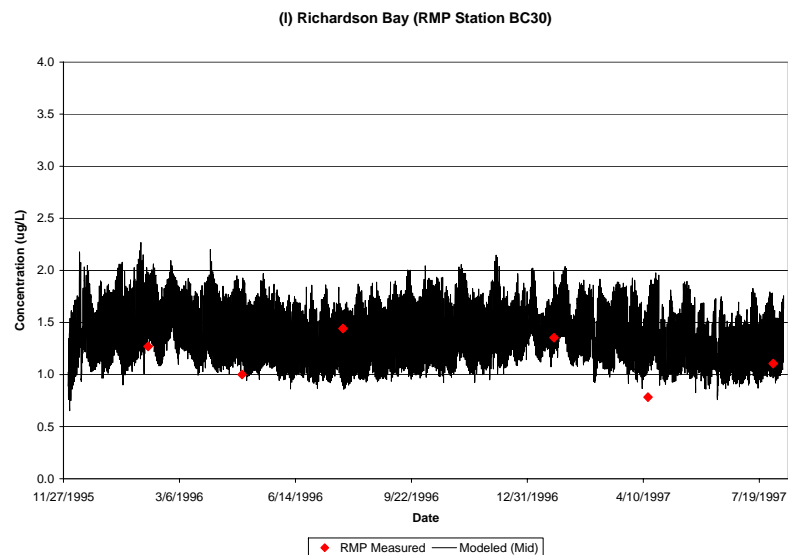
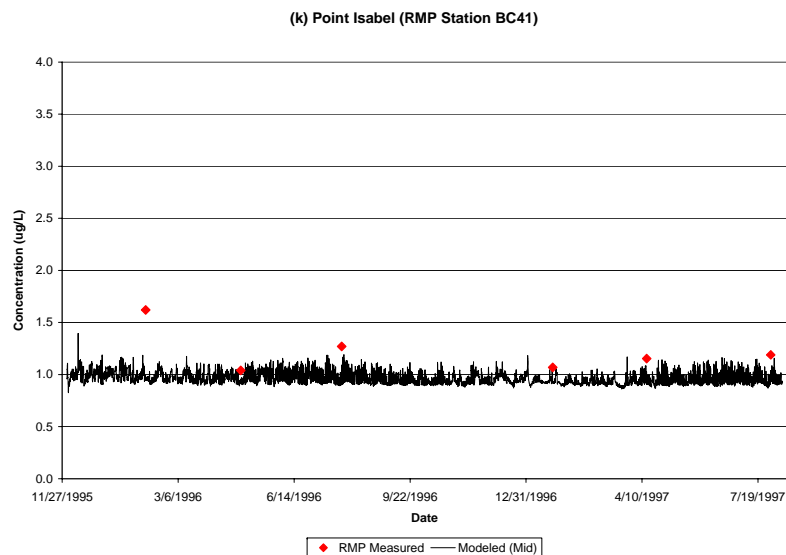
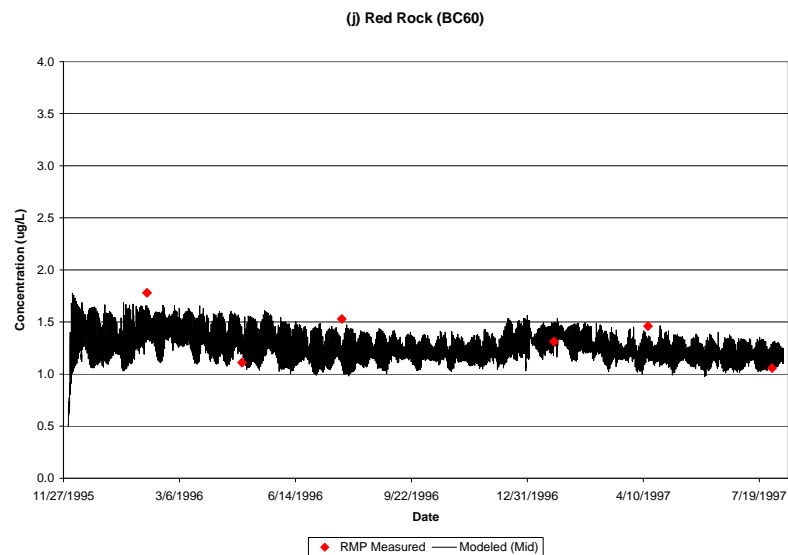
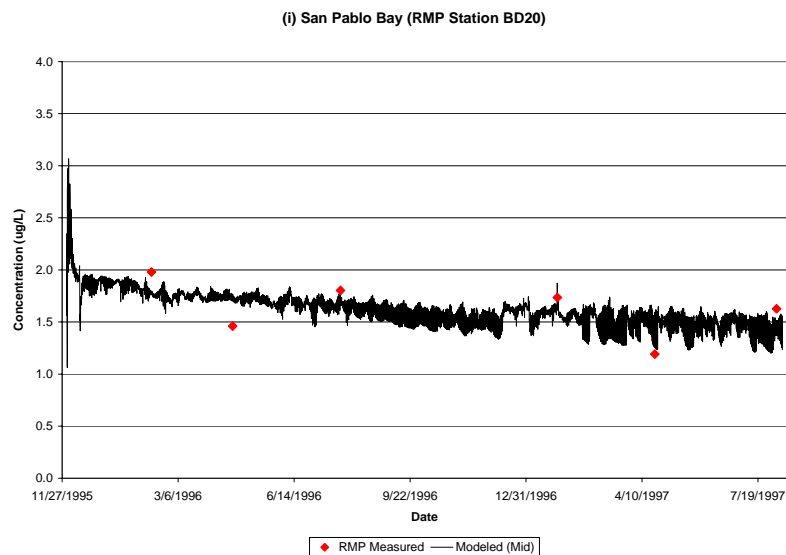


Figure 17. Comparison of Measured and Predicted Dissolved Copper Concentrations (continued)

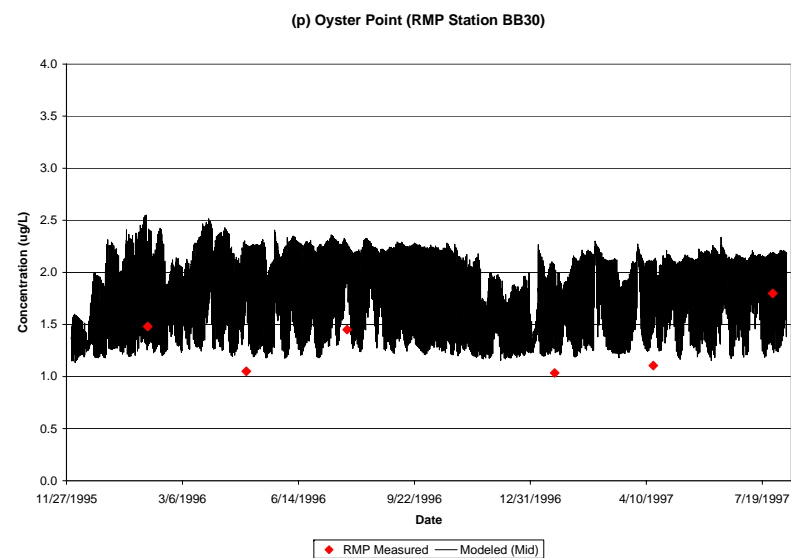
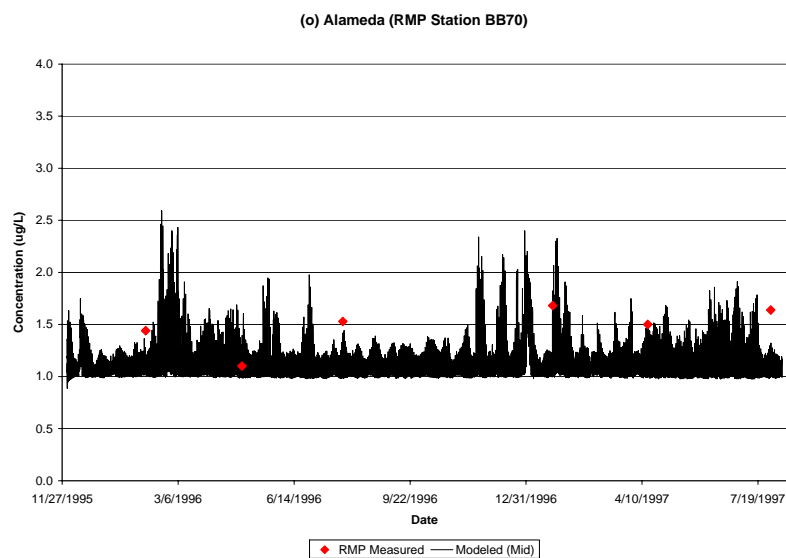
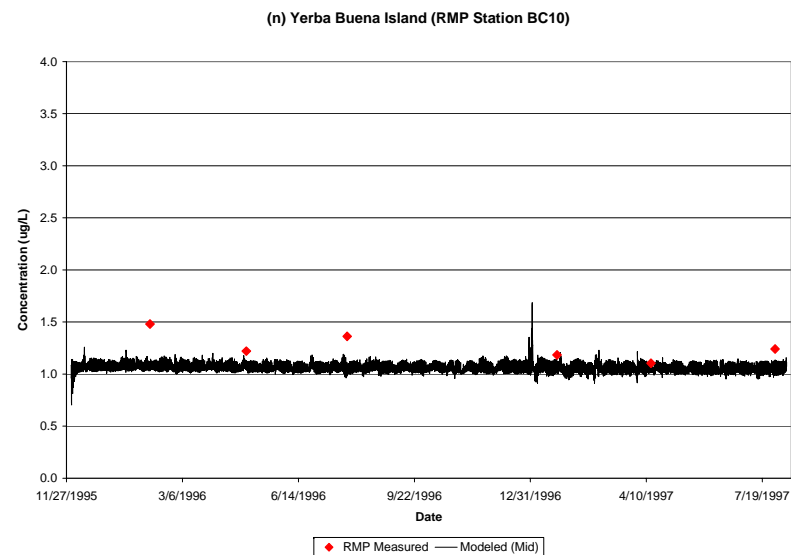
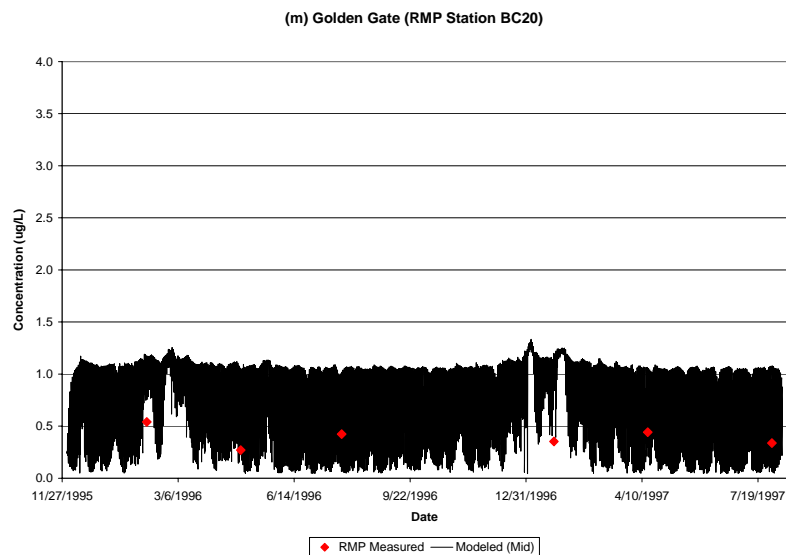


Figure 17. Comparison of Measured and Predicted Dissolved Copper Concentrations (continued)

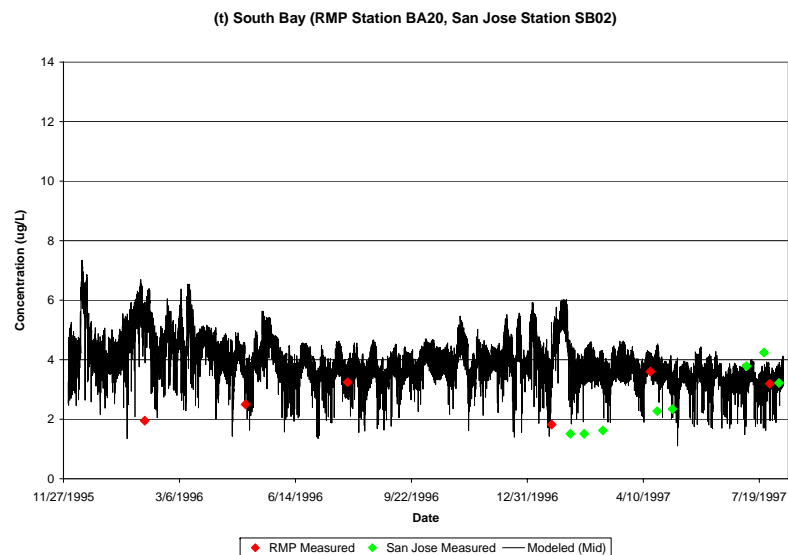
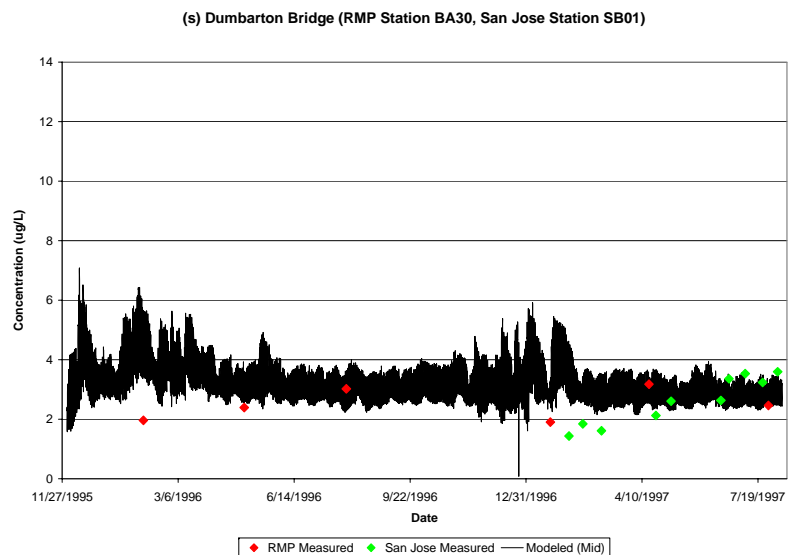
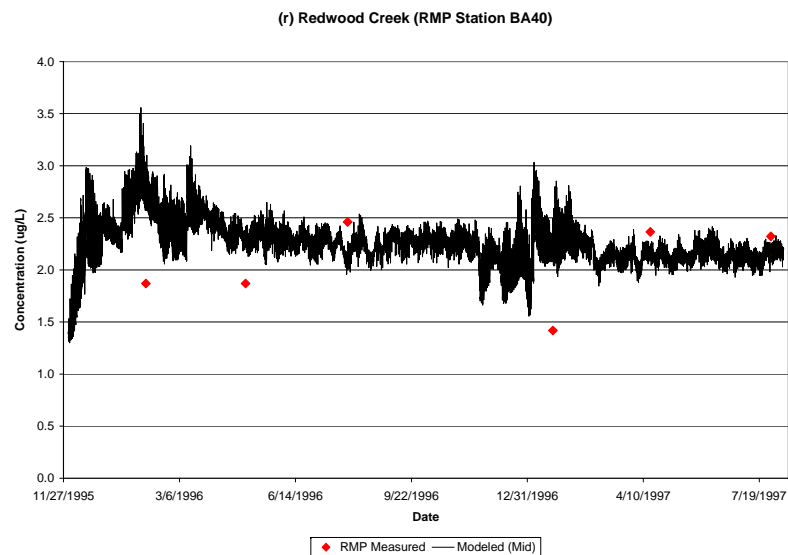
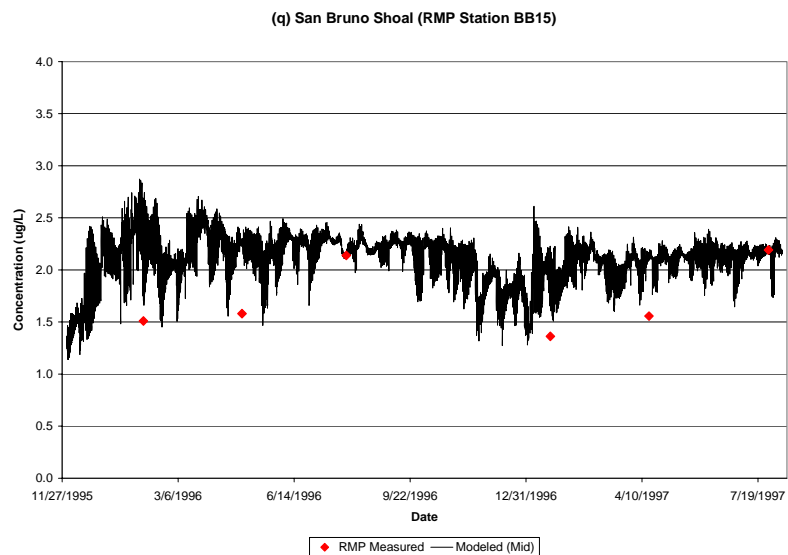
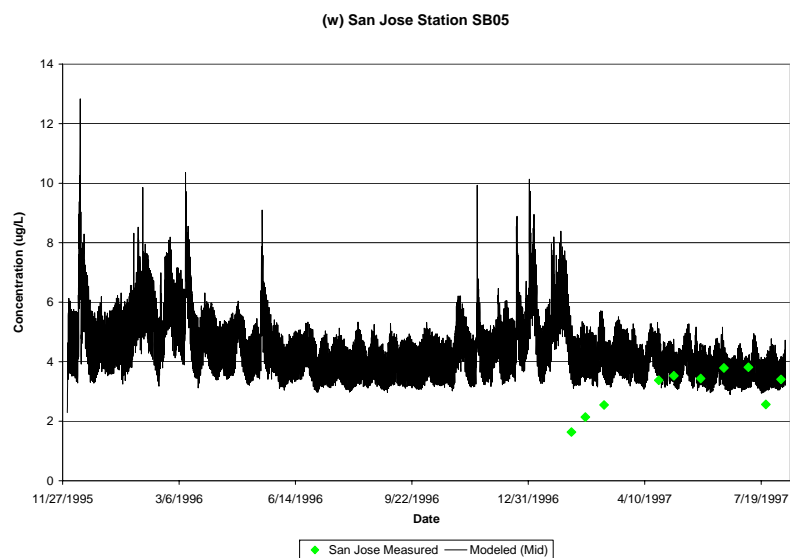
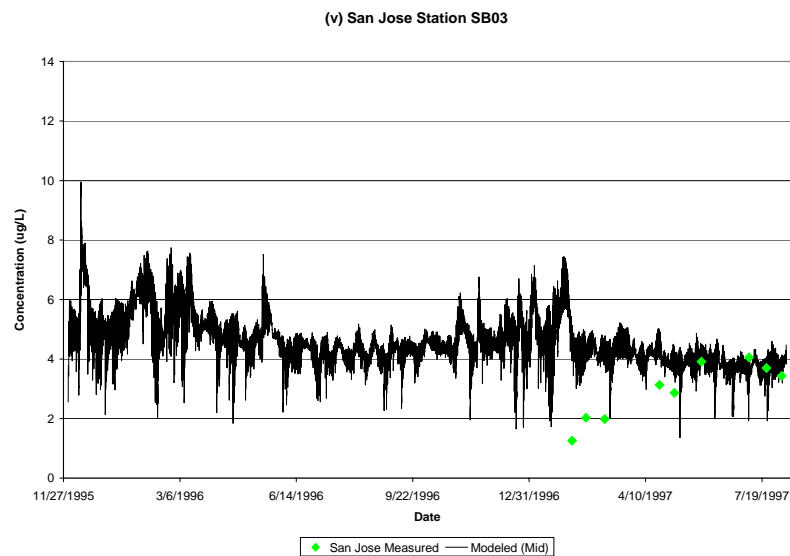
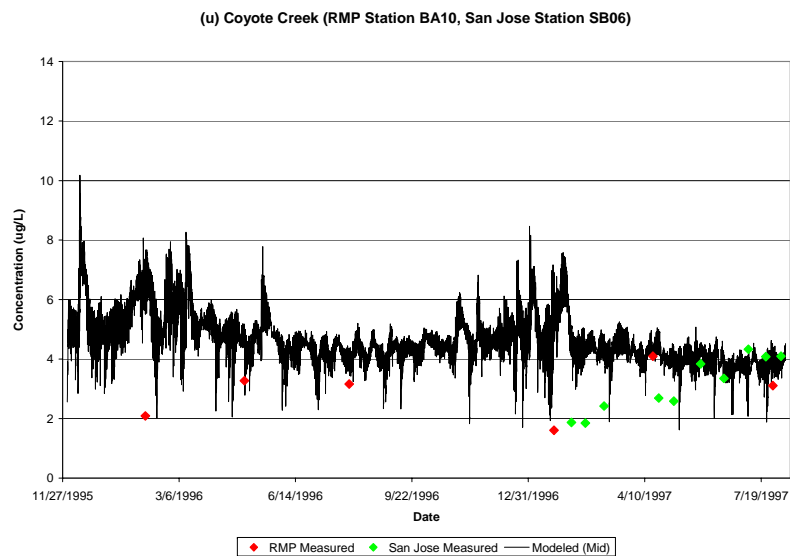
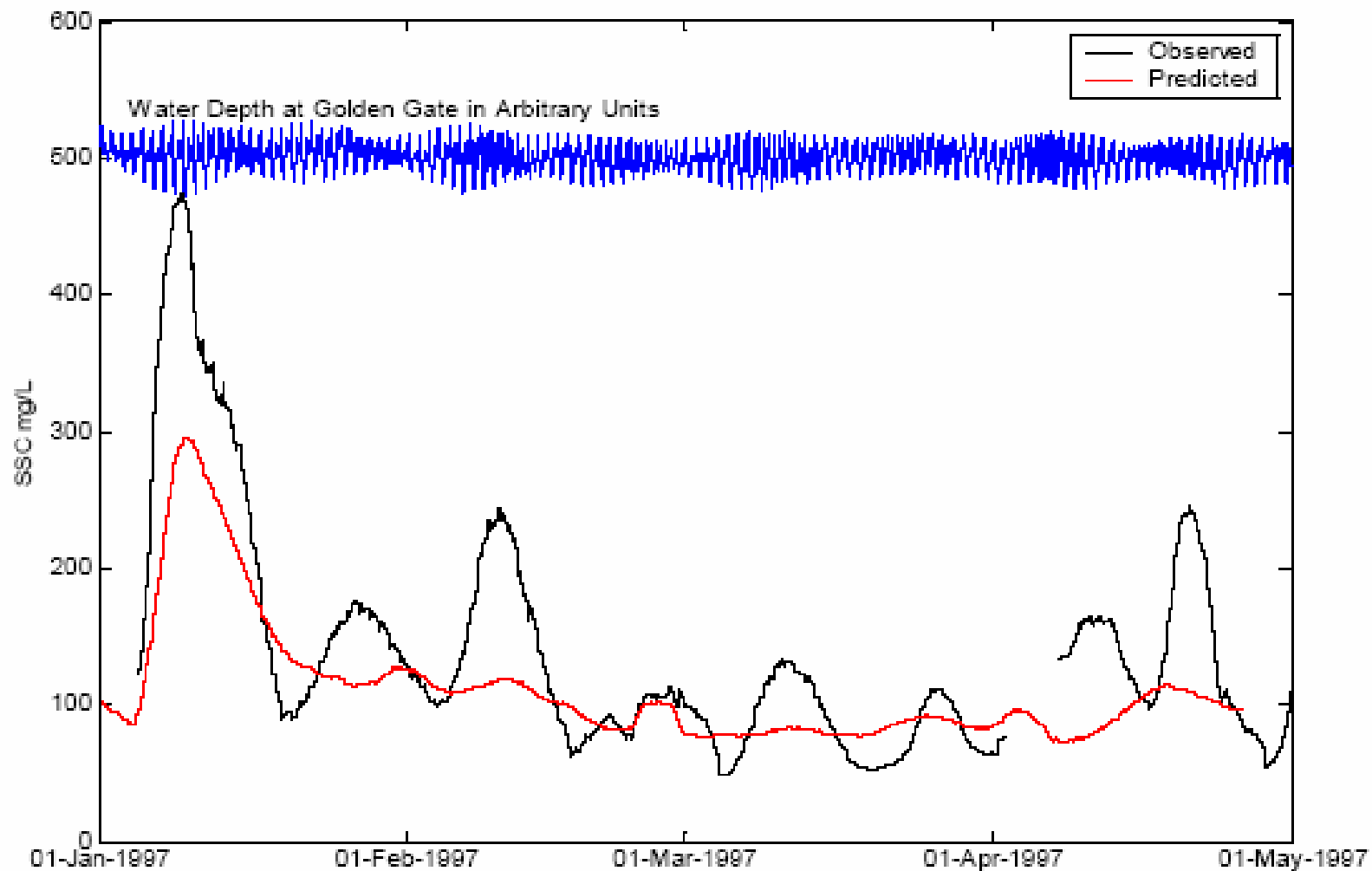


Figure 17. Comparison of Measured and Predicted Dissolved Copper Concentrations (continued)



Sources: San Jose 2007, SFEI 2007.



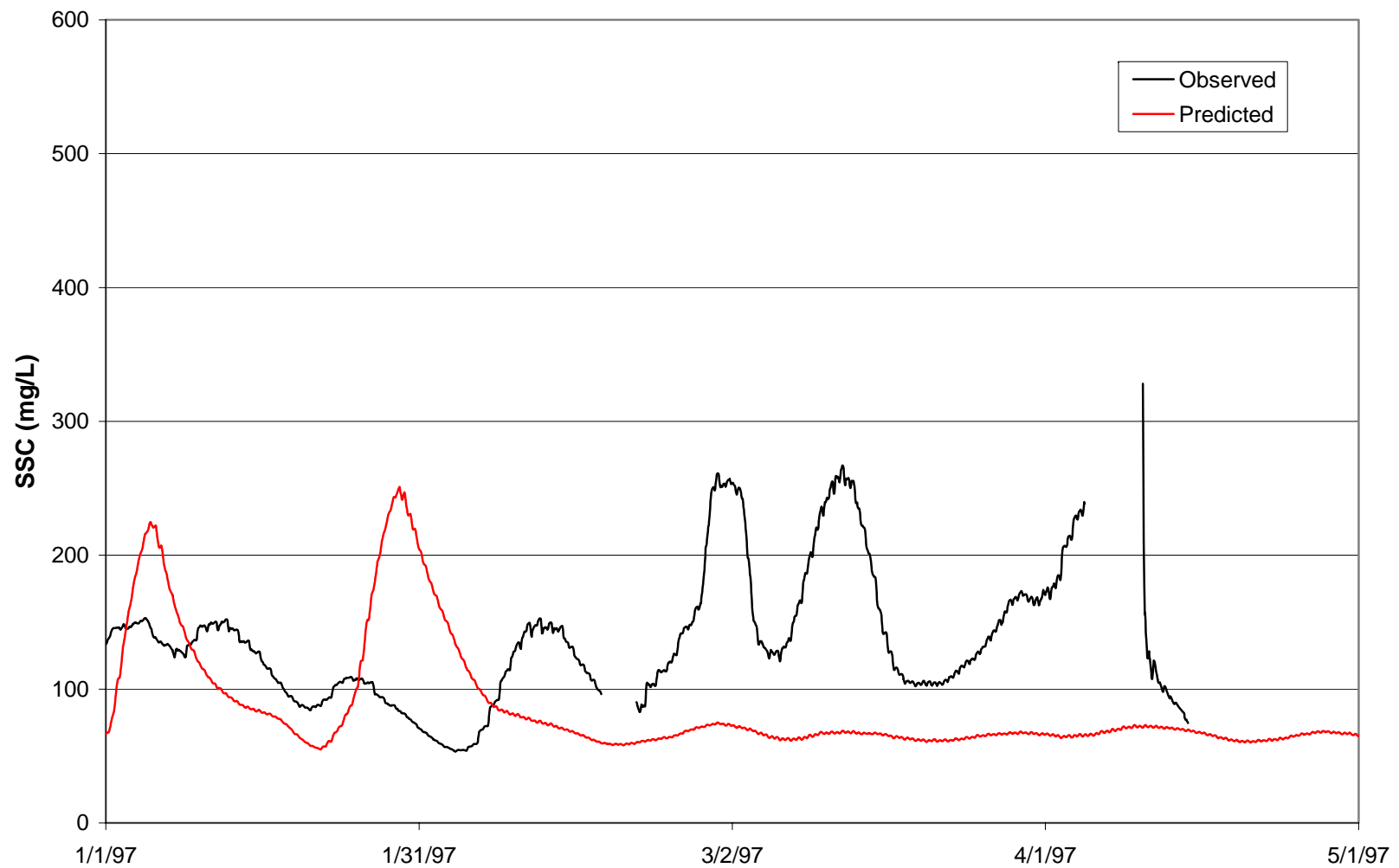
URS

Brake Pad
Partnership

26814617

Comparison of Observed and Predicted 4-Day
Running Average Suspended Sediment
Concentrations at Point San Pablo Station for 1997
Using 200-meter Model Output

FIGURE
18



URS

Brake Pad
Partnership

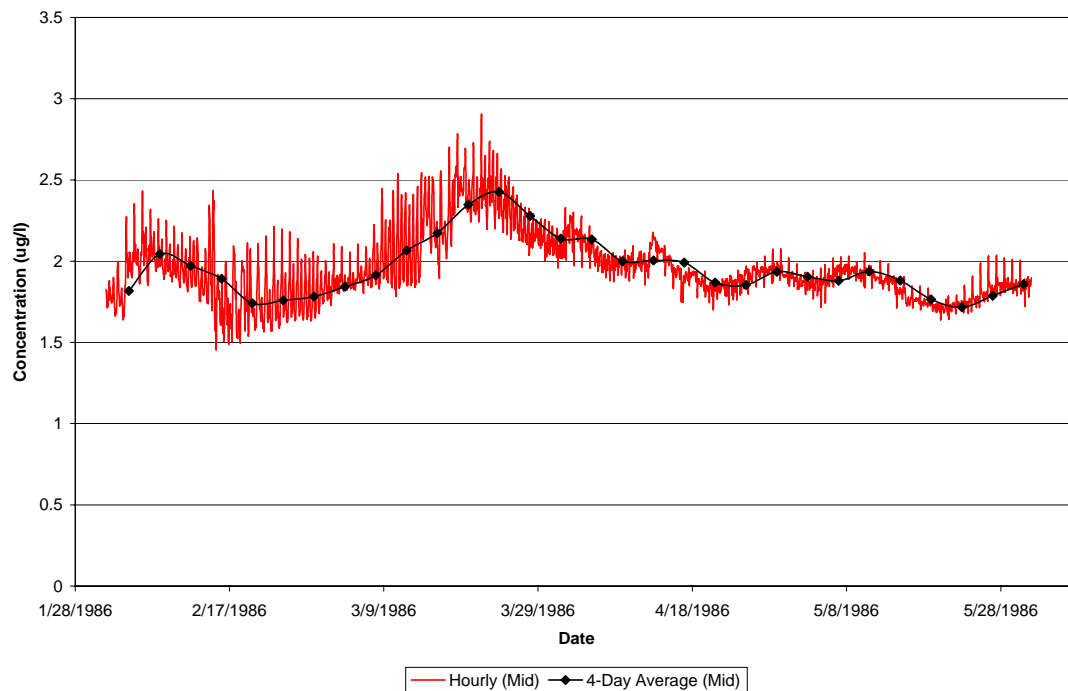
26814617

Comparison of Observed and Predicted 4-Day
Running Average Suspended Sediment
Concentrations at Dumbarton Bridge Station for 1997
Using 330-meter Model Output

FIGURE
19

Figure 20. Comparison of Selected Hourly and Average Copper Concentration Data at Redwood Creek

(a) Dissolved Copper



(b) Benthic Copper

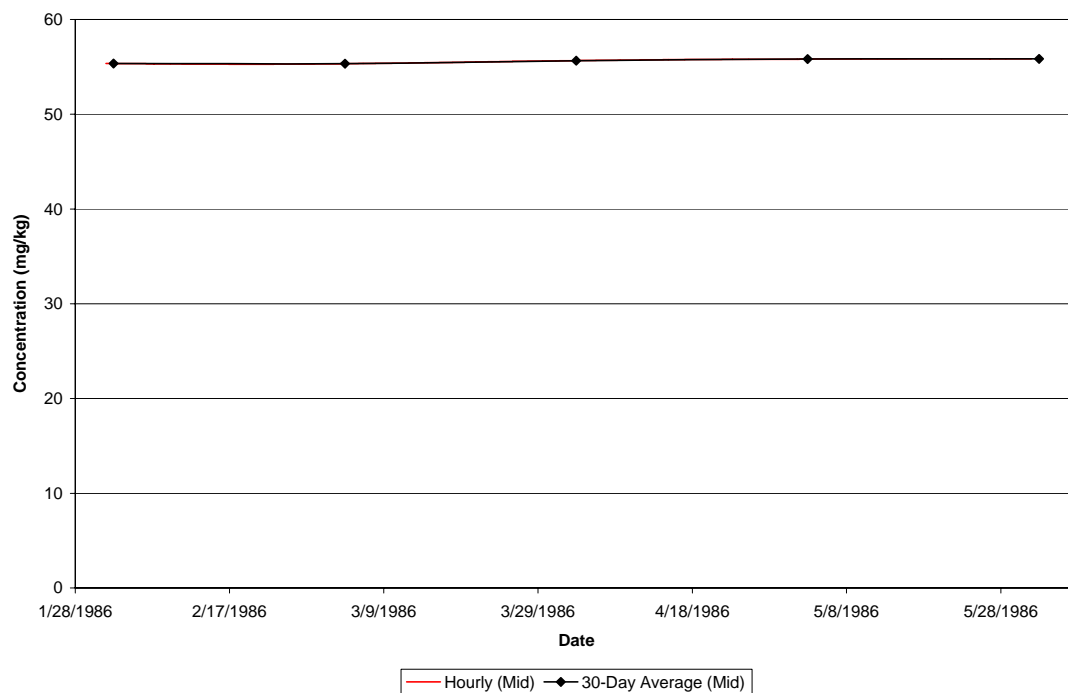


Figure 21. Dissolved Copper Concentrations for Mid and Mid-No-BP Modeled Scenarios

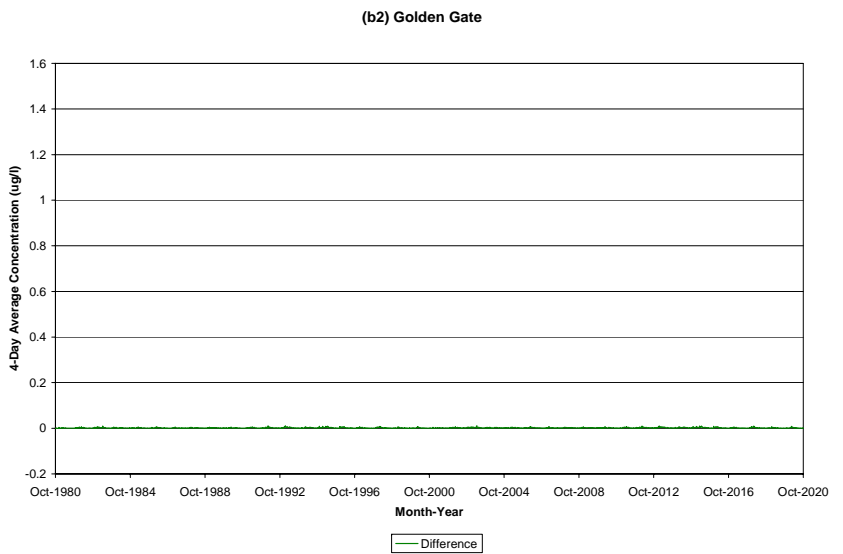
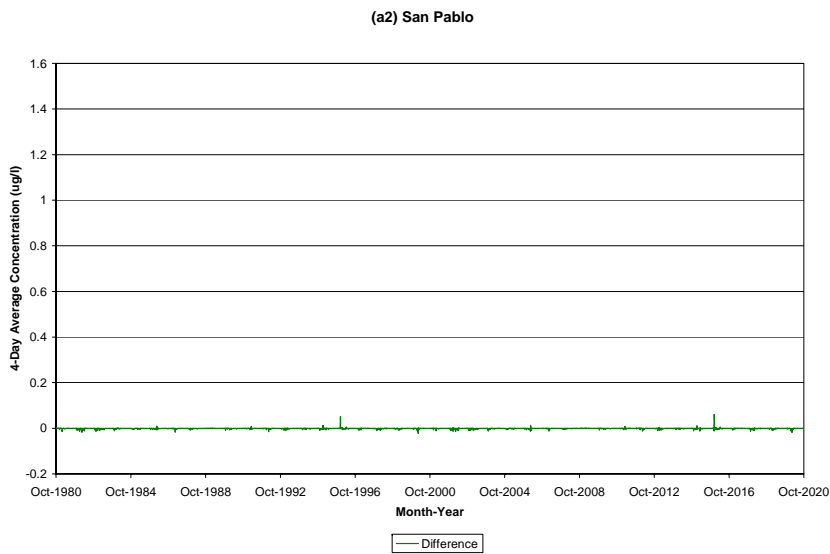
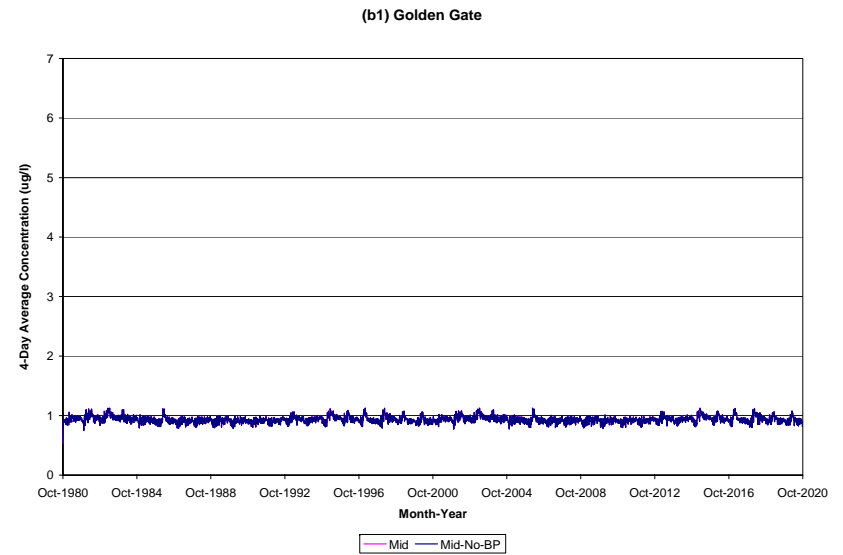
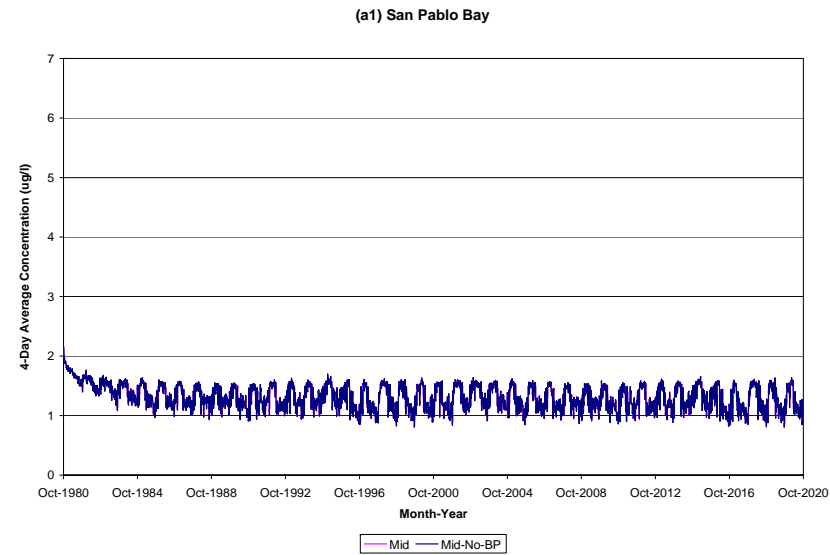


Figure 21. Dissolved Copper Concentrations for Mid and Mid-No-BP Modeled Scenarios (continued)

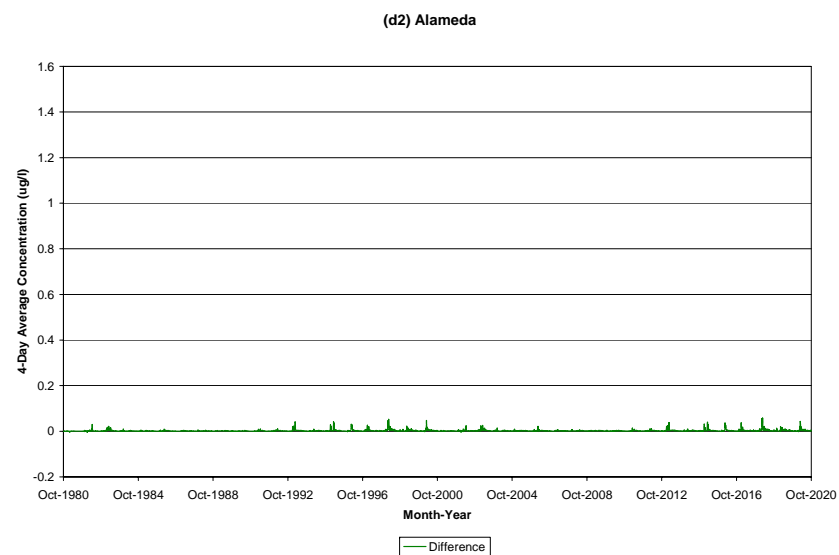
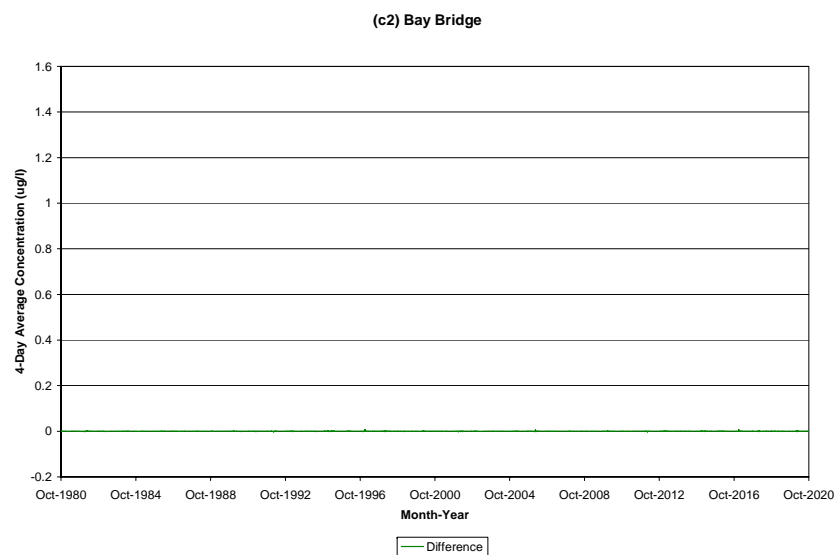
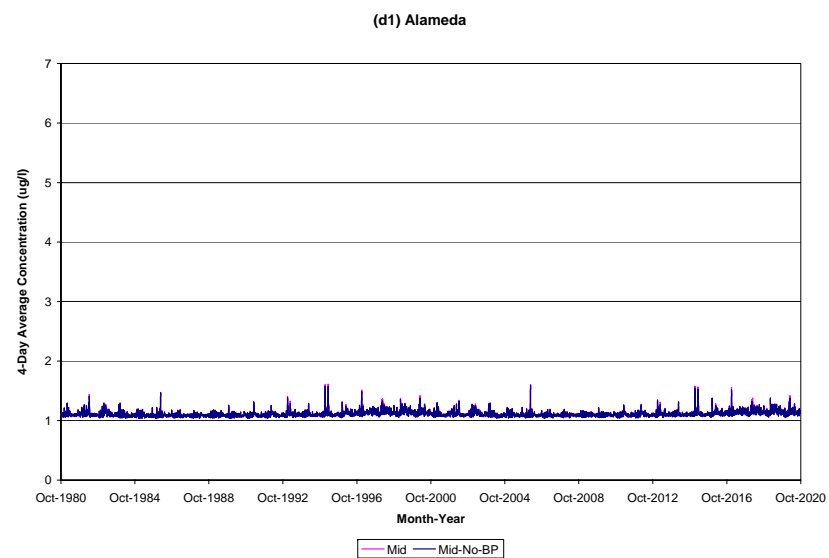
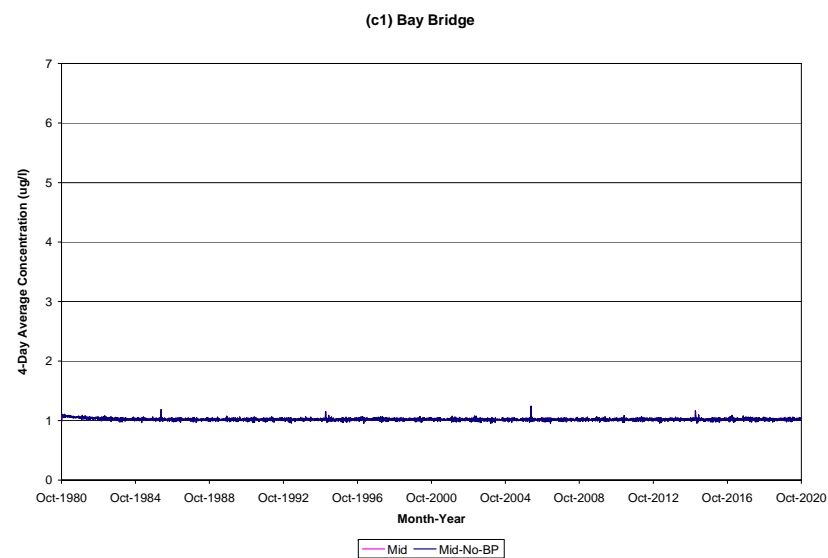


Figure 21. Dissolved Copper Concentrations for Mid and Mid-No-BP Modeled Scenarios (continued)

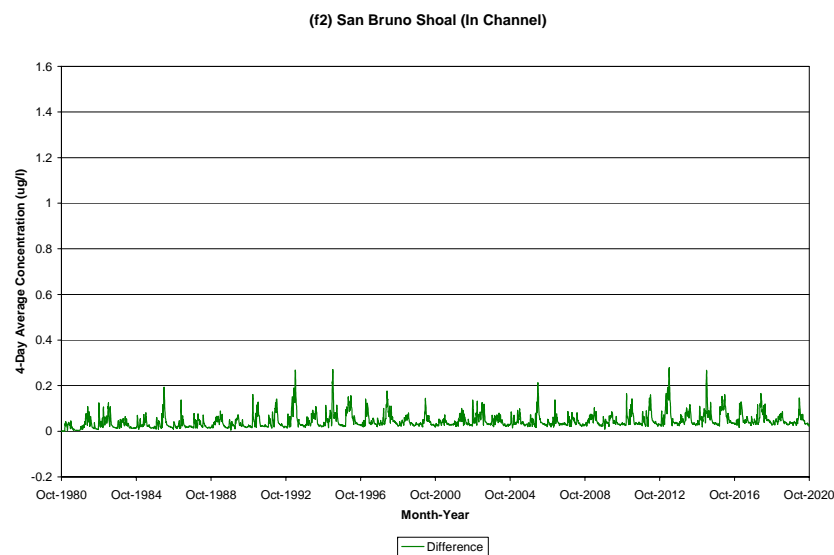
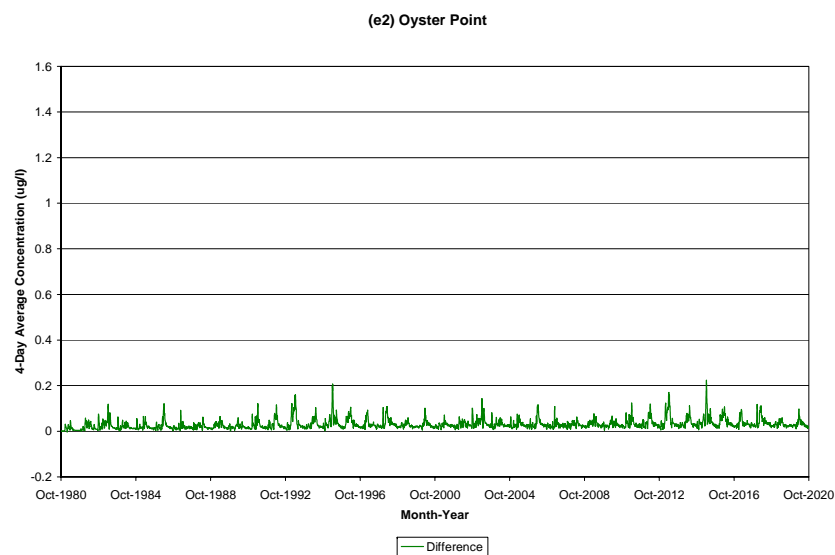
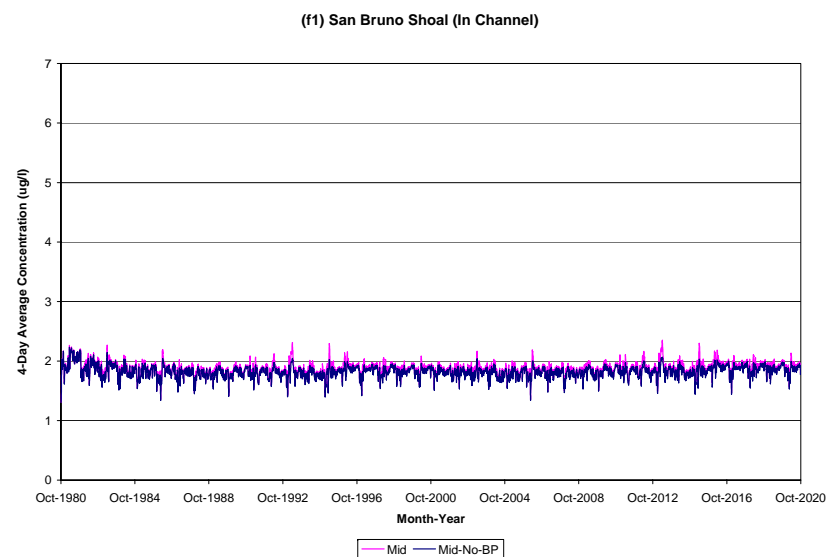
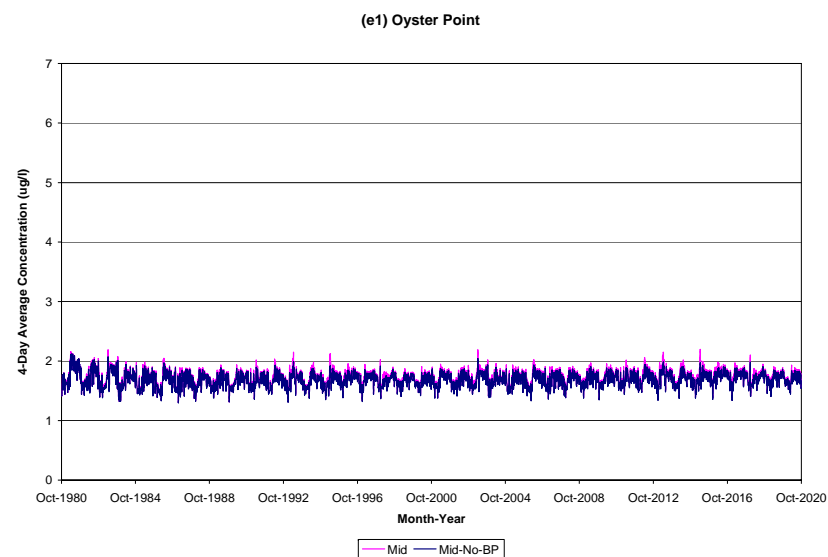


Figure 21. Dissolved Copper Concentrations for Mid and Mid-No-BP Modeled Scenarios (continued)

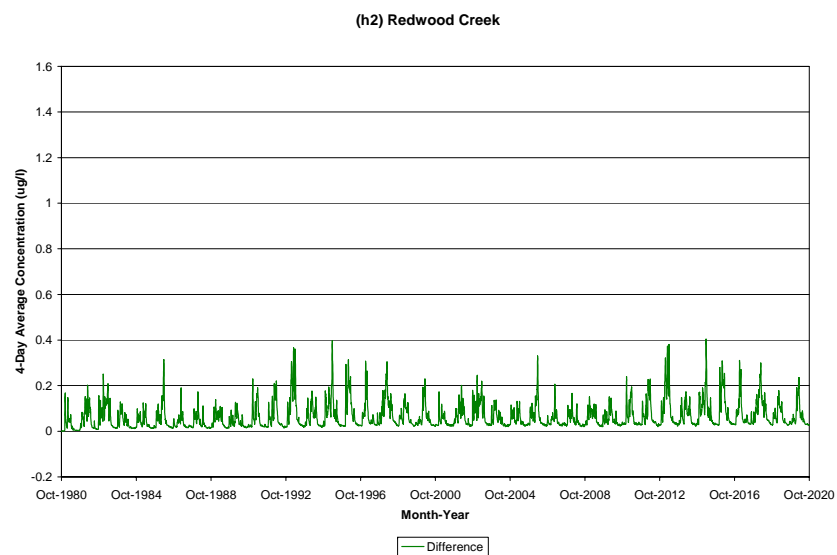
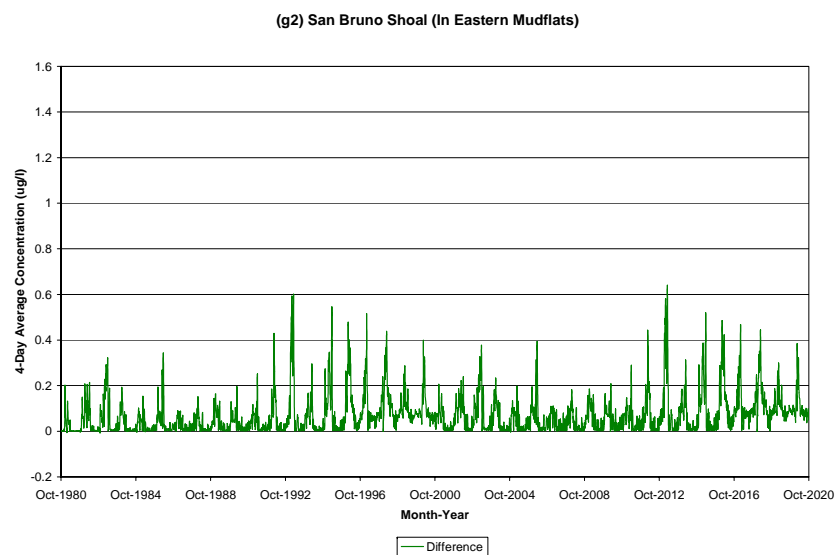
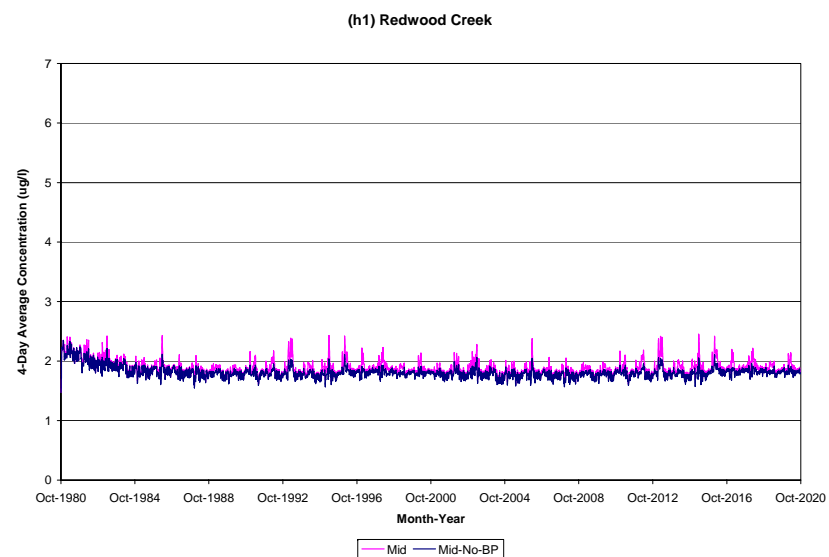
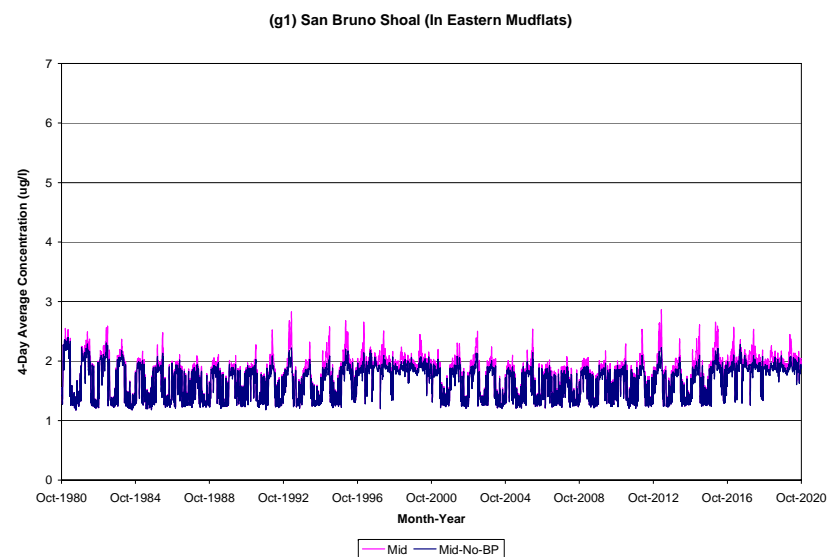


Figure 21. Dissolved Copper Concentrations for Mid and Mid-No-BP Modeled Scenarios (continued)

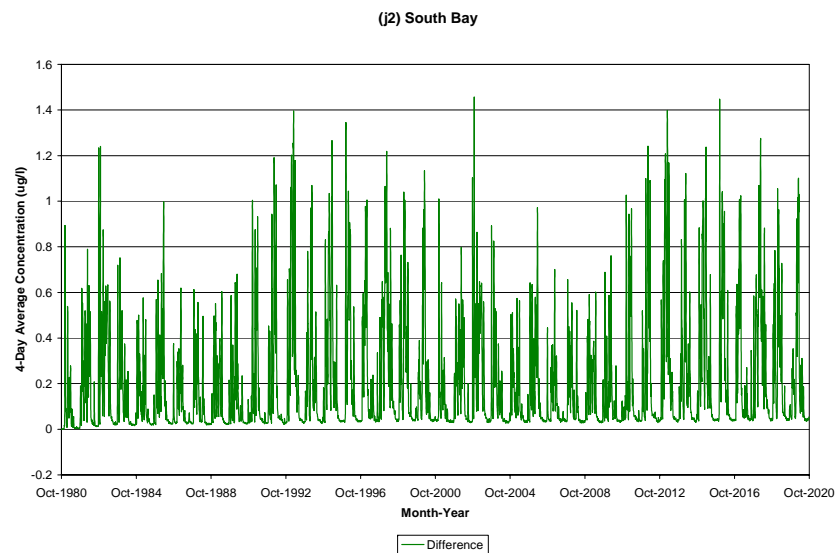
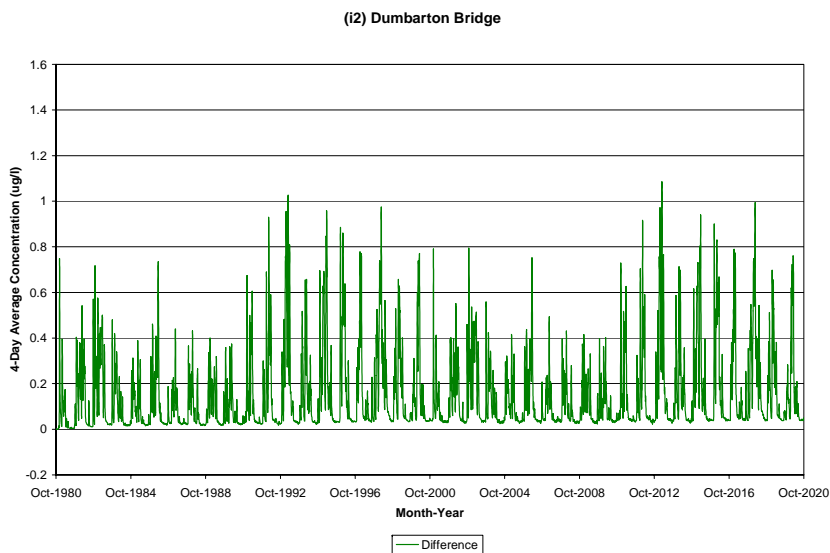
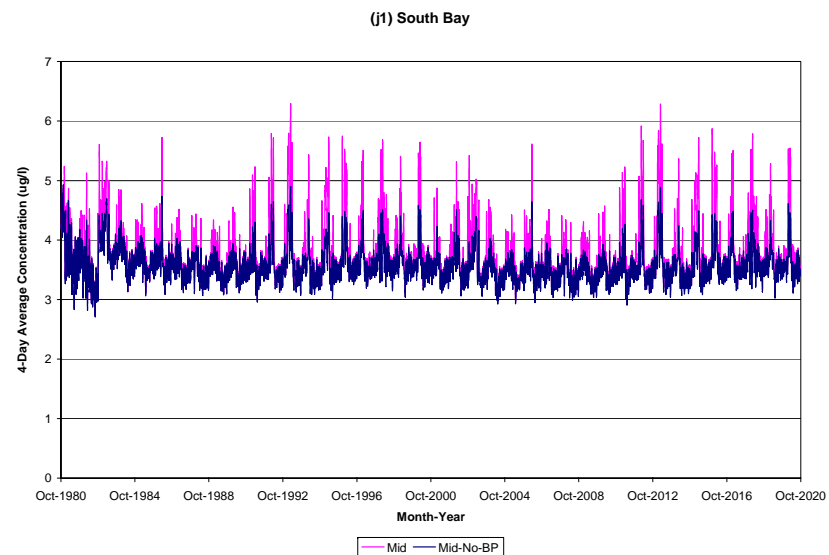
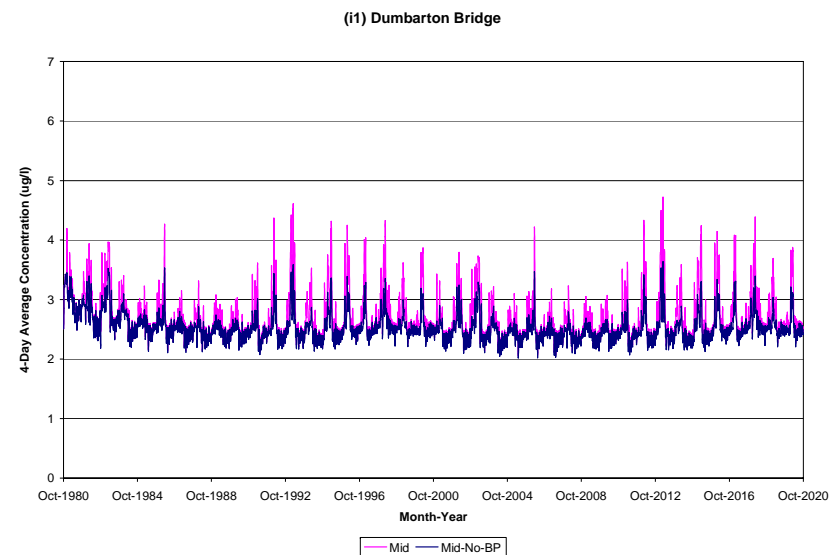


Figure 21. Dissolved Copper Concentrations for Mid and Mid-No-BP Modeled Scenarios (continued)

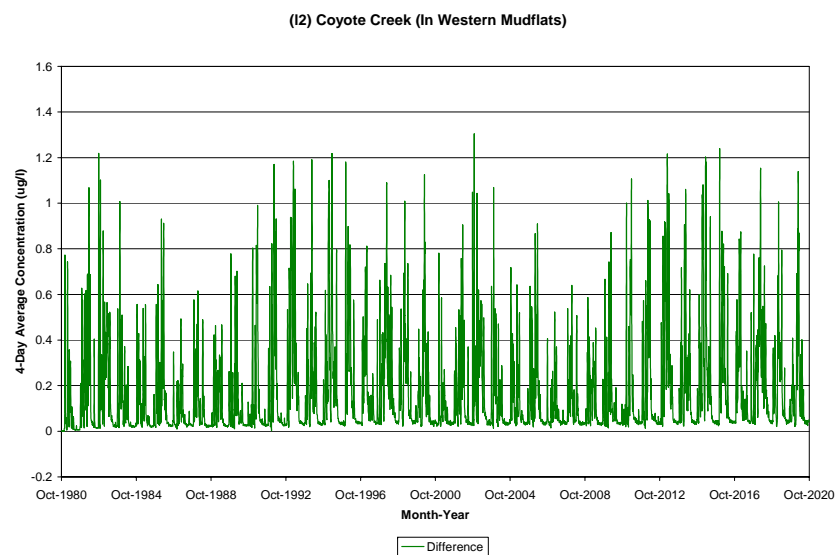
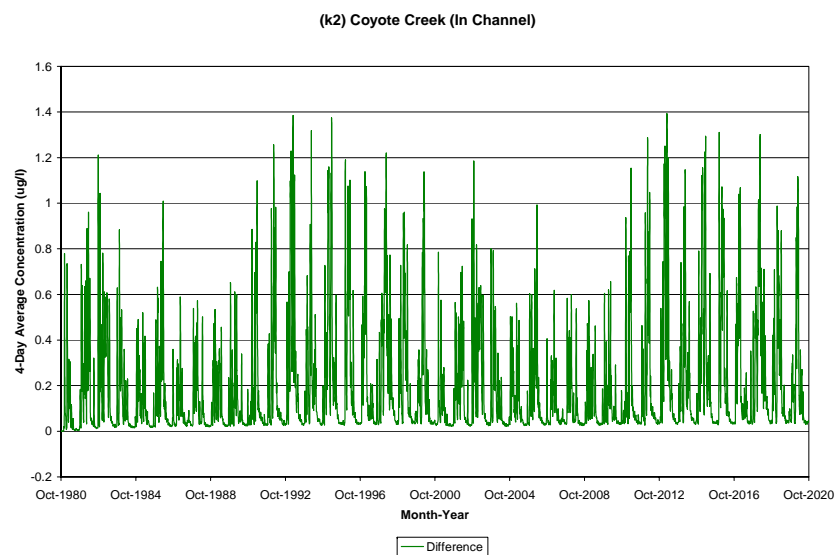
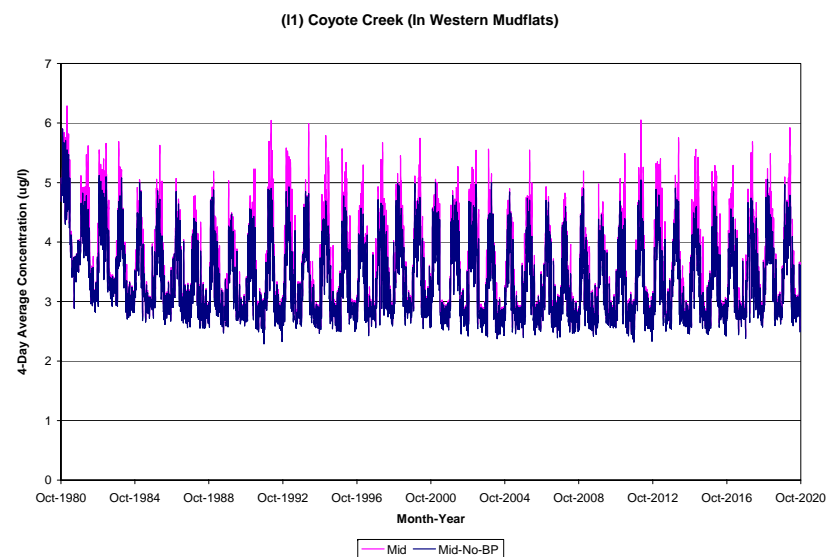
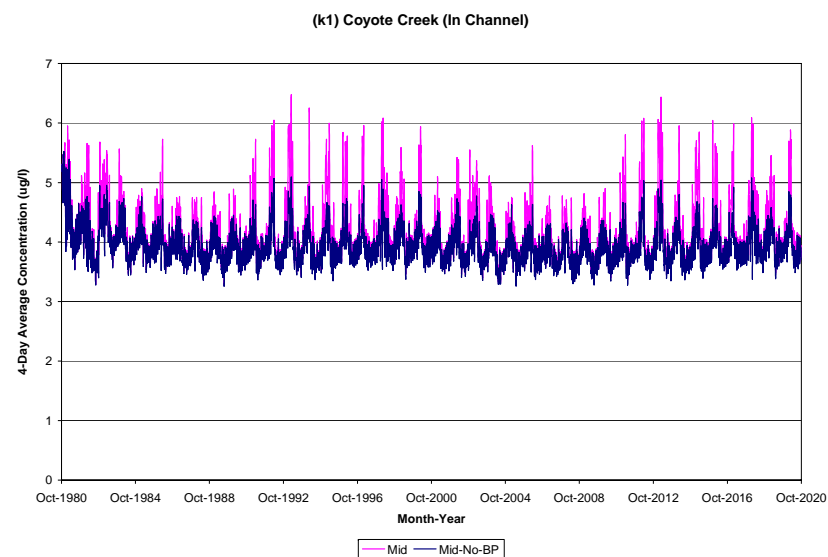


Figure 22. Benthic Copper Concentrations for Mid and Mid-No-BP Modeled Scenarios

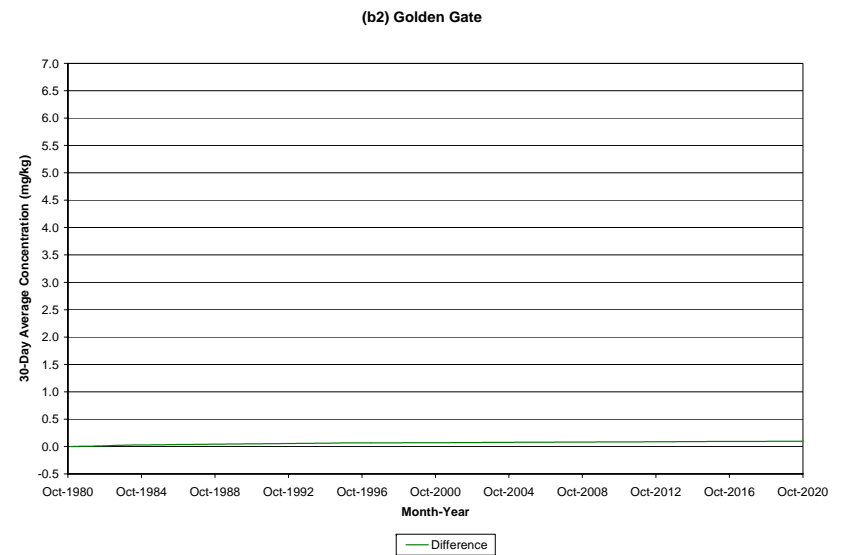
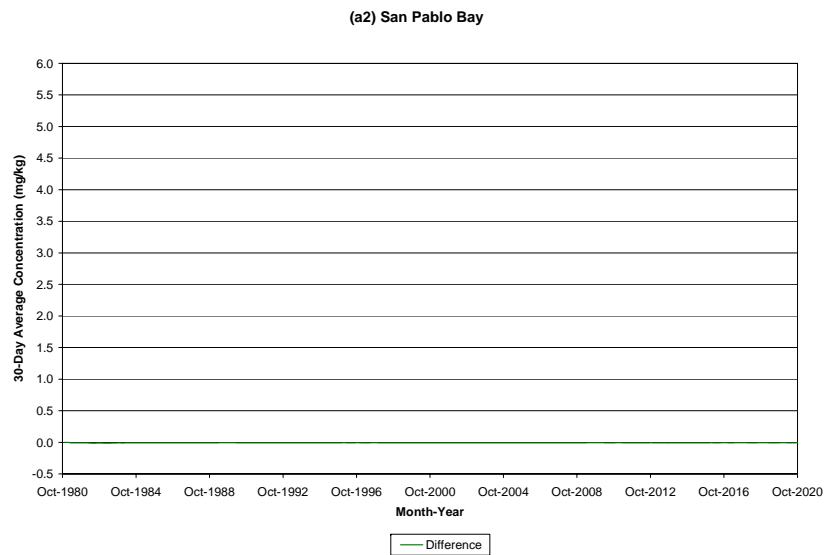
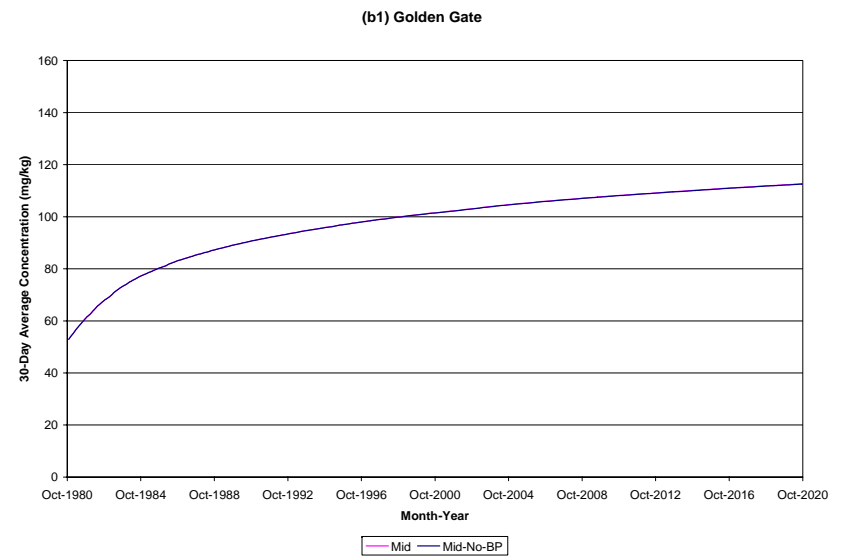
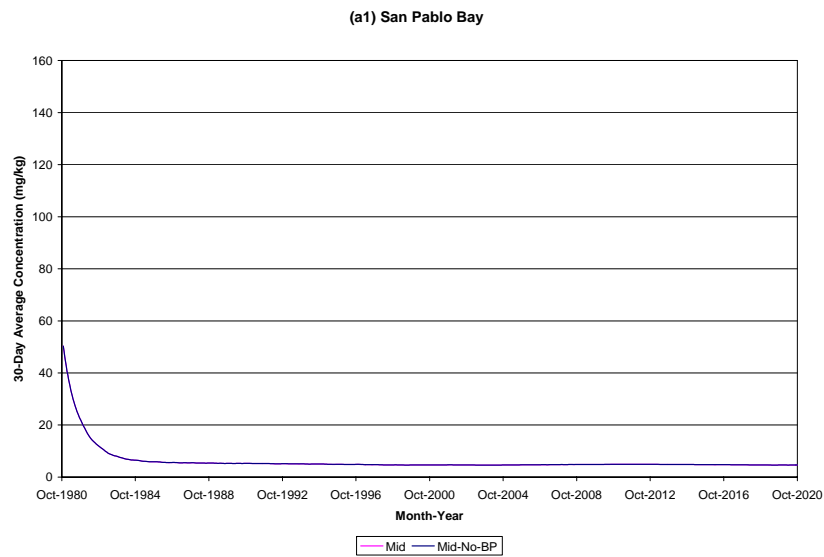


Figure 22. Benthic Copper Concentrations for Mid and Mid-No-BP Modeled Scenarios (continued)

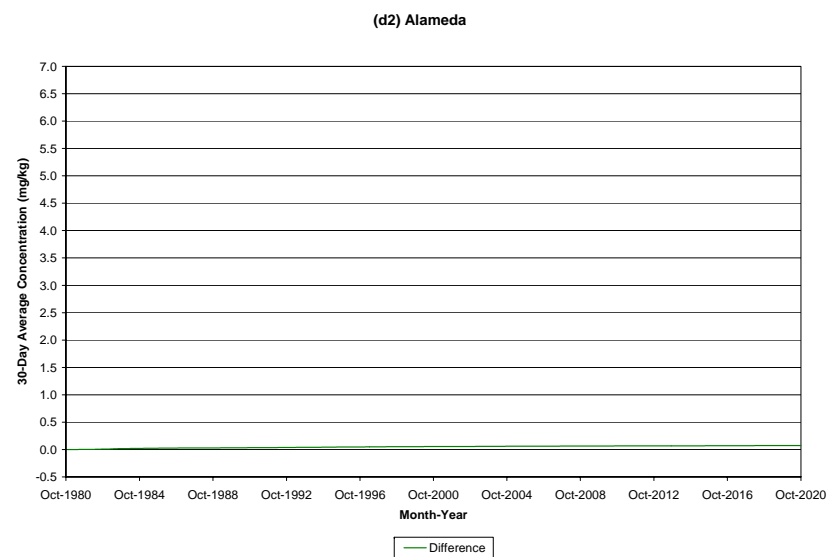
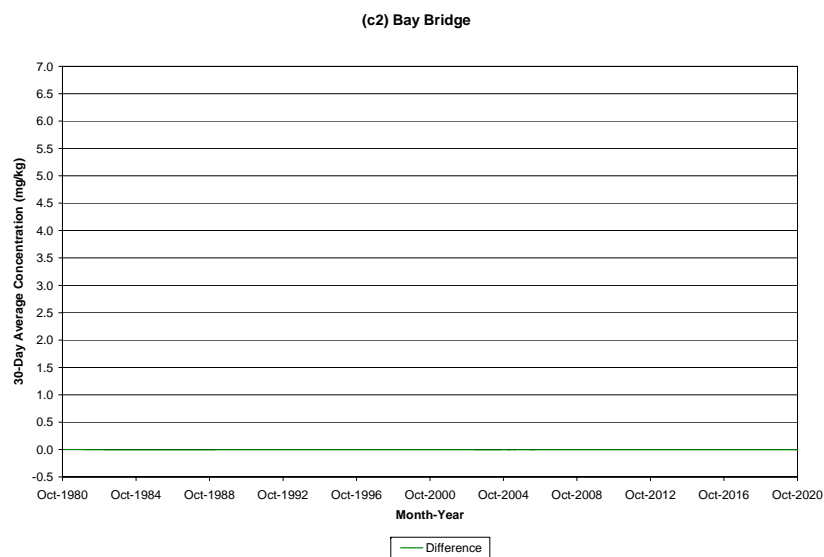
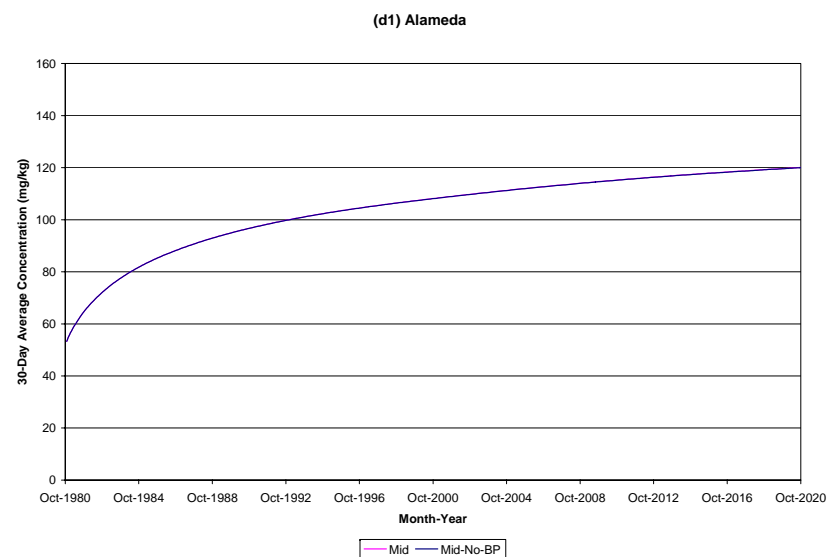
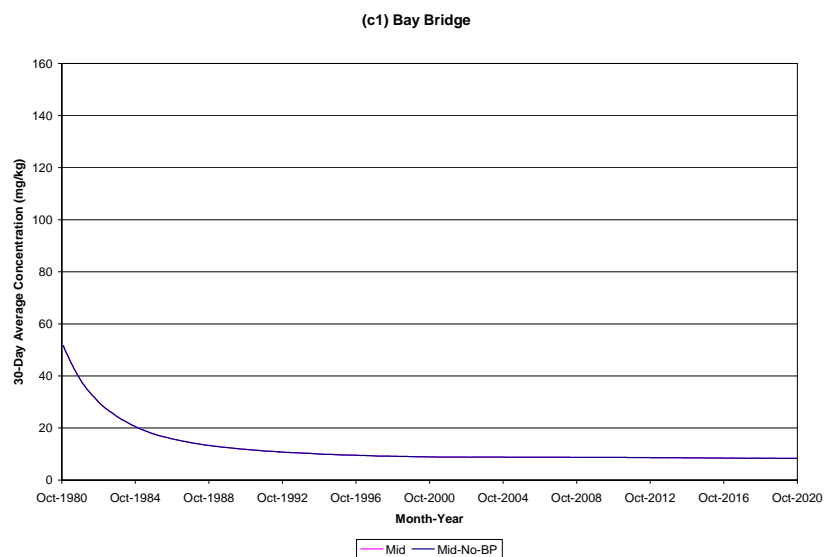


Figure 22. Benthic Copper Concentrations for Mid and Mid-No-BP Modeled Scenarios (continued)

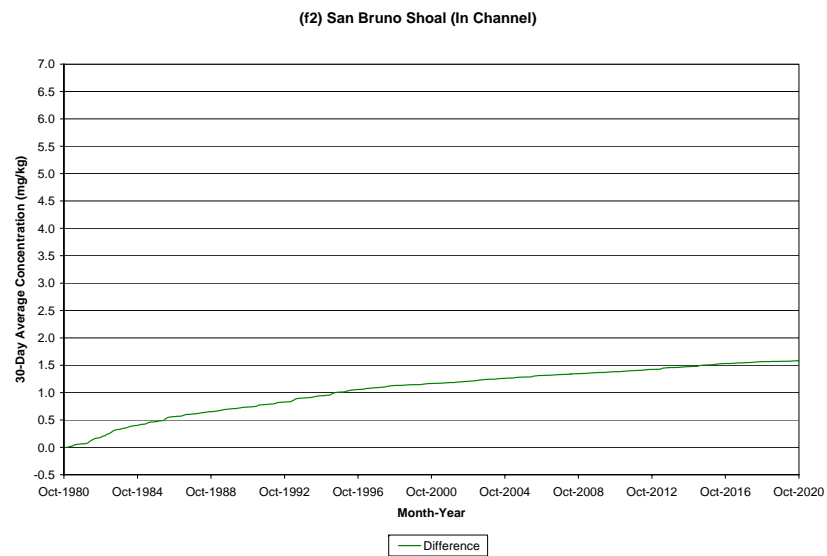
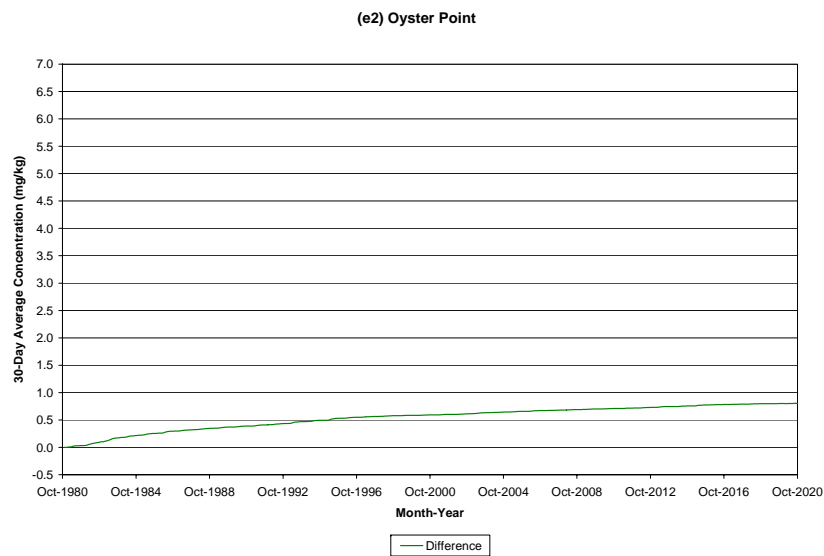
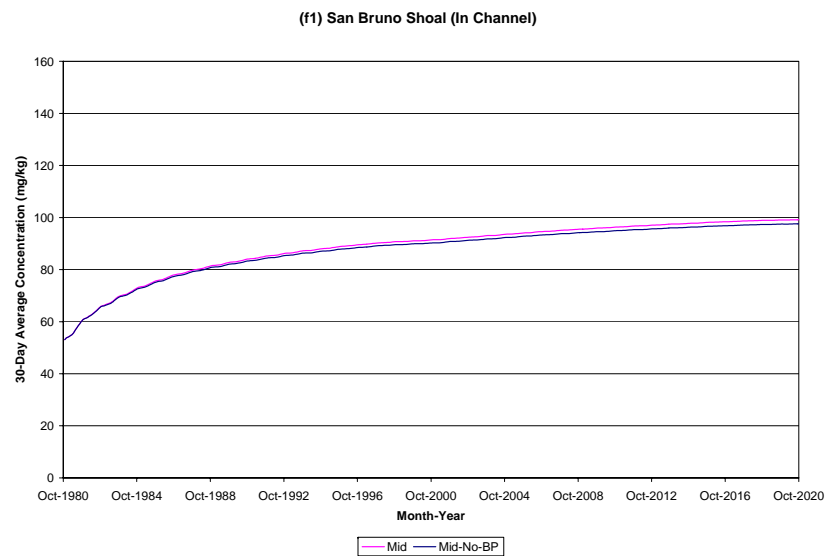
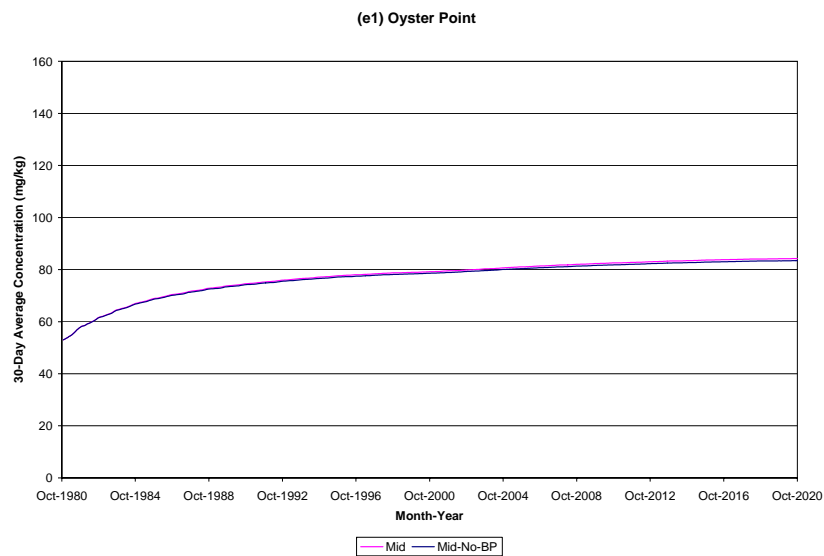


Figure 22. Benthic Copper Concentrations for Mid and Mid-No-BP Modeled Scenarios (continued)

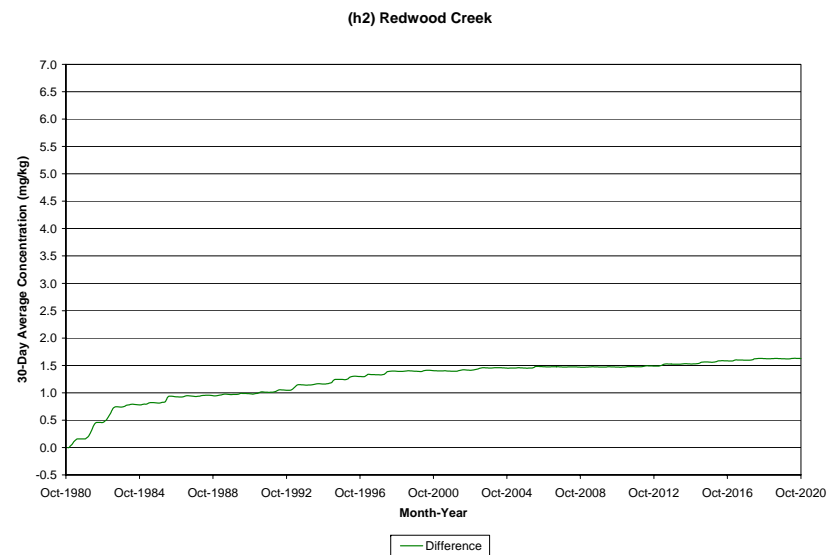
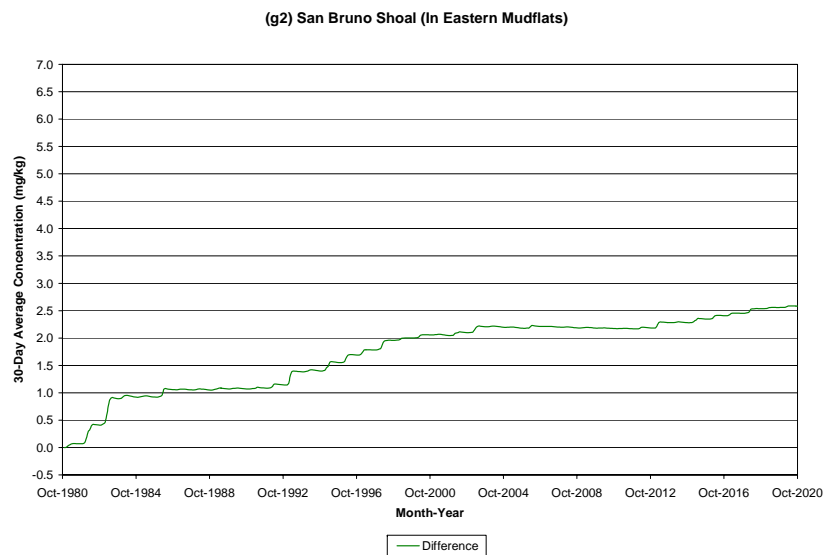
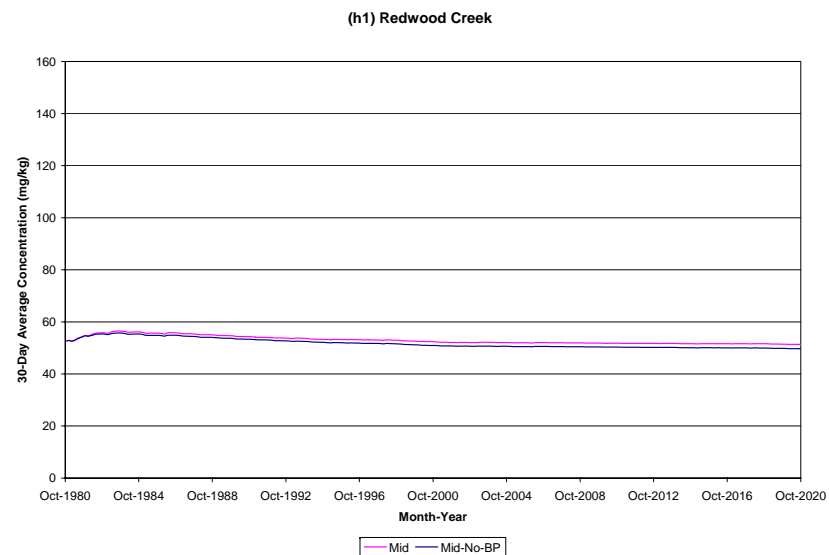
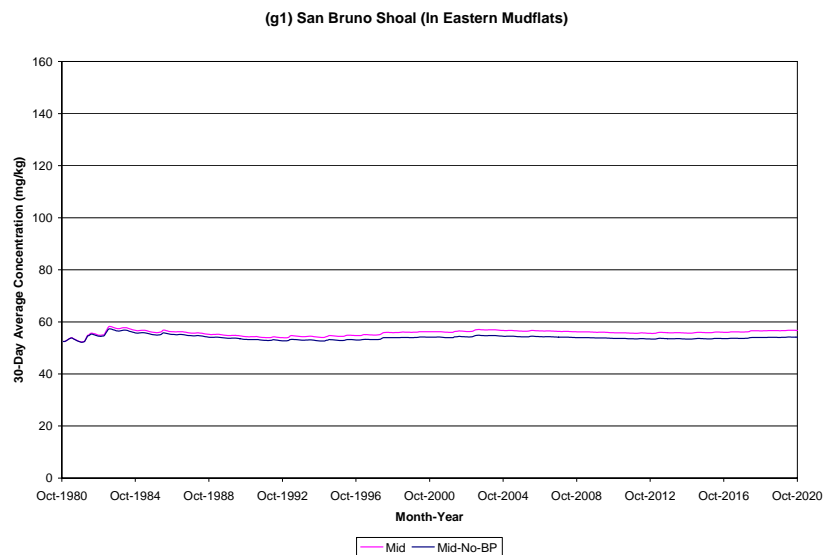


Figure 22. Benthic Copper Concentrations for Mid and Mid-No-BP Modeled Scenarios (continued)

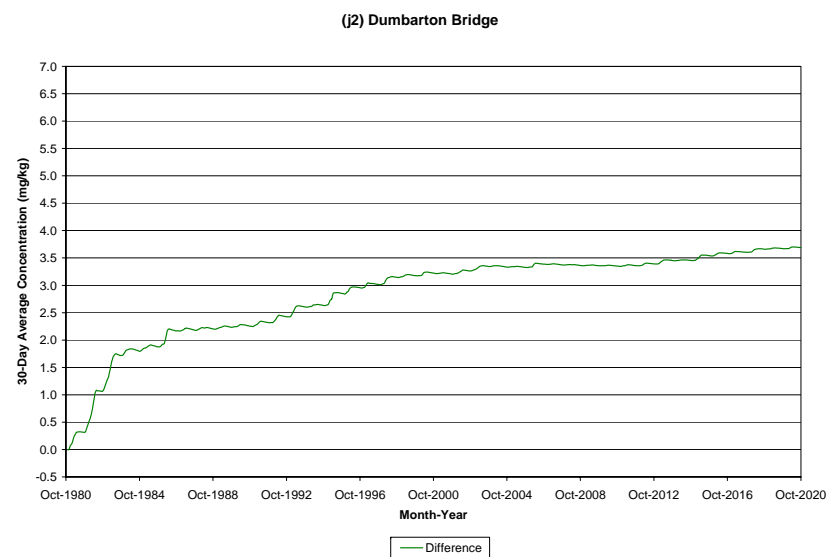
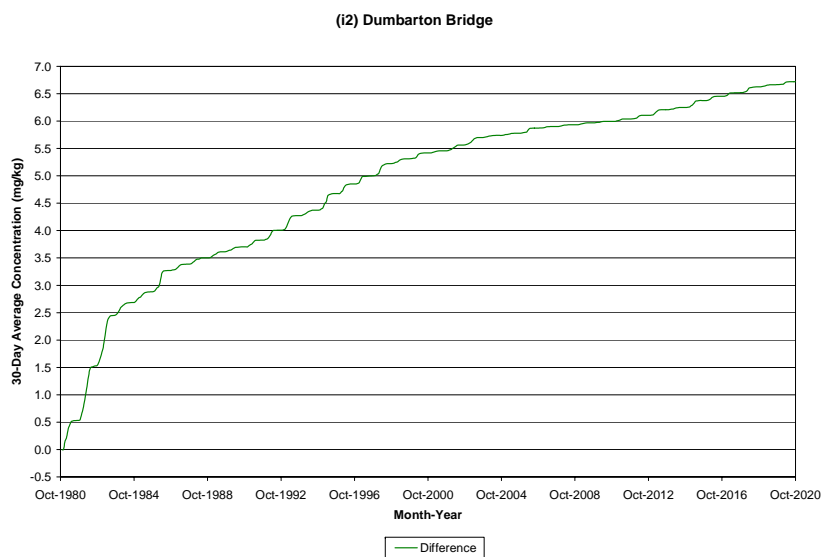
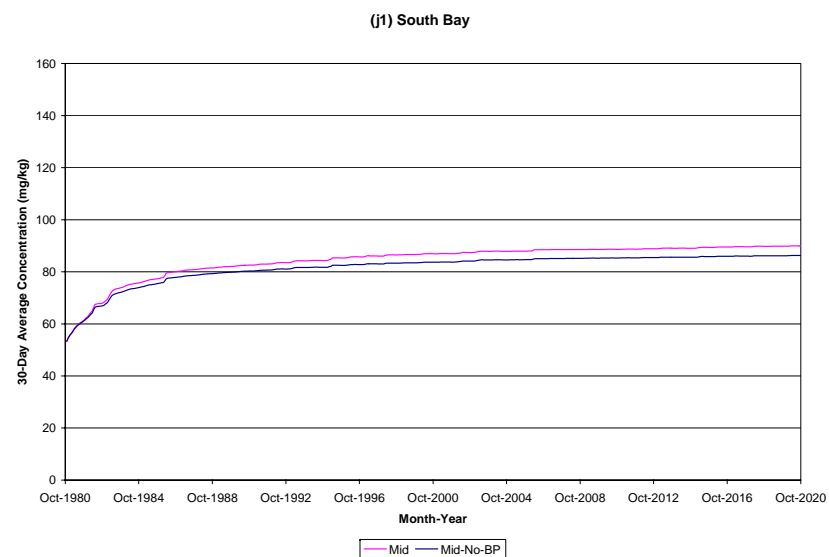
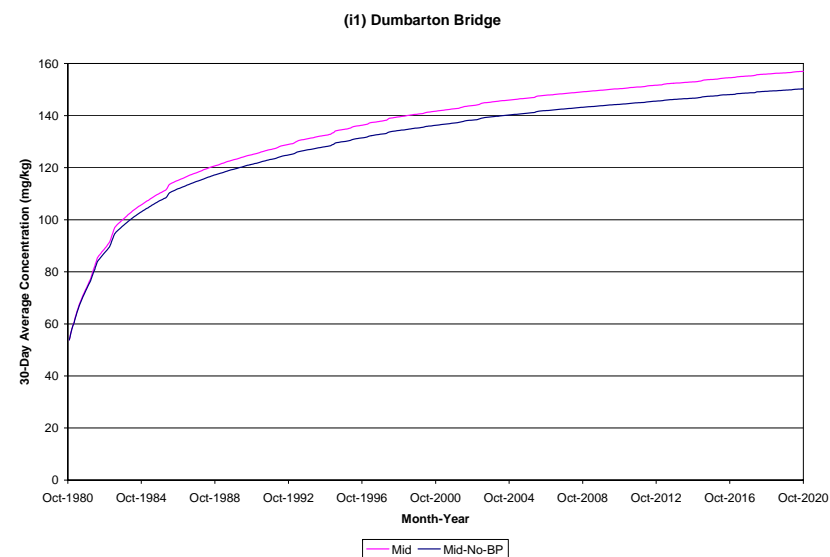


Figure 22. Benthic Copper Concentrations for Mid and Mid-No-BP Modeled Scenarios (continued)

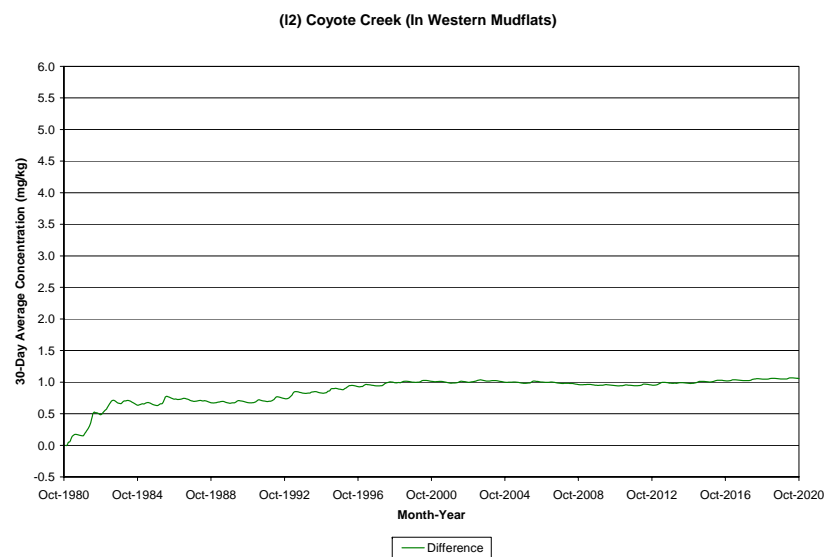
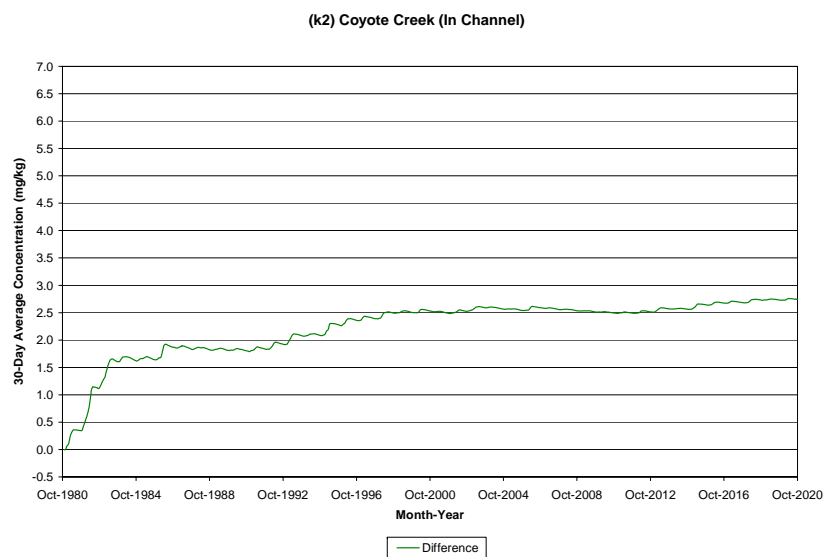
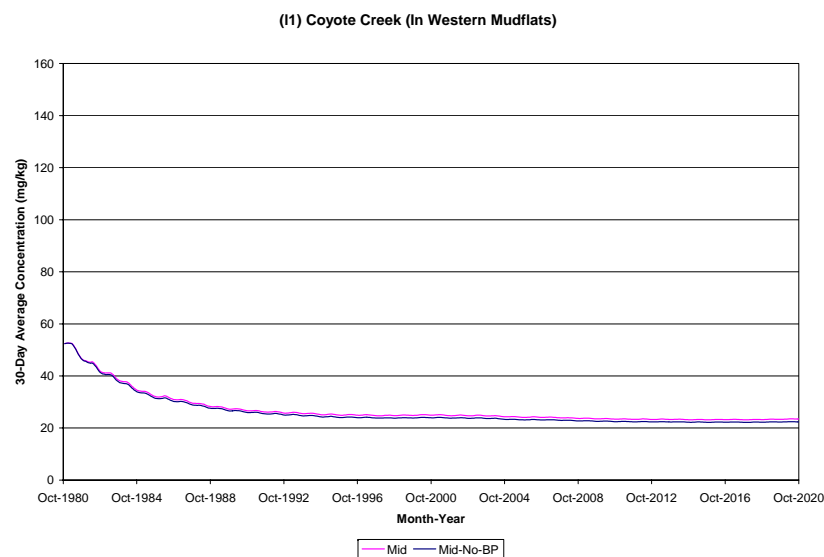
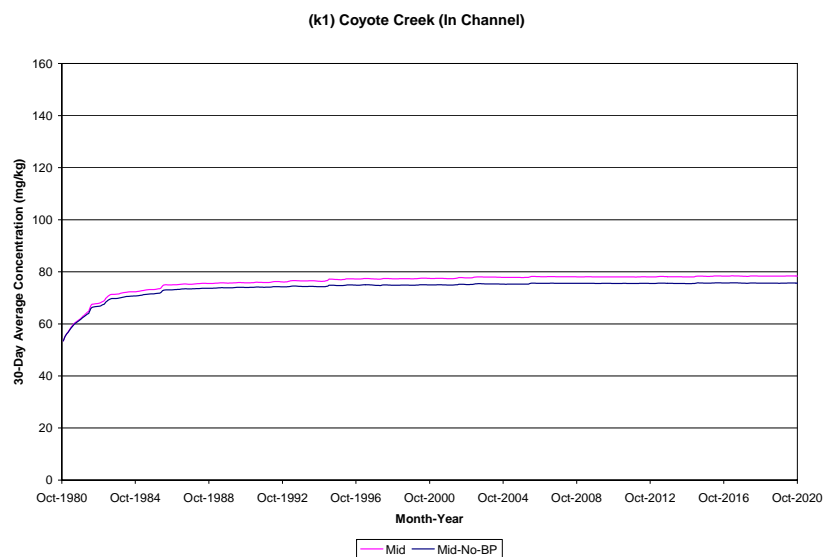


Figure 23. Cumulative Probabilities for Mid and Mid-No-BP Modeled Scenarios

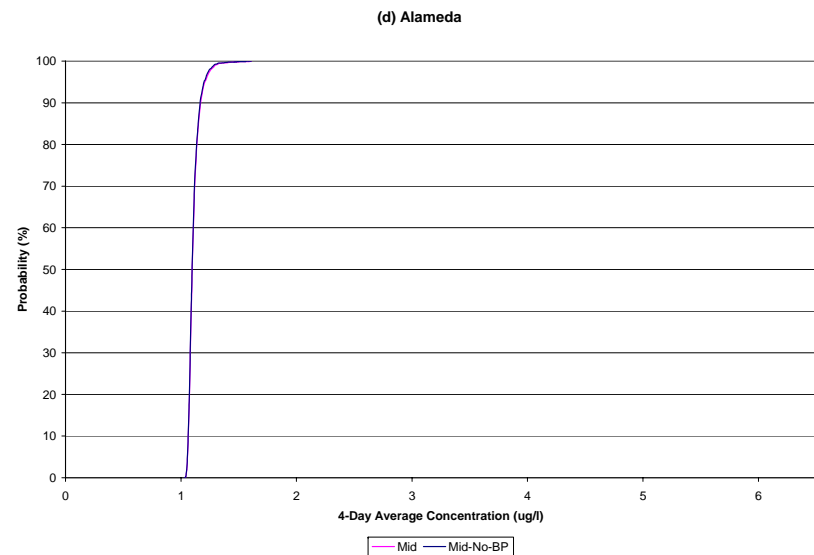
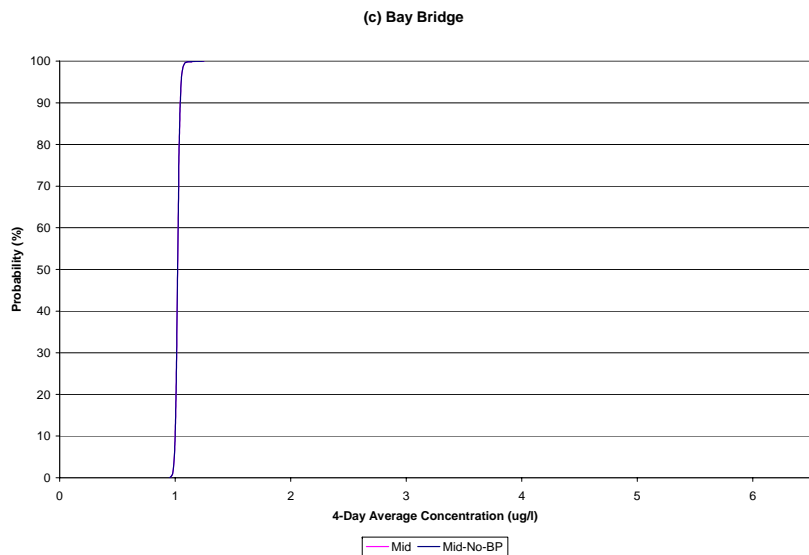
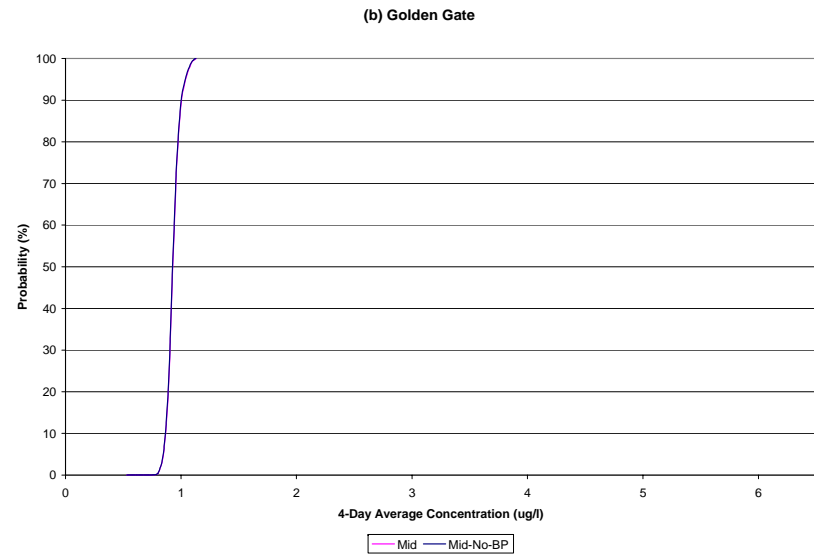
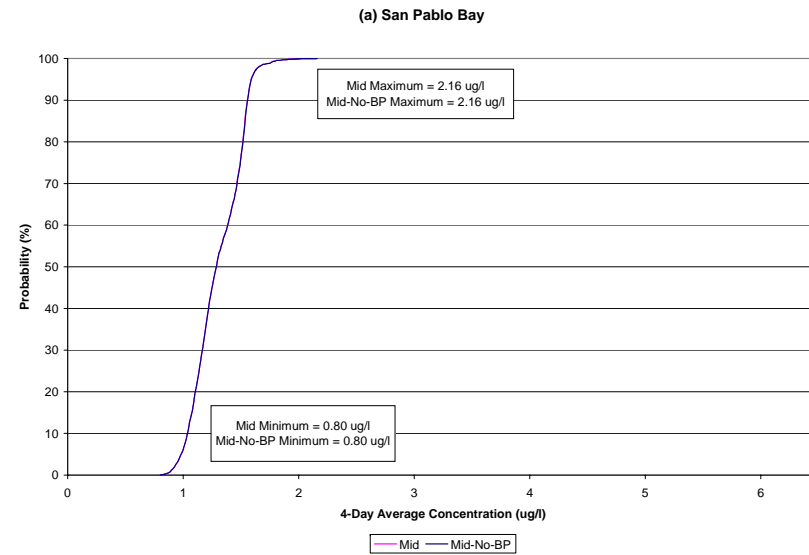


Figure 23. Cumulative Probabilities for Mid and Mid-No-BP Modeled Scenarios (continued)

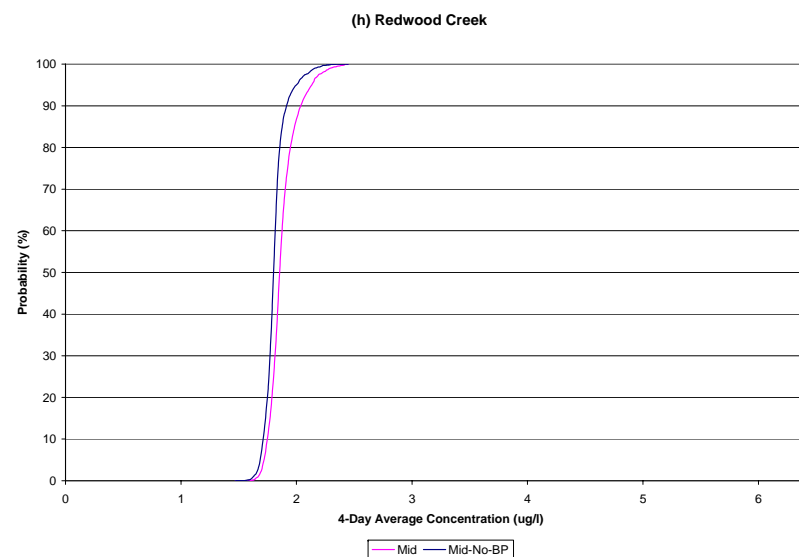
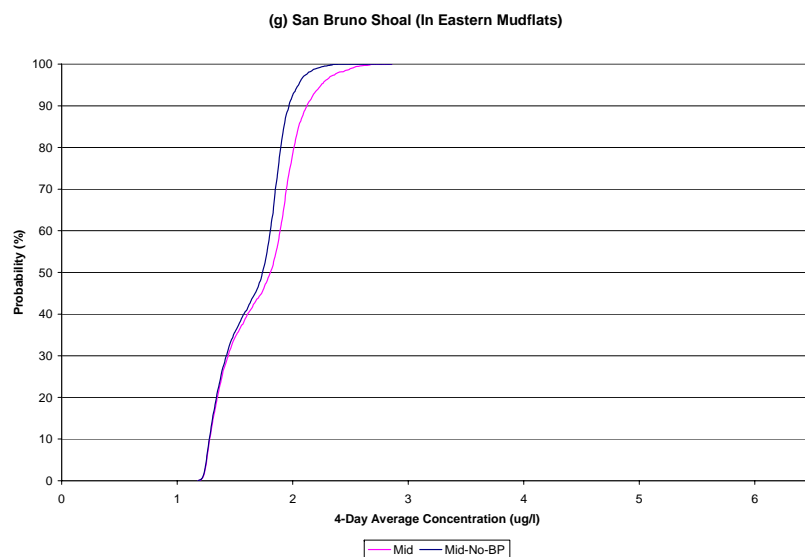
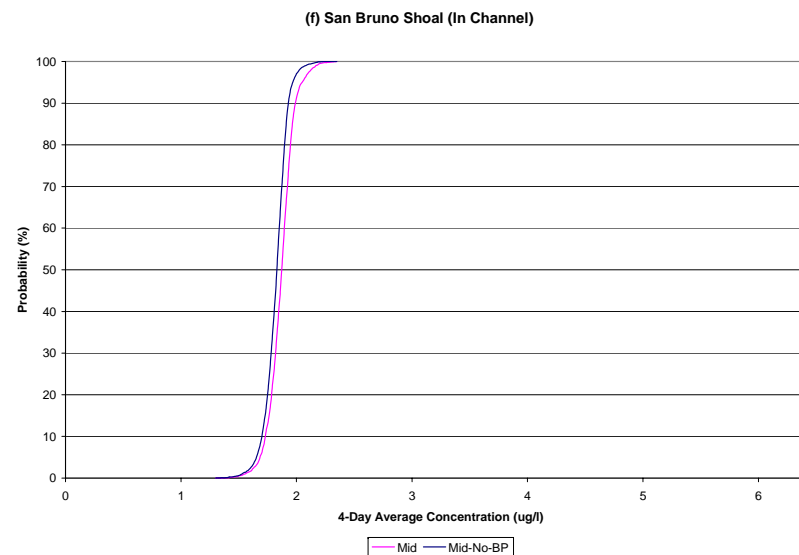
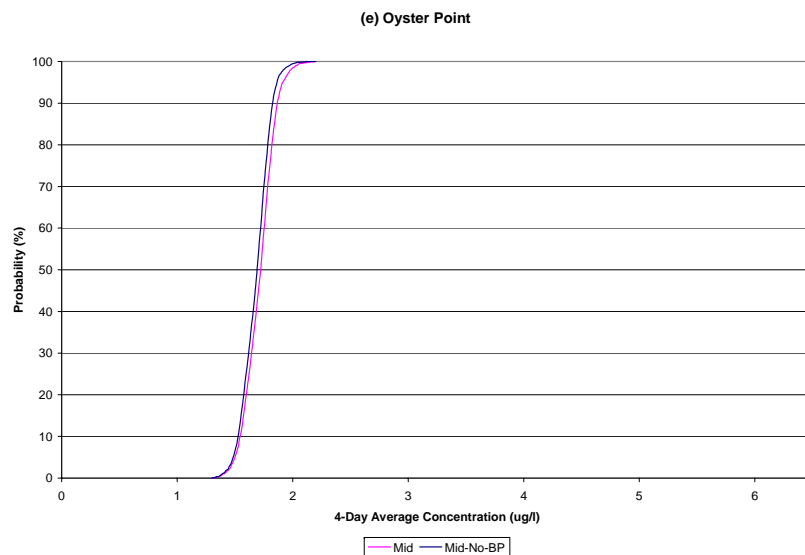


Figure 23. Cumulative Probabilities for Mid and Mid-No-BP Modeled Scenarios (continued)

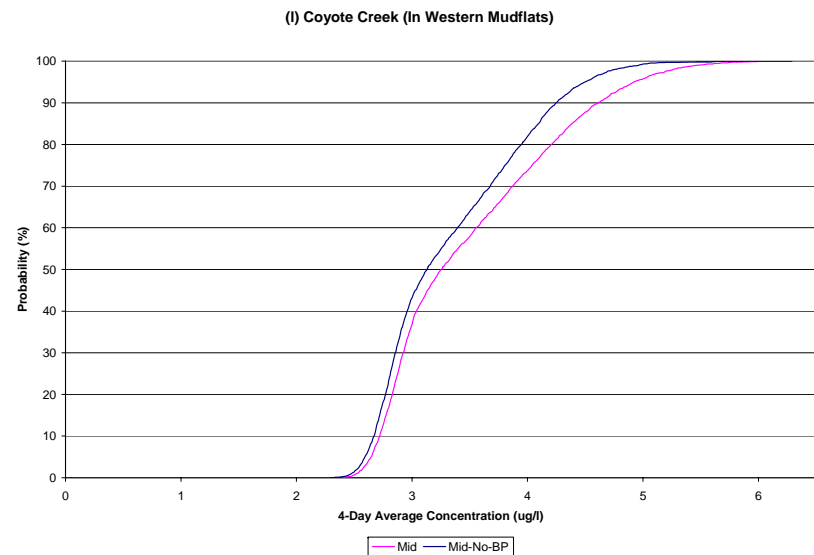
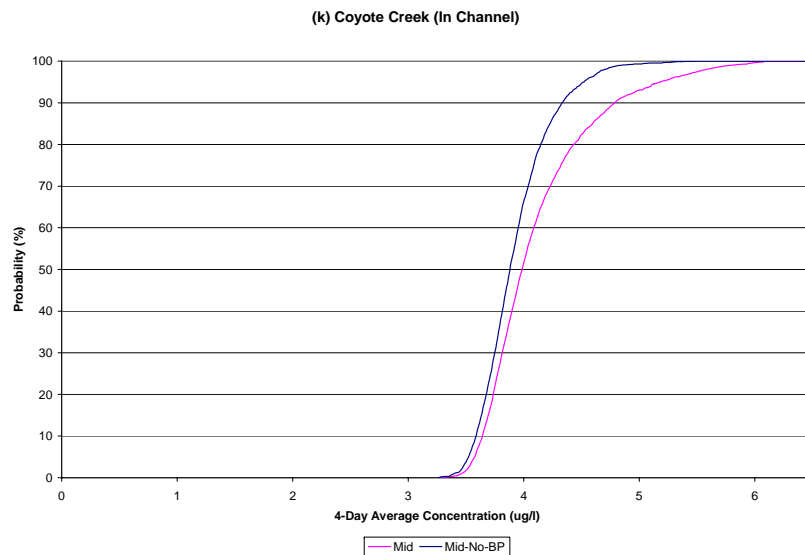
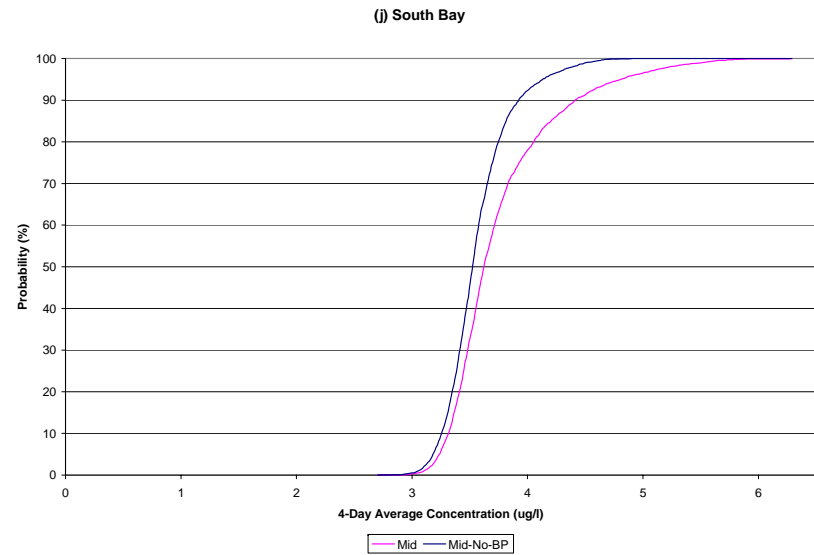
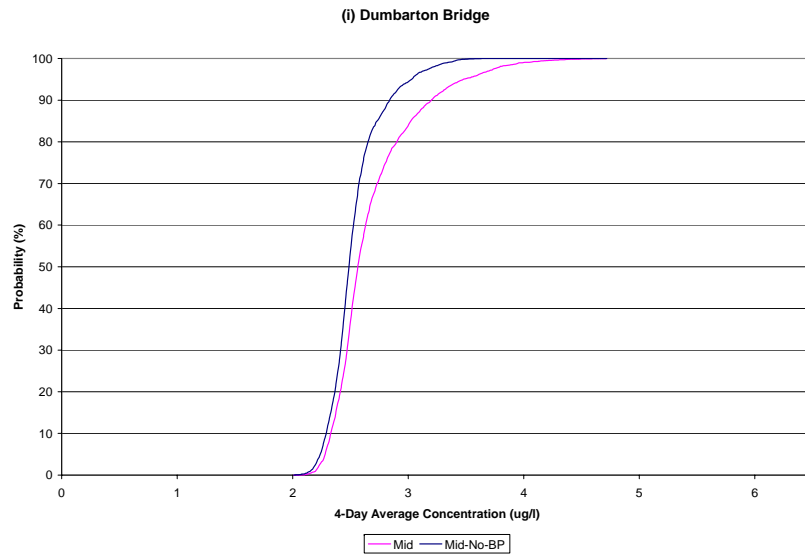


Figure 24. Cumulative Probabilities for Scenario Differences at Coyote Creek (In Channel)

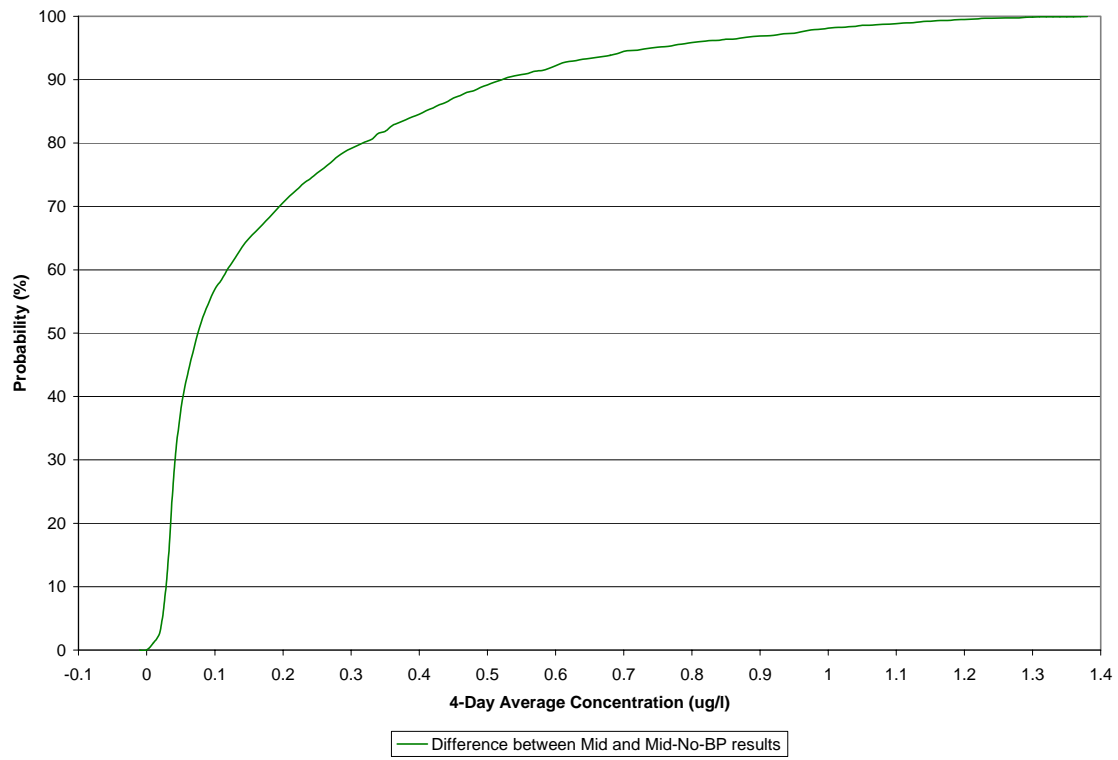
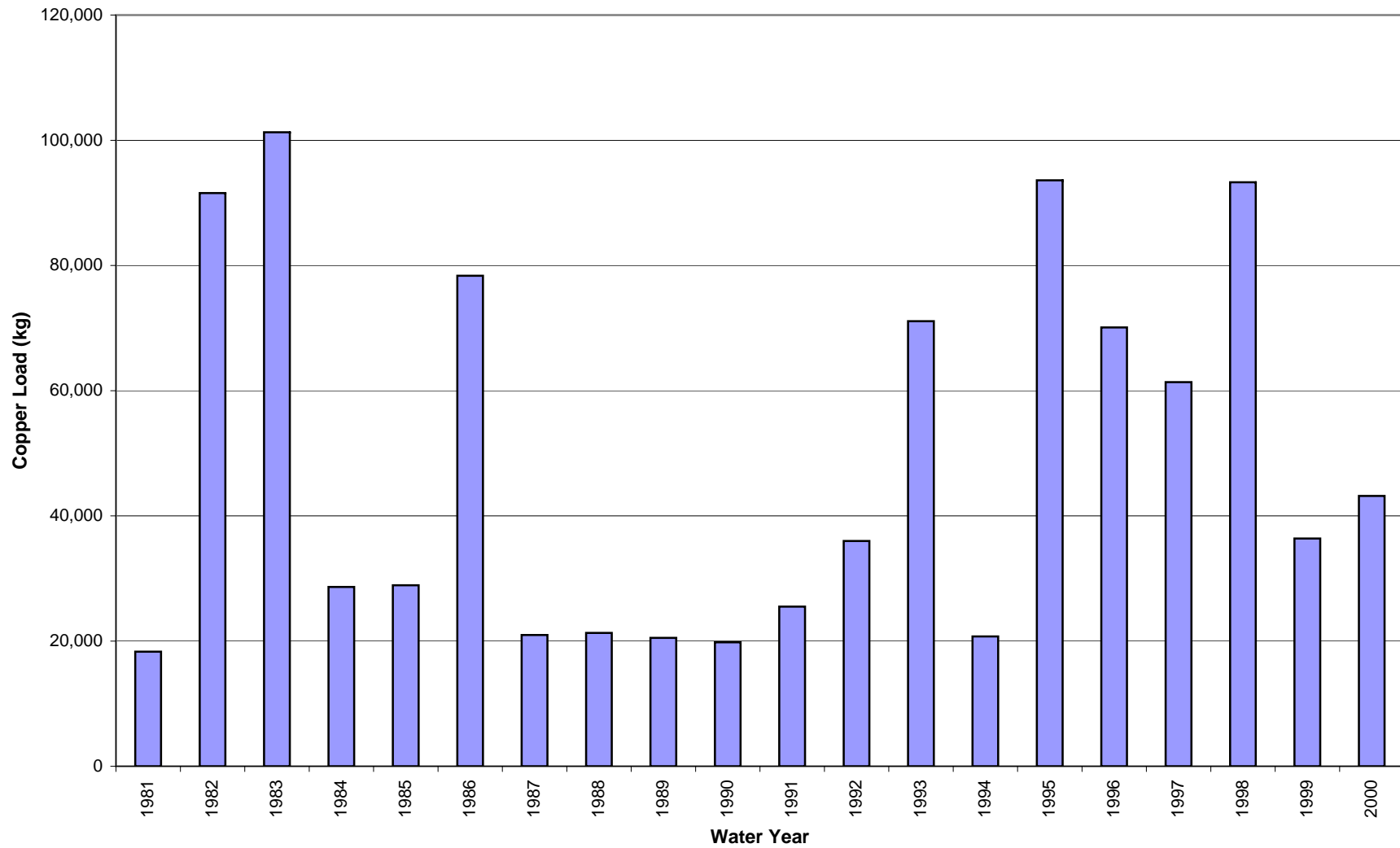
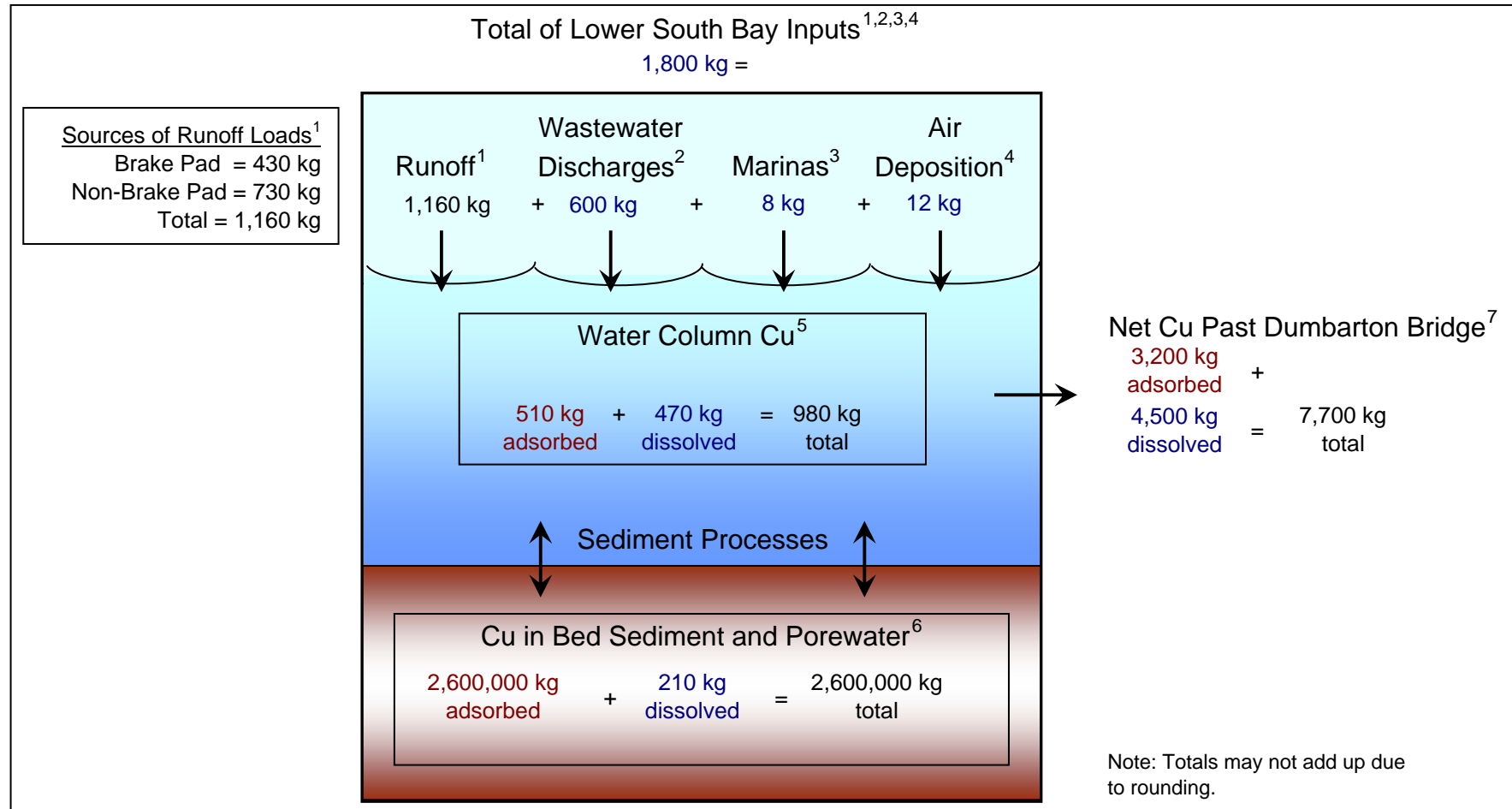


Figure 25. Annual Copper Loads in Tributary Runoff from Watershed Model



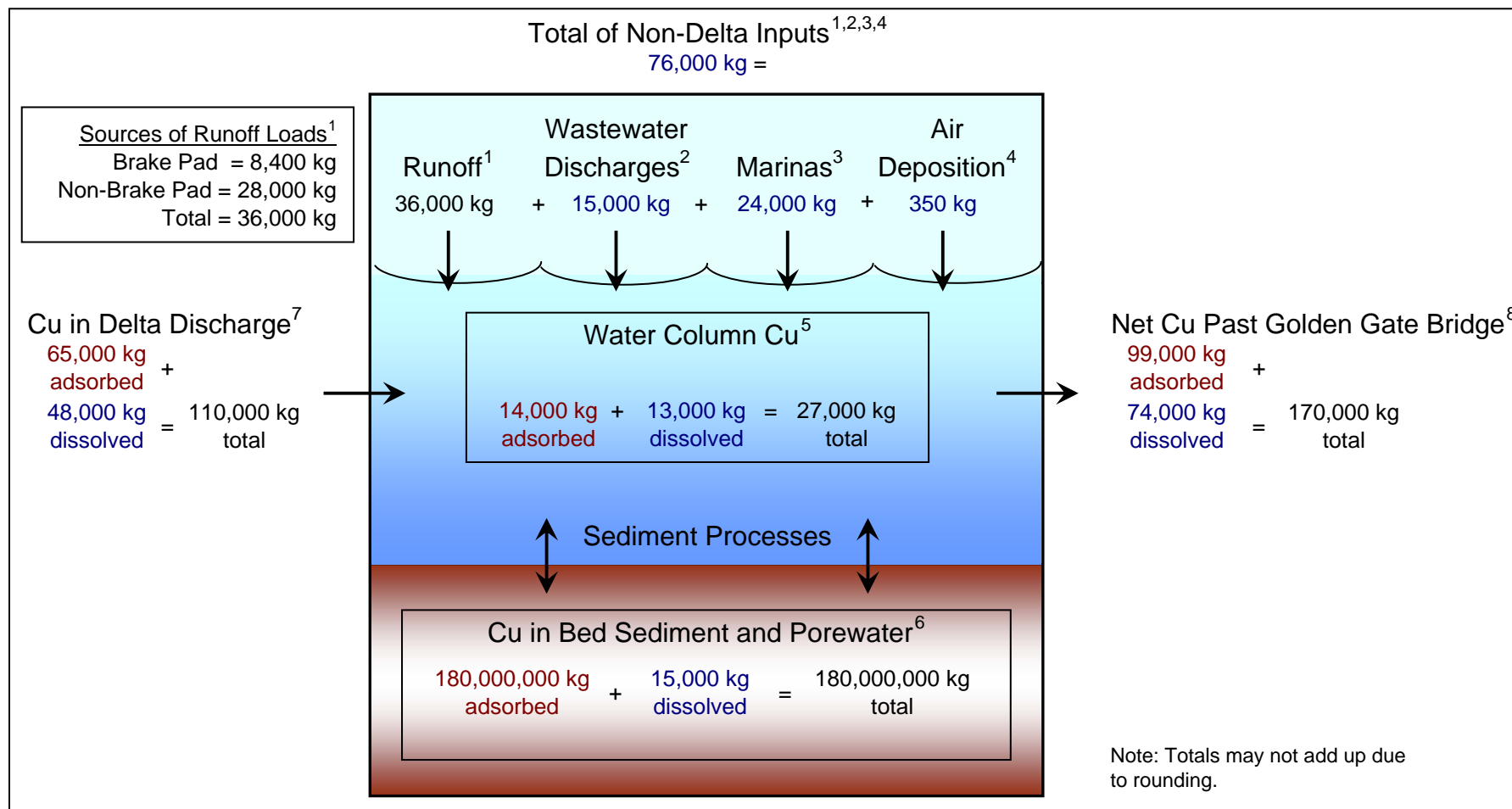
Source of loads: Output from BPP-supplied watershed model (AQUA TERRA 2007).

Figure 26. Copper Inventory for Lower South San Francisco Bay During 1997 Dry Season (February to September)



- ¹ Runoff loads are from the BPP-supplied watershed model for February through September of 1997 and include a dissolved fraction (850 kg) and an adsorbed fraction (310 kg). The portion of the runoff load attributed to brake pads is from the average annual percentage determined by AQUA TERRA (2007) for the Mid-Brakes scenario. This most likely overestimates the contribution from brake pads since the modeled period consists mainly of the dry season when hardly any runoff loads can be attributed to brake pads.
- ² Loads in wastewater discharges for the modeled period are based on the average of daily (when available) or monthly average flows and concentrations for 1996 and 1997 from NPDES self-monitoring reports. Copper was assumed to be in the dissolved state.
- ³ Marina loads are from the BPP-supplied copper release study and include copper from pressure-treated wood used in marine construction and copper released from antifouling coatings used on boats (Rosselot 2006). This category also includes copper loads from algaecides released to shoreline surface waters.
- ⁴ The annual average rates of wet and dry deposition to the Bay were obtained from the BPP-supplied air deposition model (AER 2007). The amount of deposition changes depending on the number of days with precipitation during the modeled period.
- ⁵ The load of copper in the water column is based on the average modeled amounts at the beginning and end of the modeled period from February through September of 1997.
- ⁶ The load of copper in the sediment is based on the average modeled amounts at the beginning and end of the modeled period from February through September of 1997.
- ⁷ The net flux of copper past the Dumbarton Bridge was calculated from the model output between February and September of 1997.

Figure 27. Copper Inventory for San Francisco Bay During Water Year 1999



¹ Runoff loads are from the BPP-supplied watershed model for Water Year 1999 and include a dissolved fraction (14000 kg) and an adsorbed fraction (23000 kg). The portion of the runoff load attributed to brake pads is from the average annual percentage determined by AQUA TERRA (2007) for the Mid-Brakes scenario.

² Loads in wastewater discharges for the modeled period are based on the average of daily (when available) or monthly average flows and concentrations for 1996 and 1997 from NPDES self-monitoring reports. Copper was assumed to be in the dissolved state.

³ Marina loads are from the BPP-supplied copper release study and include copper from pressure-treated wood used in marine construction and copper released from antifouling coatings used on boats (Rosselot 2006). This category also includes copper loads from algaecides released to shoreline surface waters.

⁴ The annual average rates of wet and dry deposition to the Bay were obtained from the BPP-supplied air deposition model (AER 2007). The amount of deposition changes depending on the number of days with precipitation during the modeled period.

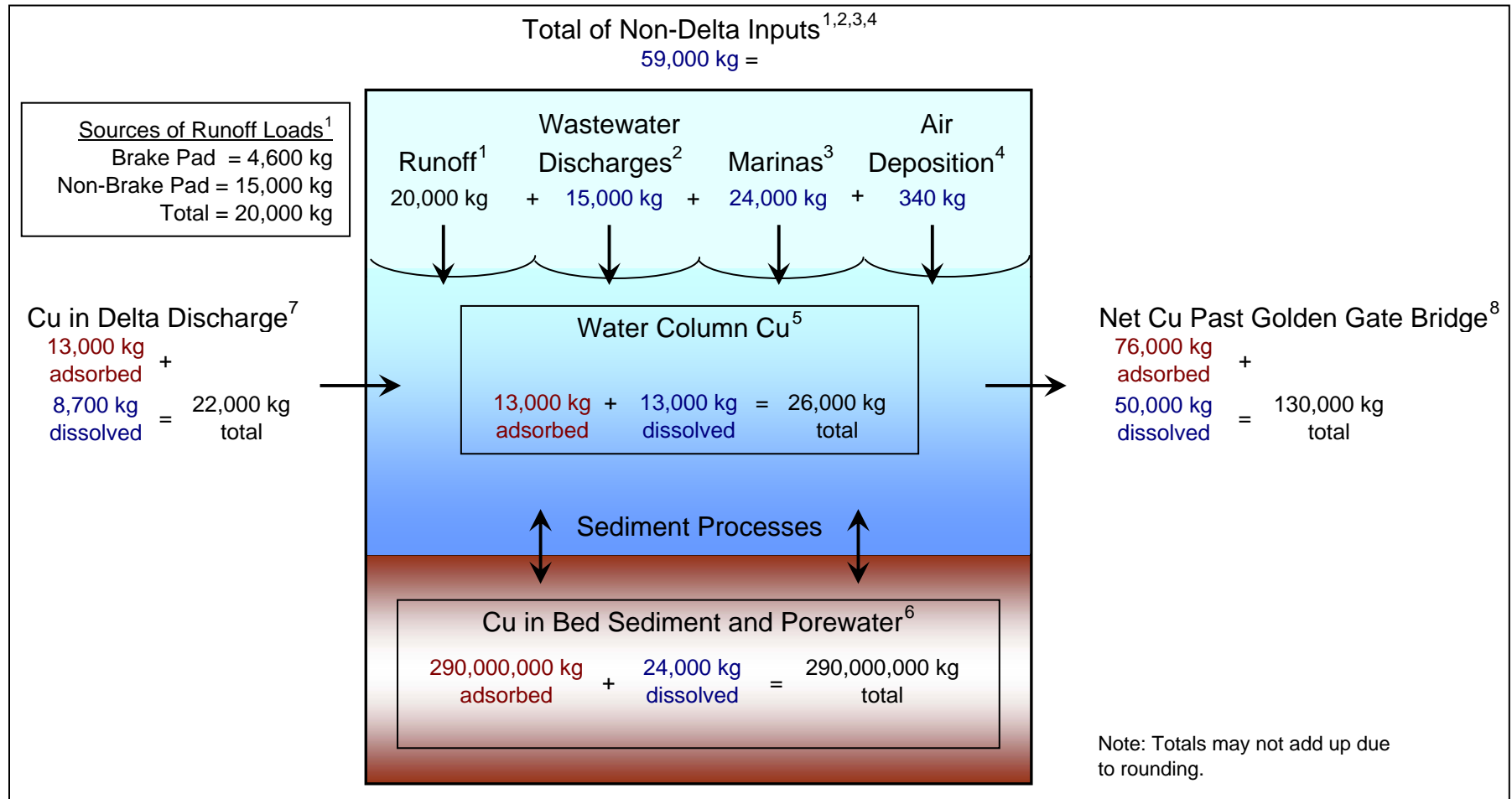
⁵ The load of copper in the water column is based on the average modeled amounts at the beginning and end of Water Year 1999.

⁶ The load of copper in the sediment is based on the average modeled amounts at the beginning and end of Water Year 1999.

⁷ The load of copper in the Delta discharge is from the model input for Water Year 1999.

⁸ The net flux of copper past the Golden Gate was calculated from the model output during Water Year 1999.

Figure 28. Copper Inventory for San Francisco Bay During Water Year 2010 Using Hydrology for Water Year 1990



¹ Runoff loads are from the BPP-supplied watershed model for Water Year 1990. This year was repeated as the hydrologic input for Water Year 2010. The loads include a dissolved fraction (8700 kg) and an adsorbed fraction (11000 kg). The portion of the runoff load attributed to brake pads is from the average annual percentage determined by AQUA TERRA (2007) for the Mid-Brakes scenario.

² Loads in wastewater discharges for the modeled period are based on the average of daily (when available) or monthly average flows and concentrations for 1996 and 1997 from NPDES self-monitoring reports. Copper was assumed to be in the dissolved state.

³ Marina loads are from the BPP-supplied copper release study and include copper from pressure-treated wood used in marine construction and copper released from antifouling coatings used on boats (Rosselot 2006). This category also includes copper loads from algaecides released to shoreline surface waters.

⁴ The annual average rates of wet and dry deposition to the Bay were obtained from the BPP-supplied air deposition model (AER 2007). The amount of deposition changes depending on the number of days with precipitation during the modeled period.

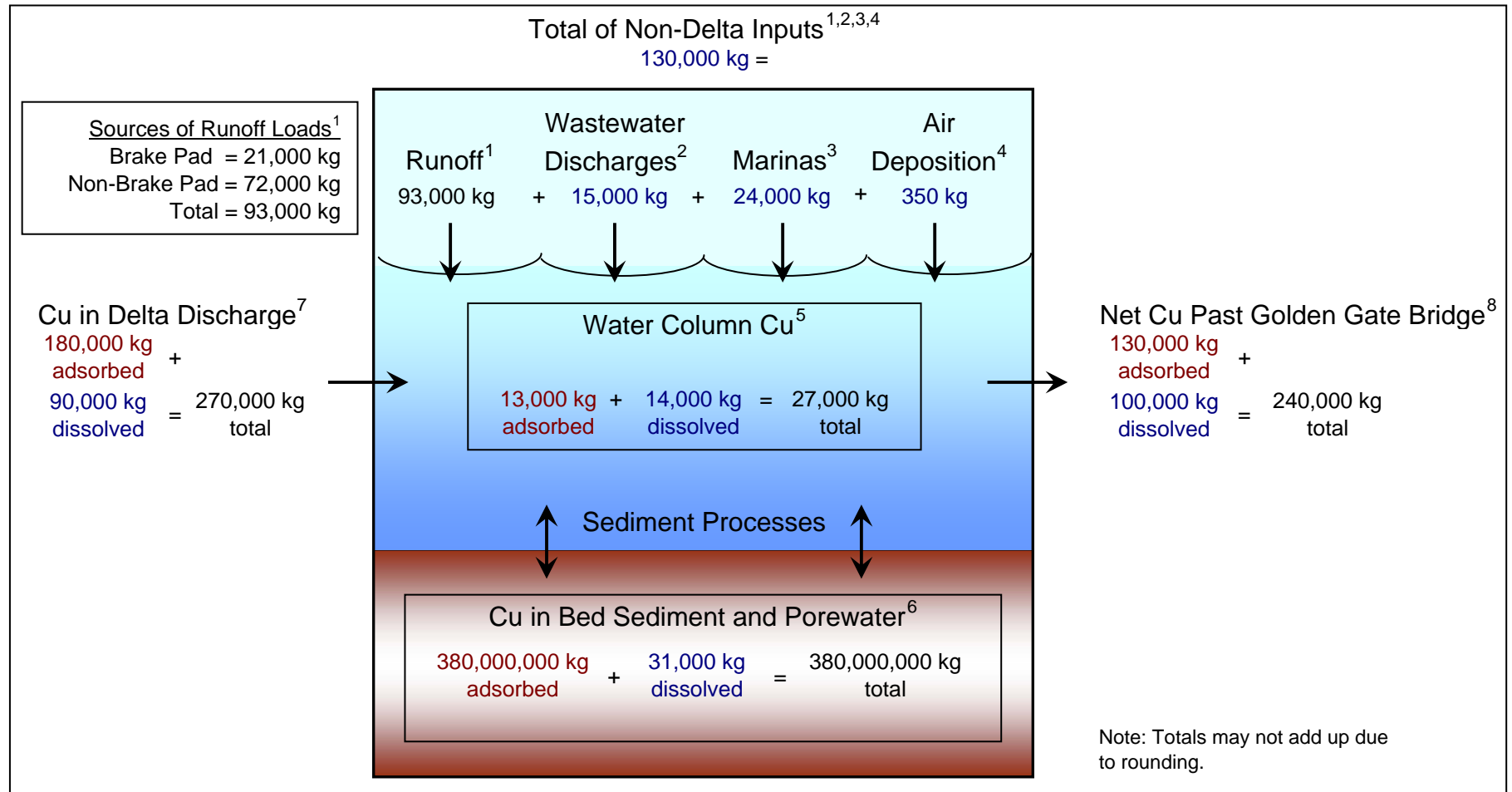
⁵ The load of copper in the water column is based on the average modeled amounts at the beginning and end of Water Year 2010.

⁶ The load of copper in the sediment is based on the average modeled amounts at the beginning and end of Water Year 2010.

⁷ The load of copper in the Delta discharge is from the model input for Water Year 1990. This year was repeated as the hydrologic input for Water Year 2010.

⁸ The net flux of copper past the Golden Gate was calculated from the model output during Water Year 2010.

Figure 29. Copper Inventory for San Francisco Bay During Water Year 2018 Using Hydrology for Water Year 1998



¹ Runoff loads are from the BPP-supplied watershed model for Water Year 1998. This year was repeated as the hydrologic input for Water Year 2018. The loads include a dissolved fraction (29000 kg) and an adsorbed fraction (65000 kg). The portion of the runoff load attributed to brake pads is from the average annual percentage determined by AQUA TERRA (2007) for the Mid-Brakes scenario.

² Loads in wastewater discharges for the modeled period are based on the average of daily (when available) or monthly average flows and concentrations for 1996 and 1997 from NPDES self-monitoring reports. Copper was assumed to be in the dissolved state.

³ Marina loads are from the BPP-supplied copper release study and include copper from pressure-treated wood used in marine construction and copper released from antifouling coatings used on boats (Rosselot 2006). This category also includes copper loads from algacides released to shoreline surface waters.

⁴ The annual average rates of wet and dry deposition to the Bay were obtained from the BPP-supplied air deposition model (AER 2007). The amount of deposition changes depending on the number of days with precipitation during the modeled period.

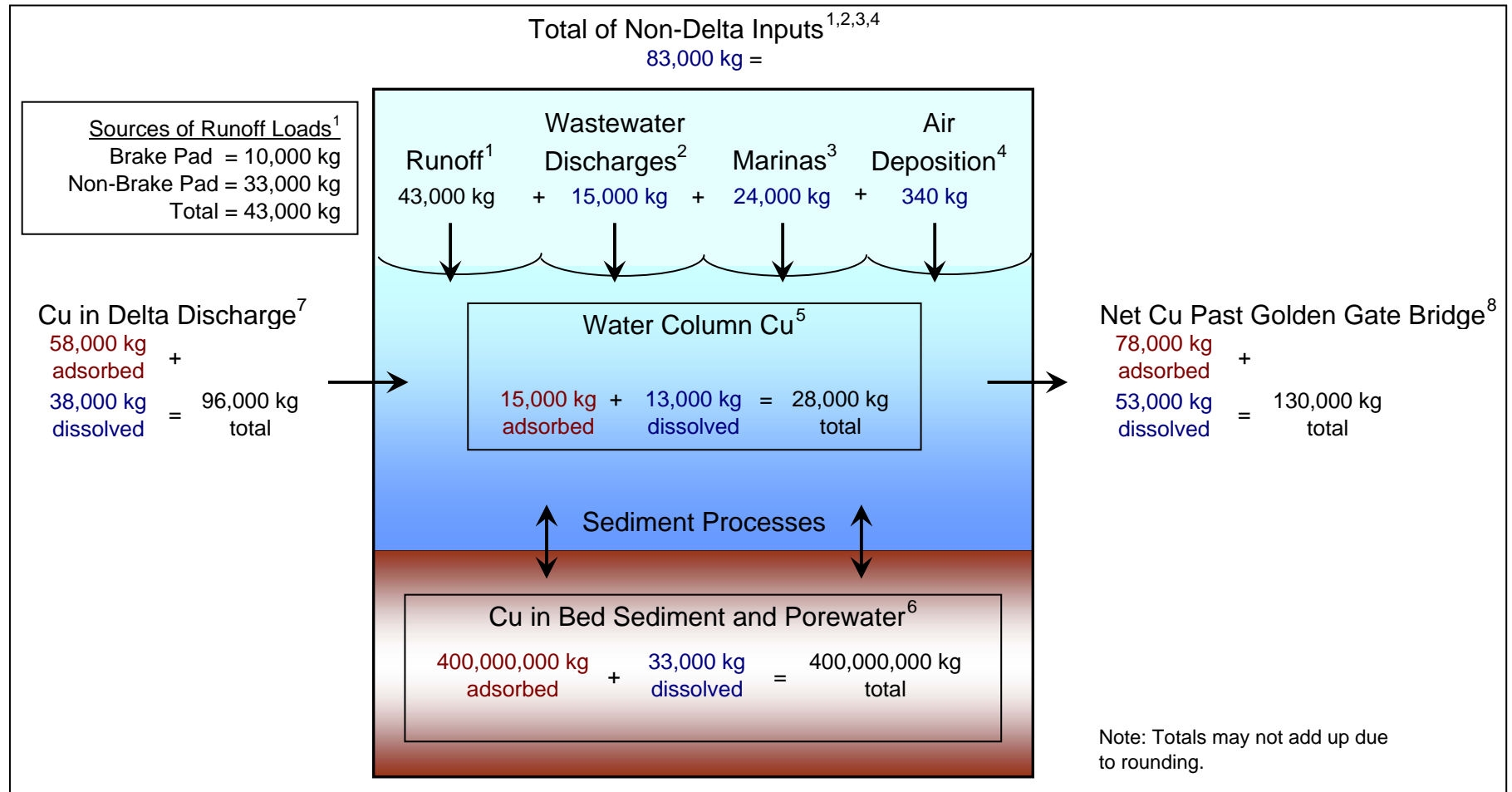
⁵ The load of copper in the water column is based on the average modeled amounts at the beginning and end of Water Year 2018.

⁶ The load of copper in the sediment is based on the average modeled amounts at the beginning and end of Water Year 2018.

⁷ The load of copper in the Delta discharge is from the model input for Water Year 1998. This year was repeated as the hydrologic input for Water Year 2018.

⁸ The net flux of copper past the Golden Gate was calculated from the model output during Water Year 2018.

Figure 30. Copper Inventory for San Francisco Bay During Water Year 2020 Using Hydrology for Water Year 2000



¹ Runoff loads are from the BPP-supplied watershed model for Water Year 2000. This year was repeated as the hydrologic input for Water Year 2020. The loads include a dissolved fraction (15000 kg) and an adsorbed fraction (28000 kg). The portion of the runoff load attributed to brake pads is from the average annual percentage determined by AQUA TERRA (2007) for the Mid-Brakes scenario.

² Loads in wastewater discharges for the modeled period are based on the average of daily (when available) or monthly average flows and concentrations for 1996 and 1997 from NPDES self-monitoring reports. Copper was assumed to be in the dissolved state.

³ Marina loads are from the BPP-supplied copper release study and include copper from pressure-treated wood used in marine construction and copper released from antifouling coatings used on boats (Rosselot 2006). This category also includes copper loads from algacides released to shoreline surface waters.

⁴ The annual average rates of wet and dry deposition to the Bay were obtained from the BPP-supplied air deposition model (AER 2007). The amount of deposition changes depending on the number of days with precipitation during the modeled period.

⁵ The load of copper in the water column is based on the average modeled amounts at the beginning and end of Water Year 2020.

⁶ The load of copper in the sediment is based on the average modeled amounts at the beginning and end of Water Year 2020.

⁷ The load of copper in the Delta discharge is from the model input for Water Year 2000. This year was repeated as the hydrologic input for Water Year 2020.

⁸ The net flux of copper past the Golden Gate was calculated from the model output during Water Year 2020.

Figure 31. Sensitivity of Dissolved Copper Concentration to Copper Loads

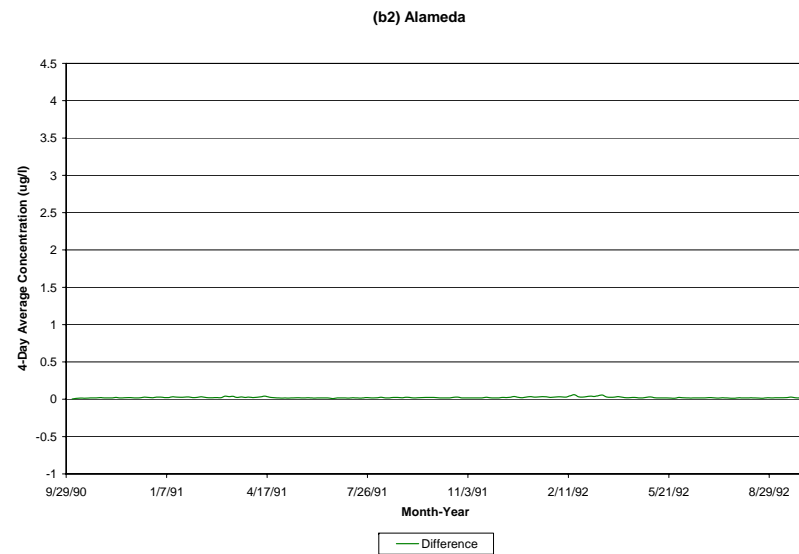
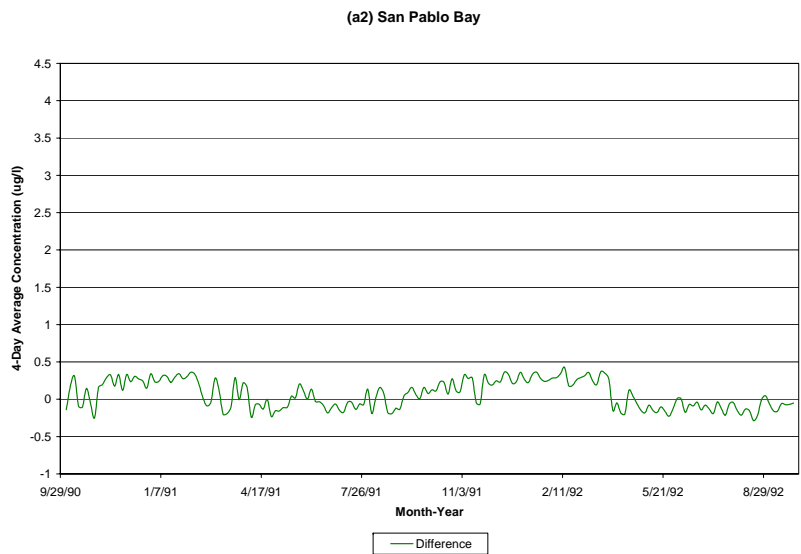
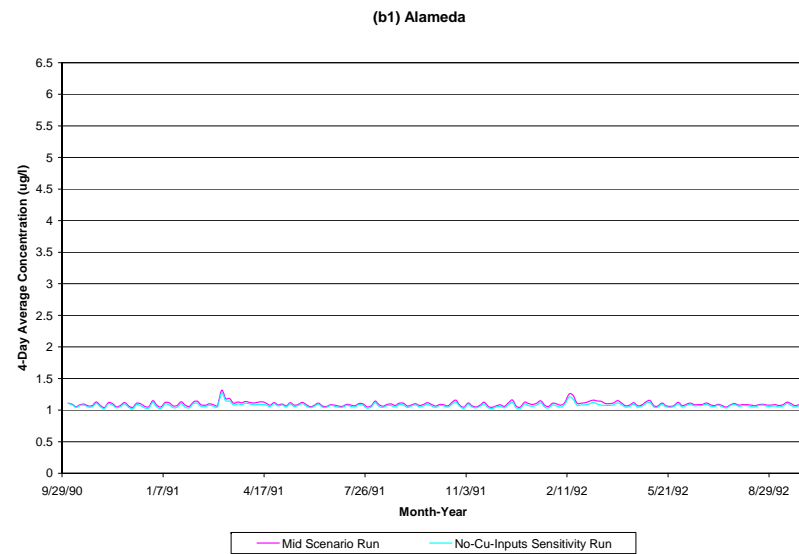
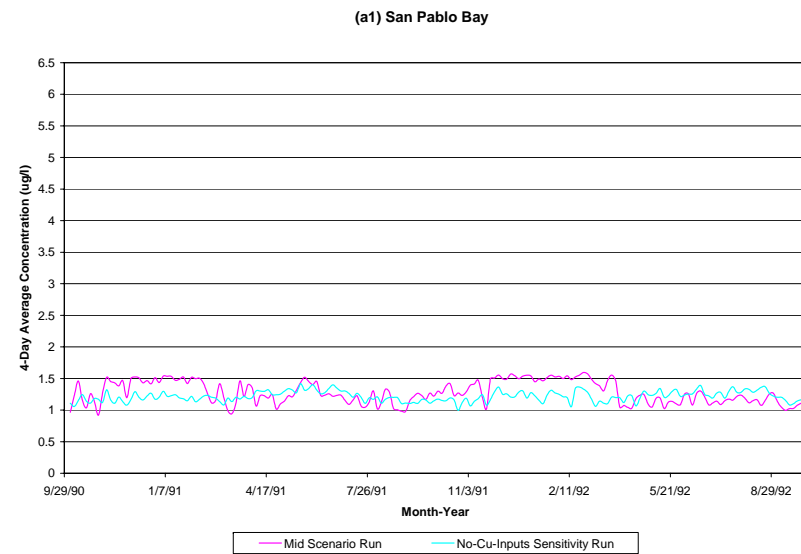
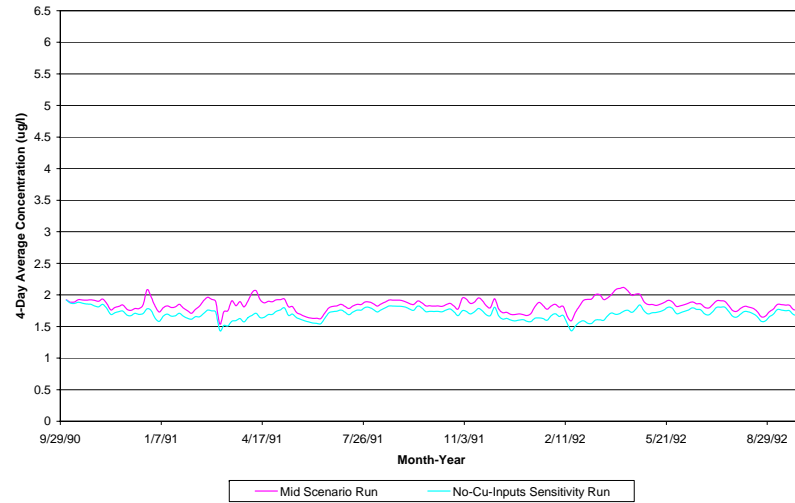
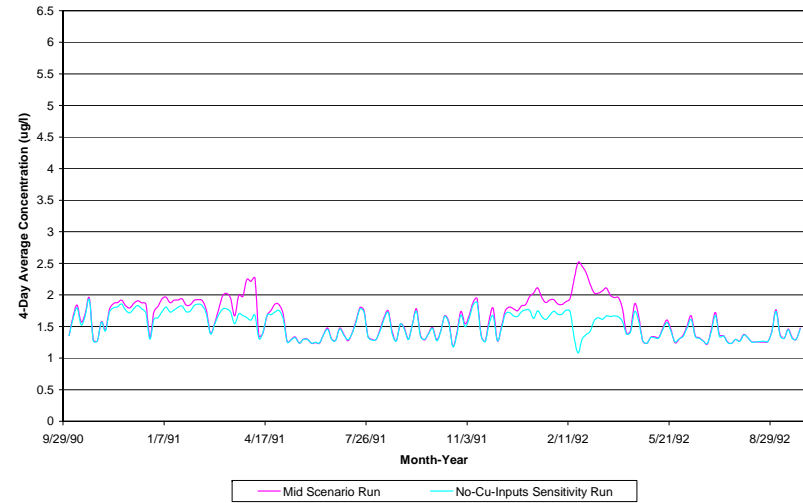


Figure 31. Sensitivity of Dissolved Copper Concentration to Copper Loads (continued)

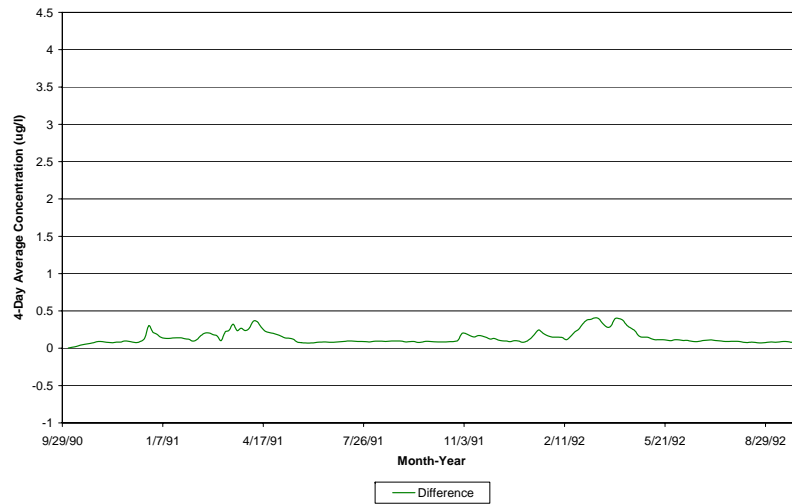
(c1) San Bruno Shoal (In Channel)



(d1) San Bruno Shoal (In Eastern Mudflats)



(c2) San Bruno Shoal (In Channel)



(d2) San Bruno Shoal (In Eastern Mudflats)

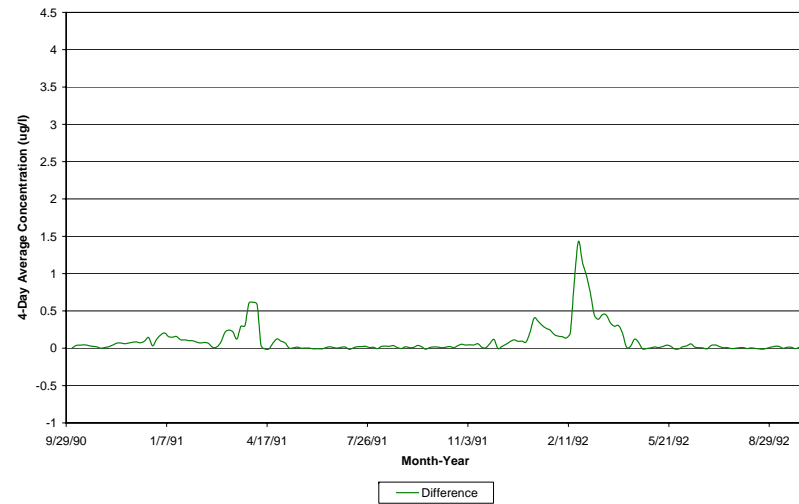
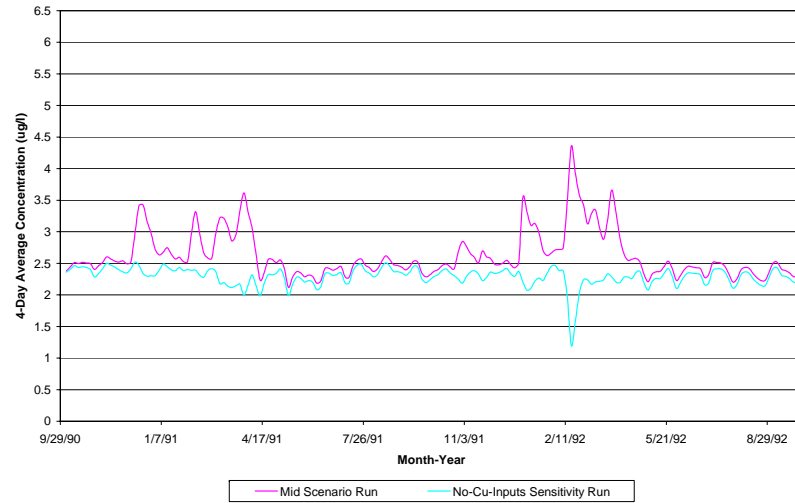
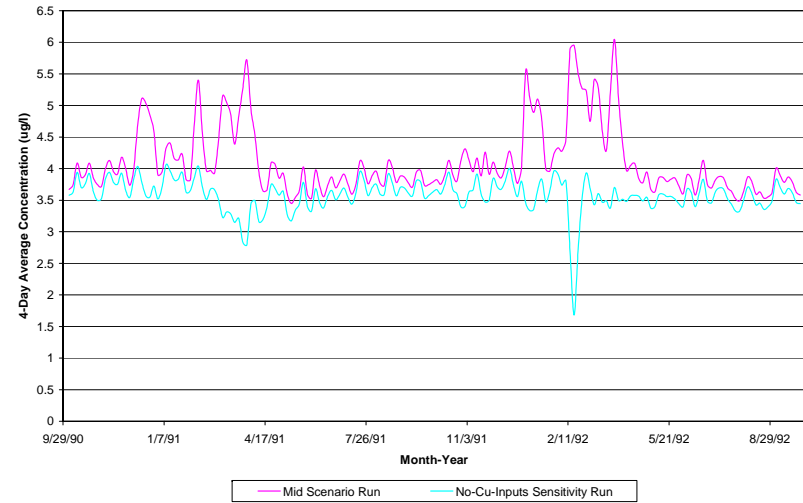


Figure 31. Sensitivity of Dissolved Copper Concentration to Copper Loads (continued)

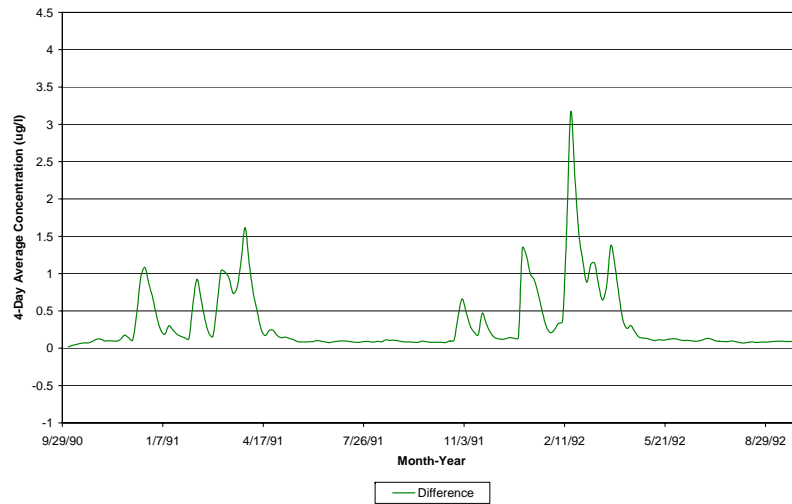
(e1) Dumbarton Bridge



(f1) Coyote Creek (In Channel)



(e2) Dumbarton Bridge



(f2) Coyote Creek (In Channel)

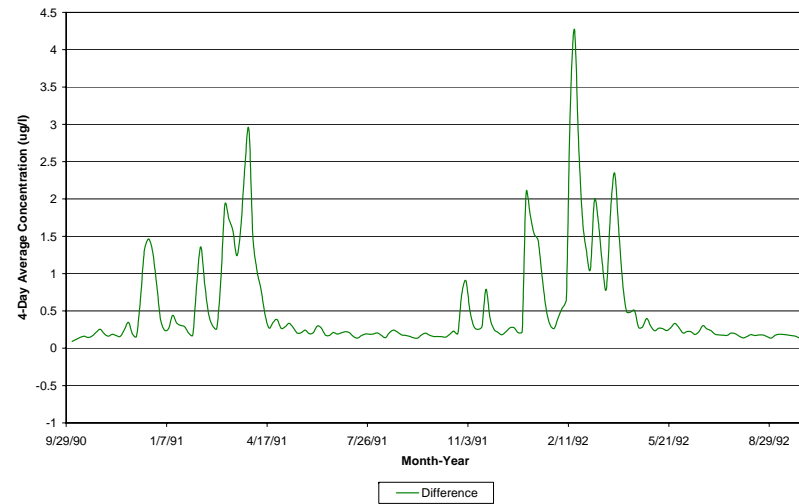


Figure 32. Sensitivity of Benthic Copper Concentration to Copper Loads, Coyote Creek (In Channel)

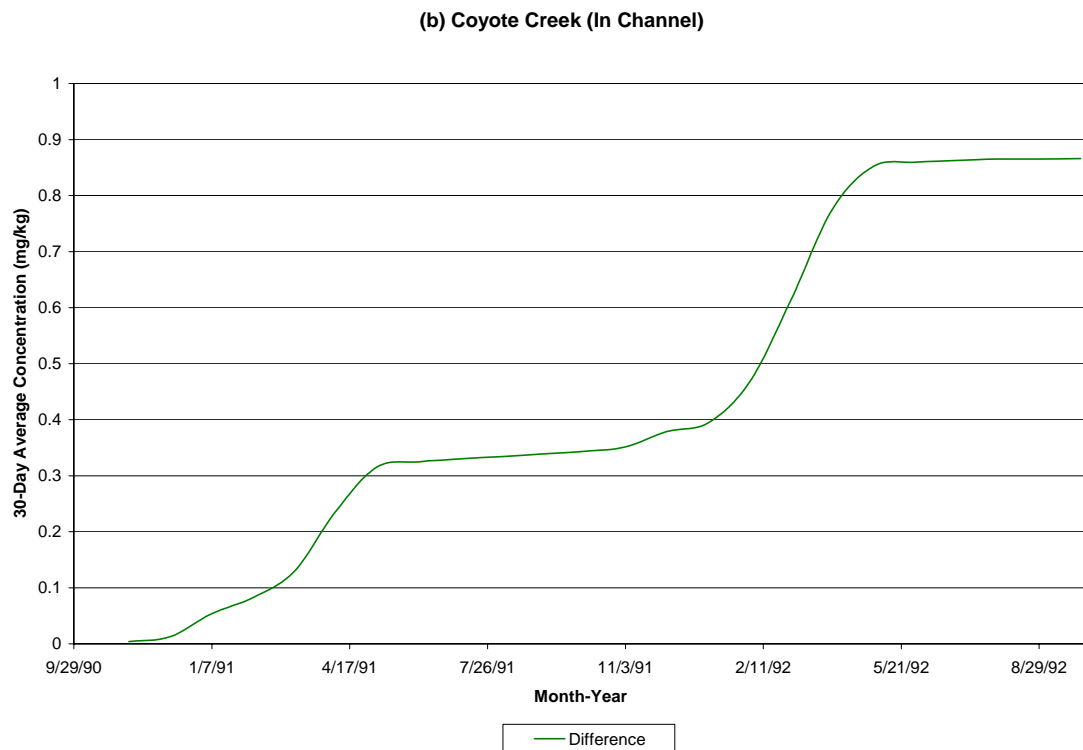
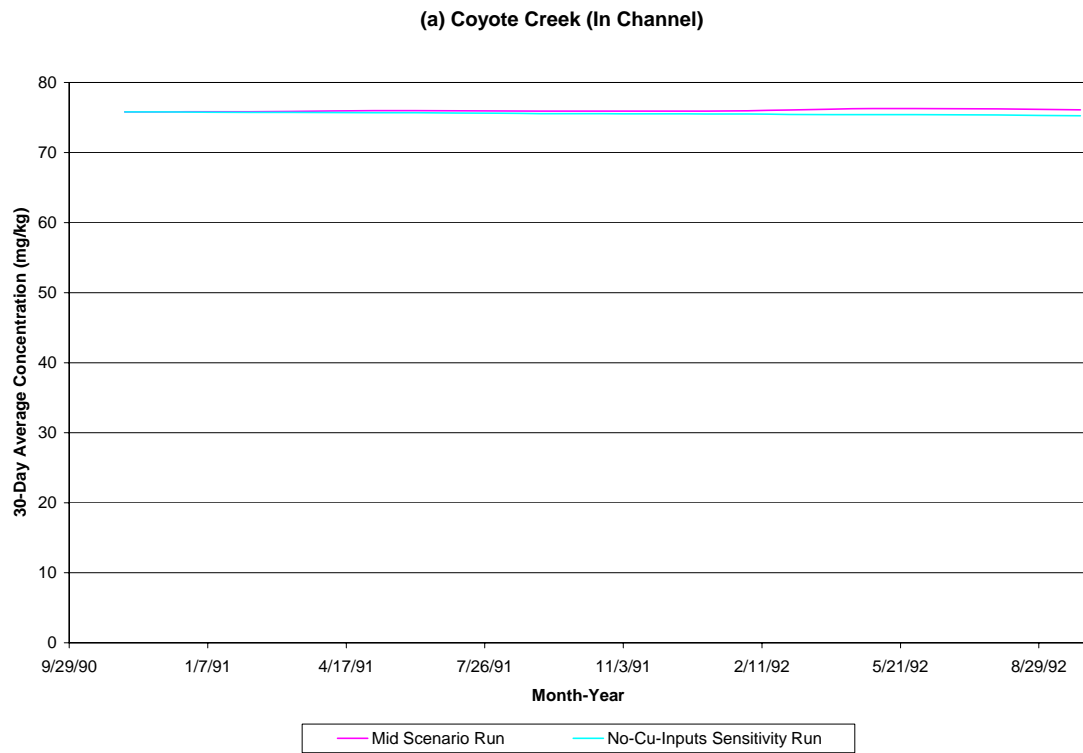


Figure 33. Sensitivity of Dissolved Copper Concentration to Initial Benthic Copper Conditions

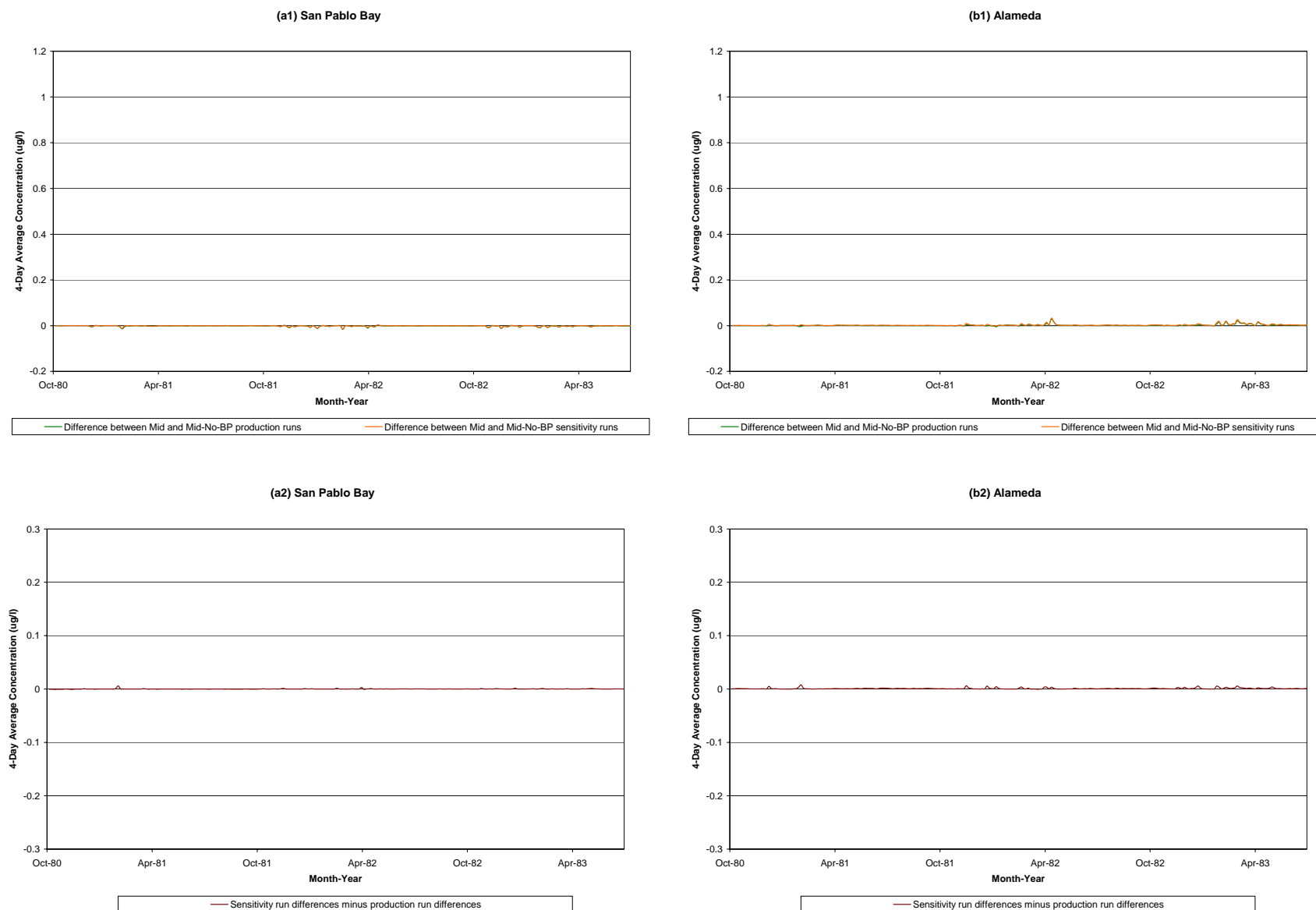
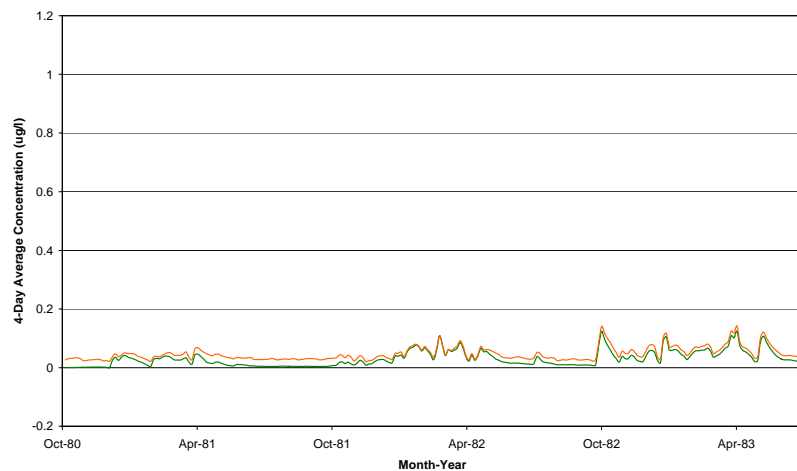


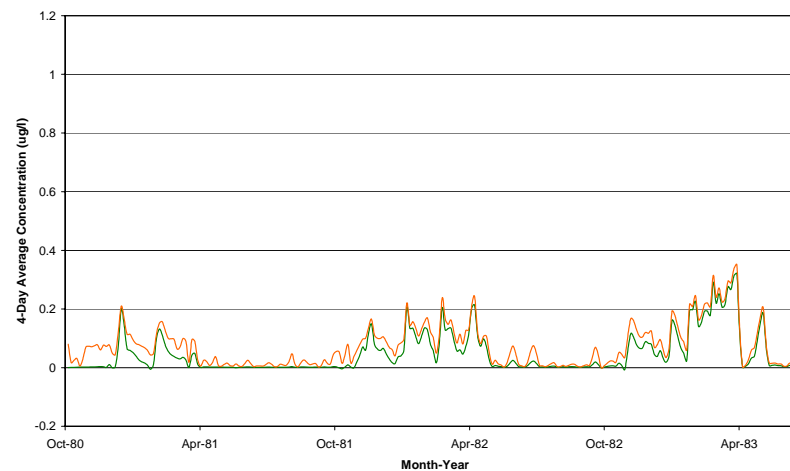
Figure 33. Sensitivity of Dissolved Copper Concentration to Initial Benthic Copper Conditions (continued)

(c1) San Bruno Shoal (In Channel)



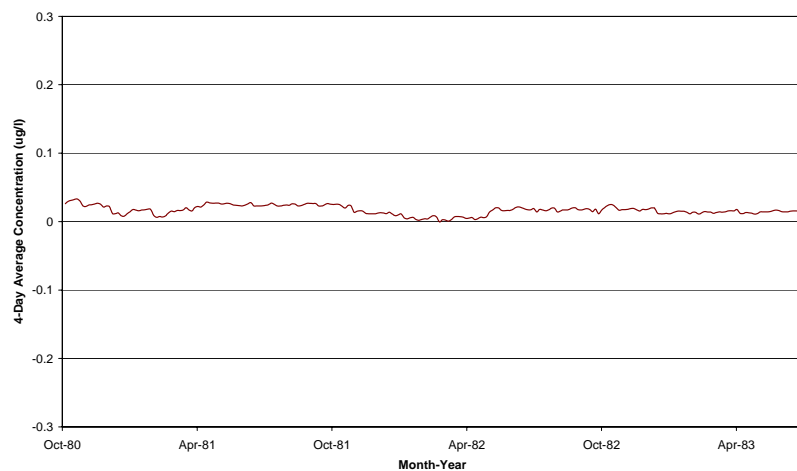
— Difference between Mid and Mid-No-BP production runs — Difference between Mid and Mid-No-BP sensitivity runs

(d1) San Bruno Shoal (In Eastern Mudflats)



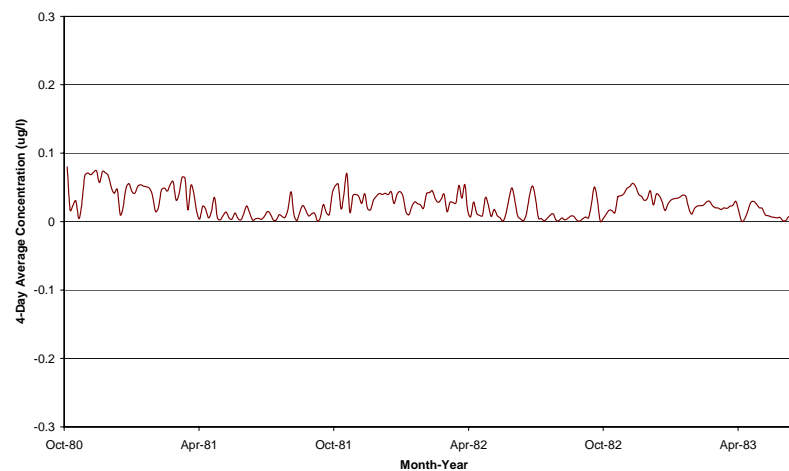
— Difference between Mid and Mid-No-BP production runs — Difference between Mid and Mid-No-BP sensitivity runs

(c2) San Bruno (In Channel)



— Sensitivity run differences minus production run differences

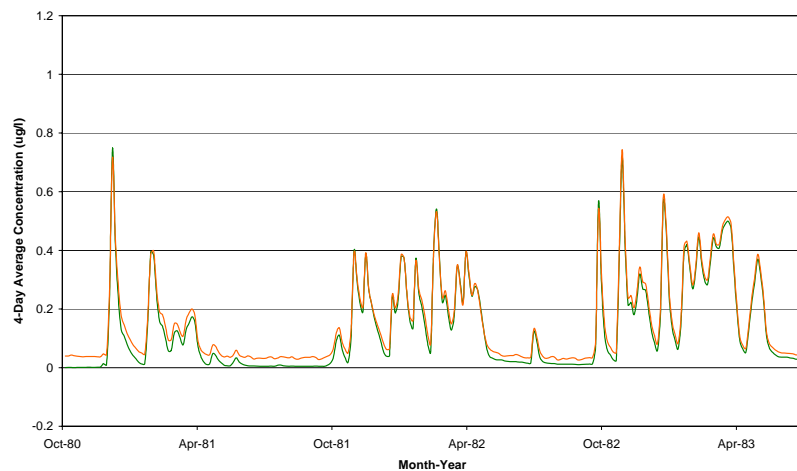
(d2) San Bruno (In Eastern Mudflats)



— Sensitivity run differences minus production run differences

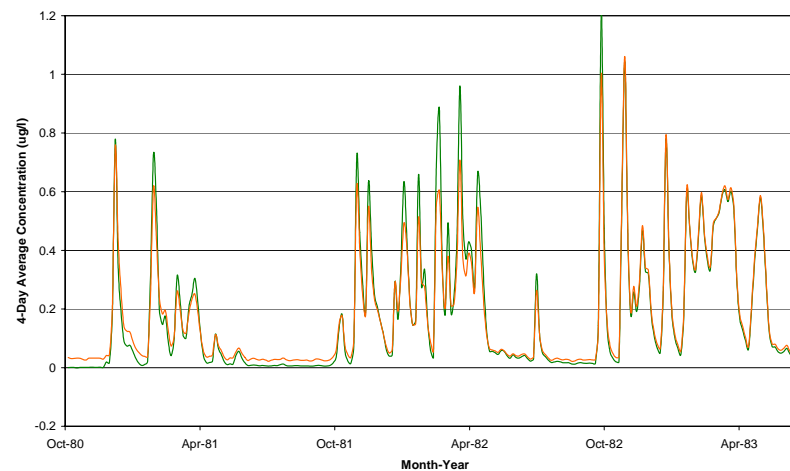
Figure 33. Sensitivity of Dissolved Copper Concentration to Initial Benthic Copper Conditions (continued)

(e1) Dumbarton Bridge



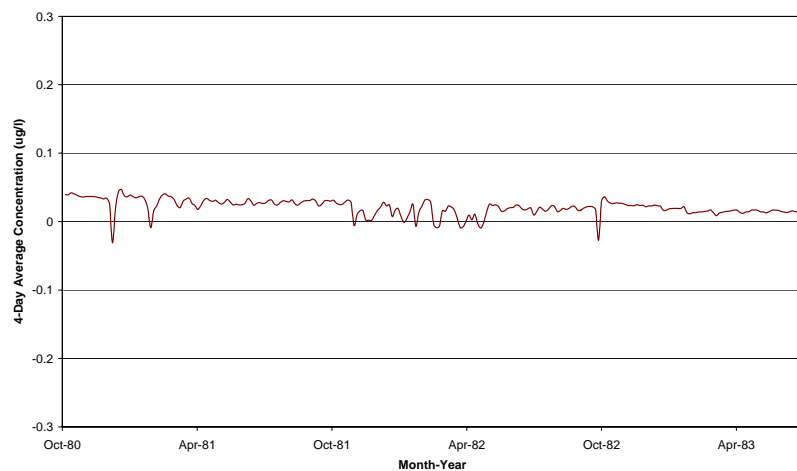
— Difference between Mid and Mid-No-BP production runs — Difference between Mid and Mid-No-BP sensitivity runs

(f1) Coyote Creek (In Channel)



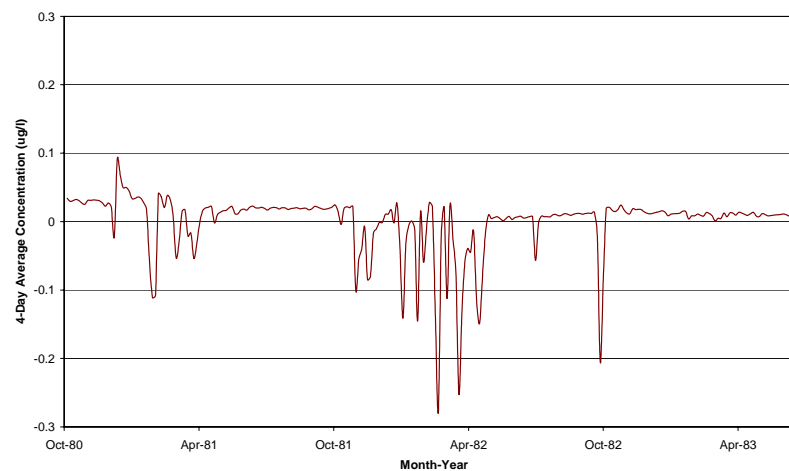
— Difference between Mid and Mid-No-BP production runs — Difference between Mid and Mid-No-BP sensitivity runs

(e2) Dumbarton Bridge



— Sensitivity run differences minus production run differences

(f2) Coyote Creek (In Channel)



— Sensitivity run differences minus production run differences

Figure 34. Sensitivity of Benthic Copper Concentration to Initial Benthic Copper Conditions

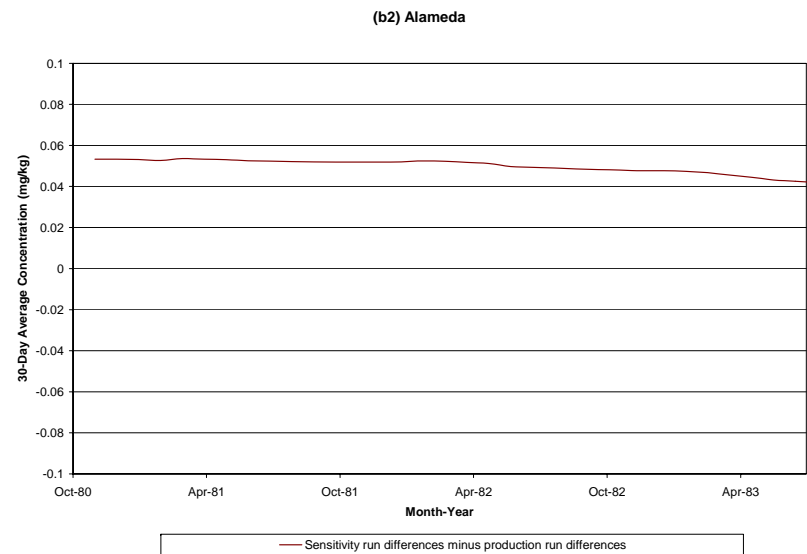
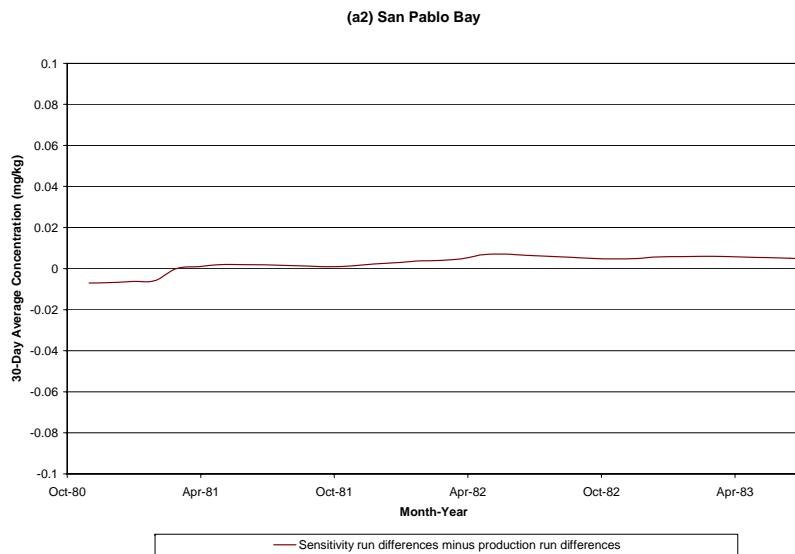
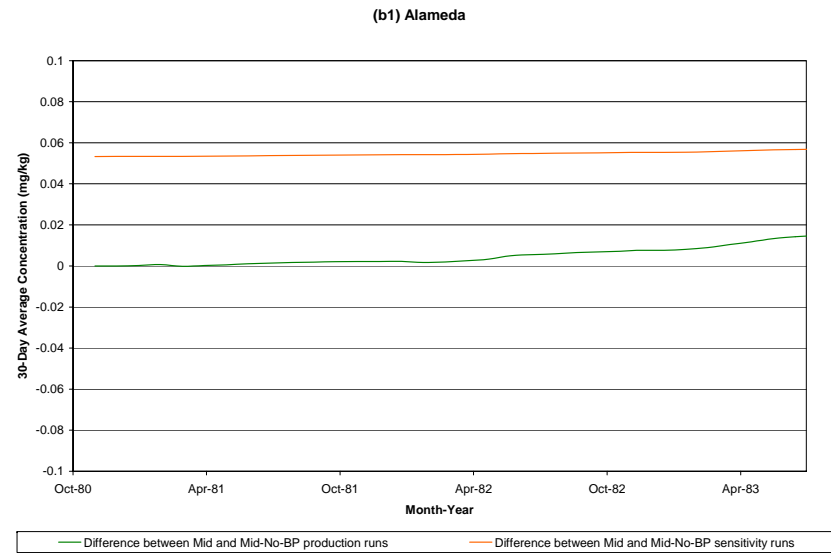
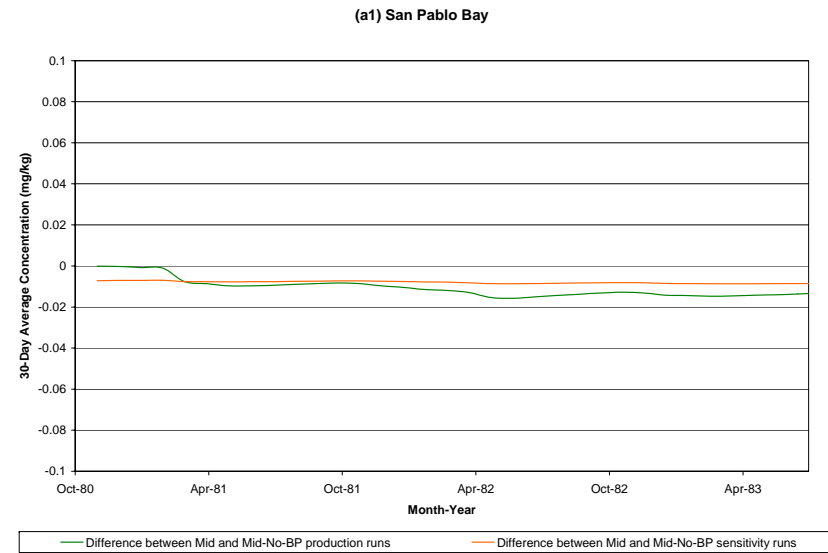
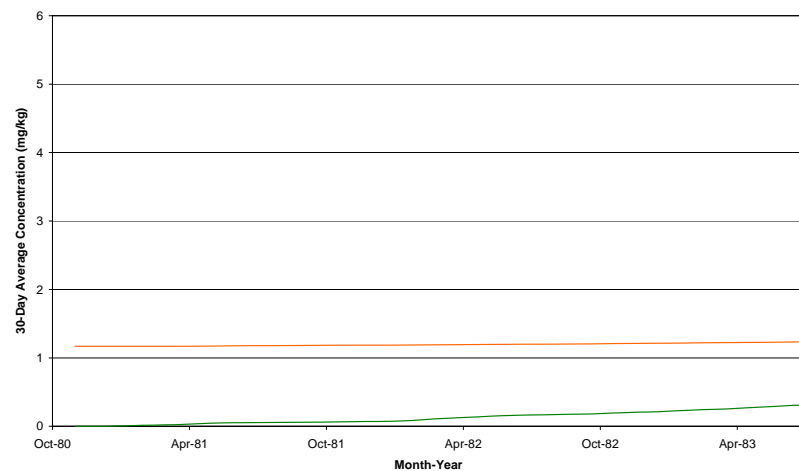


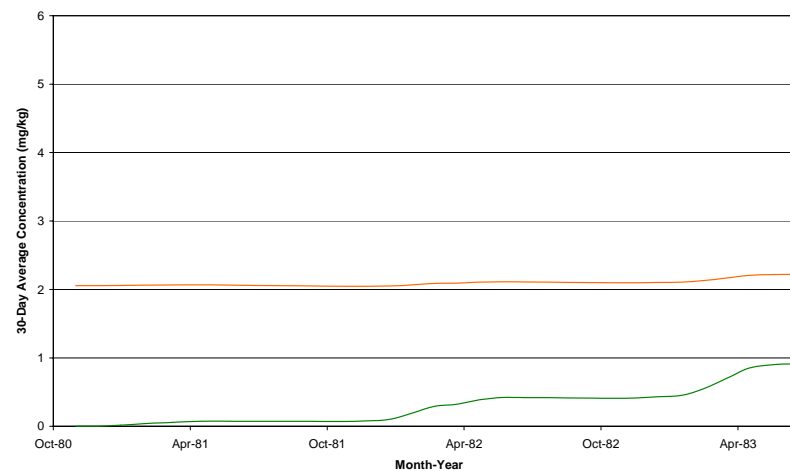
Figure 34. Sensitivity of Benthic Copper Concentration to Initial Benthic Copper Conditions (continued)

(c1) San Bruno Shoal (In Channel)



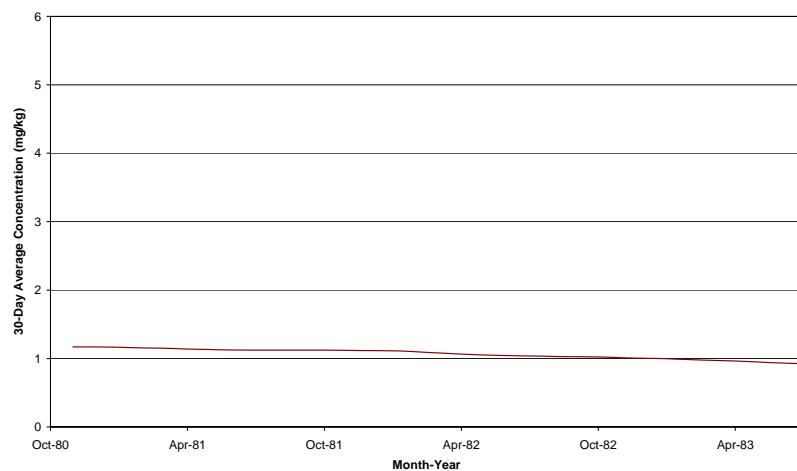
— Difference between Mid and Mid-No-BP production runs — Difference between Mid and Mid-No-BP sensitivity runs

(d1) San Bruno Shoal (In Eastern Mudflats)



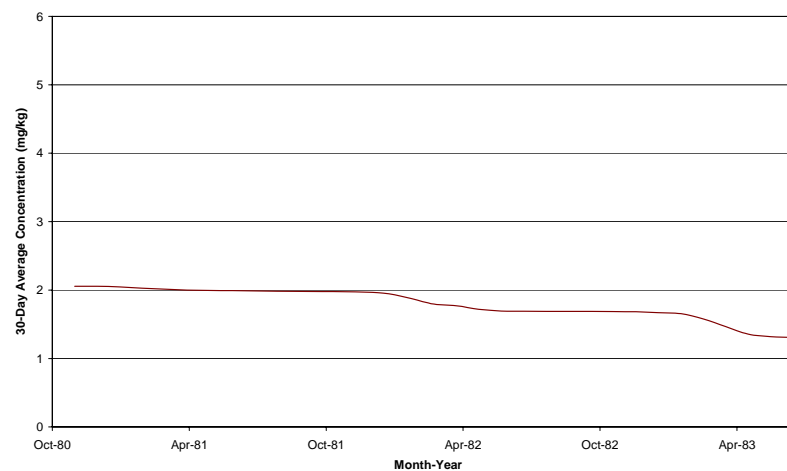
— Difference between Mid and Mid-No-BP production runs — Difference between Mid and Mid-No-BP sensitivity runs

(c2) San Bruno Shoal (In Channel)



— Sensitivity run differences minus production run differences

(d2) San Bruno Shoal (In Eastern Mudflat)



— Sensitivity run differences minus production run differences

Figure 34. Sensitivity of Benthic Copper Concentration to Initial Benthic Copper Conditions (continued)

